STUDIES ON STABILITY CHARACTERISTICS OF MOX AND METAL FUELED FAST REACTOR CORES

by

ANURAJ V L

PHYS 02 2012 04 018

Indira Gandhi Centre for Atomic Research, Kalpakkam

A thesis submitted to the

Board of Studies in Physical Sciences

In partial fulfillment of requirements for the Degree of

DOCTOR OF PHILOSOPHY

of

HOMI BHABHA NATIONAL INSTITUTE

August 2019

Homi Bhabha National Institute

Recommendations of the Viva Voce Board

As members of the Viva Voce Board, we certify that we have read the dissertation prepared by Anuraj V L entitled 'Studies on stability characteristics of MOX and metal fueled fast reactor cores' and recommend that it may be accepted as fulfilling the dissertation requirement for the Degree of Doctor of Philosophy.

Chairman - Dr. K. Velusamy By VC for 14/12/2020 (Dean, PS)

Guide/Convener - Dr. K. Devan 14/12/2020

Examiner - Dr. Bruno Merk By VC for 14/12/2020 (Dean PS)

Member 1 - Dr. M. T. Jose 14/12/2020

Member 2 - Dr. G. Raghavan

Technology advisor - Dr. G. S. Srinivasan 14/12/2020

Final approval and acceptance of this dissertation is contingent upon the candidate's submission of the final copies of the dissertation to HBNI.

I hereby certify that I have read this dissertation prepared under my direction and recommend that it may be accepted as fulfilling the dissertation requirement

Date: 14.12.2020

Place: Kalpakkam

Guide 14/12/2020

STATEMENT BY AUTHOR

This dissertation has been submitted in partial fulfillment of requirements for an advanced degree at Homi Bhabha National Institute (HBNI) and is deposited in the Library to be made available to borrowers under rules of the HBNI.

Brief quotations from this dissertation are allowable without special permission, provided that accurate acknowledgment of source is made. Requests for permission for extended quotation from or reproduction of this manuscript in whole or in part may be granted by the Competent Authority of HBNI when in his or her judgment the proposed use of the material is in the interests of scholarship. In all other instances, however, permission must be obtained from the author.

Anuraj V. L

DECLARATION

I, hereby declare that the investigation presented in the thesis has been carried out by me. The work is original and has not been submitted earlier as a whole or in part for a degree / diploma at this or any other Institution / University.

Anuraj V. L

List of Publications arising from the thesis

Journal

1. "Stability characteristics of the 500 MW Indian PFBR", Anuraj V. L., G. S. Srinivasan, and K. Devan, *Nuclear Technology and Radiation Protection*, **2015**, *Vol 30-2*, pp 113-123. (DOI: 10.2298/NTRP1502113A)

2. "Stability characteristics of metal fueled fast reactor cores", Anuraj V. L., A. Riyas, G. S. Srinivasan, K. Devan and Abhitab Bachchan, *Nuclear Engineering and Design*, **2018**, *Vol. 340*, pp 318-324. (DOI: 10.1016/j.nucengdes.2018.10.005)

3. "Safety aspects of medium sized LMFBR core for reactivity oscillations due to seismic event", Anuraj V. L., G. S. Srinivasan, and K. Devan, *Nuclear Engineering and Design*, **2019**, *Vol. 351*, pp 143-148. (DOI: 10.1016/j.nucengdes.2019.05.033)

Conferences

1. "Dynamic power coefficient of reactivity calculations and stability analysis with perturbation worths based on ABBN 93 cross section set", Anuraj V. L. and G. S. Srinivasan, *National Symposium on Radiation Physics*, **2012**.

2. "Validation of computer code PREDIS against PHENIX end of life natural convection test", Anuraj V. L., Abhitab Bachchan, T. Sathiyasheela, G. S. Srinivasan, K. Devan and P. Chellapandi, *Advances in Reactor Physics*, **2013**.

3. "Stability characteristics of a medium sized LMFBR core", Anuraj V. L., G. S. Srinivasan, A. John Arul, K. Devan and P. Chellapandi, *Advances in Reactor Physics*, **2013**.

Anuraj V. L

To my parents...

ACKNOWLEDGEMENTS

I would like to express my sincere gratitude to my advisor Dr. K. Devan for the continuous support of my Ph.D study and related research, and also for his patience, motivation, and immense knowledge. His guidance helped me in all the time of research and writing of this thesis. I could not have imagined having a better advisor and mentor for my Ph.D study.

Sincere gratitude to my forever interested, encouraging and always enthusiastic Technical advisor Dr. G. S. Srinivasan: he was always keen to help me to progress during the entire period of my Ph. D.

I would like to thank the rest of my thesis committee: Dr. K. Velusamy (chairman), Dr. G. Raghavan, and Dr. M. T. Jose, for their insightful comments and encouragement.

A special thanks to Shri. S. Raghupathy (Director- Reactor Design and Technology Group) and Dr. R. Rajaraman (Dean - Physical sciences), for their support and encouragement

I greatly appreciate the support received through the collaborative work with Dr. A. John Arul, Dr. A. Riyas, Smt. T. Sathiyasheela, and Shri. Abhitab Bachchan, on topics varying from nonlinear stability to eigen value separation.

Sincere thanks are to Dr. P. Mohanakrishnan who introduced me to the topic of fast reactor stability. Many thanks are also to Dr. Om Pal Singh and Shri. S. Ponpandi (late) who initiated the stability studies at IGCAR

I want to thank all my teachers who have taught me in the school and college for their valuable training and guidance while pursuing science.

I gratefully acknowledge the Department of Atomic Energy of India and Homi Bhabha National Institute for providing the opportunity to do this study.

I would also like to say a heartfelt thank you to my mother, Smt. B. Leela, and father Shri. K. Vijayan for always believing in me and encouraging me to follow my dreams. I am grateful to my wife Smt. Geethu Krishnan, who provided me moral and emotional support in my life and patiently taken care of the family while I was busy with my thesis. My thanks are also to my brothers, Akhil Raj, Sajeev Kumar, Hareesh and my twin sister Anjulekshmi who were always keen to know what I was doing and how I was proceeding.

My dear friends Ranjit Jovin Cyriac, Dr. P. Abdul Nishad, P. T. Rakesh, Saju T. Abraham, A. D. Arun, R. Sukanya and many others whose motivation and encouragement helped me to complete the thesis. I would also extend my sincere thanks to my friends in Kerala.

Anuraj V. L.

Contents

List of Figures

List of Tables

Chapter 1

Introduction

1.1 Concept of stability

Stability of a system is the property by which it returns to its equilibrium state from a perturbed state. There are many notions of stability and one such remark was given by Clerk Maxwell, in one of his lectures (1873) as [1]

> *"An infinitely small variation of the present state will alter only by a small quantity the state at some future time, the condition of the system, whether at rest or in motion, is said to be stable; but when an infinitely small variation in the present state may bring about a finite difference in the state of the system in a finite time, the condition of the system is said to be unstable.....*
> *It is manifested that the existence of unstable conditions renders impossible the prediction of future events, if our knowledge of the present state is only approximate, and not accurate."*

The governing equations of most dynamical systems are nonlinear in nature and no general method is available for finding their solution. However, many methods do exist to assess the stability of these systems and the linear stability analysis is the simplest and reasonably accurate. The nonlinear equations are linearized around the stable equilibrium point for performing this analysis. In general, the linear stability analysis holds good for a nonlinear system, if the perturbation is very small.

Methods of nonlinear and linear stability analyses are briefly discussed in the following sections.

1.1.1 *Nonlinear stability*

A global stability analysis in a nonlinear system has the capability to provide necessary conditions for its stability. In general, three broad approaches are followed. They are:

(i) Time domain analysis using a non-linear model, that follows the transients for various perturbations at different operating conditions.

(ii) Lyapunov's direct method.

(iii) Bifurcation theory based methods that effectively examine the solution space to arrive at information about its stability or lack of it.

Time domain analysis: A simple way of doing stability analysis is to solve the governing dynamic equations of the system in the time domain, either analytically or numerically, and find out the system response to various perturbations [2]. A large number of repeated analysis with all possible types of perturbations can show light on the stability characteristics of the system. The differential equations governing the system is to be integrated in time and the variation of output parameter with time can be observed for boundedness.

The direct method of Lyapunov: The direct method of Lyapunov is a generalization of the concept of energy in the field of theoretical mechanics[3]. The method is to identify a positive definite function of the state space variables satisfying certain conditions. If the total time derivative of the chosen function is zero or negative, the positive definite function is a Lyapunov function and the system is said to be stable. If the time derivative is negative definite (vanishing only when all its arguments are zero), the motion is asymptotically stable. The major difficulty of this approach is to find a

suitable Lyapunov function. There is no general method that exists for finding this function.

Bifurcation analysis: When some parameter is varied, If the qualitative nature of solutions of a nonlinear system changes, it is called as bifurcation. A bifurcation diagram can demonstrate the changes in the nature of solution; the horizontal axis gives the value of the parameter which is varied and the vertical axis gives the variable as a measure of solutions. The multiplicity of solutions and the emergence of instability can be assessed by this method [4].

1.1.2 *Linear stability*

In the linear stability analysis, the dynamical equations representing the system is linearized about the equilibrium point and the stability of the system is assessed. The frequency response and the root locus methods are the most classical methods of linear stability analysis.

The transfer function of a linear, time-invariant, differential equation system is defined as the ratio of the Laplace transform of the output (response function) to the Laplace transform of the input (driving function) under the assumption that all initial conditions are zero [5]. The transfer function is also defined as Laplace transform of the impulse response function. For better understanding, the system under study is represented as block diagrams, which are the pictorial representations of various functions performed by the system components. Each block actually represents the mathematical operation on the input signal which produces the output signal. Figure 1.1 (a) and (b) are the block diagrams representing the feedback loop in a linear system in time and frequency domains. The forward loop transfer function is represented as $Z(s)$ and the feedback transfer function is represented as $K(s)$. Time varying input signal is given as $r(t)$ and the output is $c(t)$. The difference between input and feedback

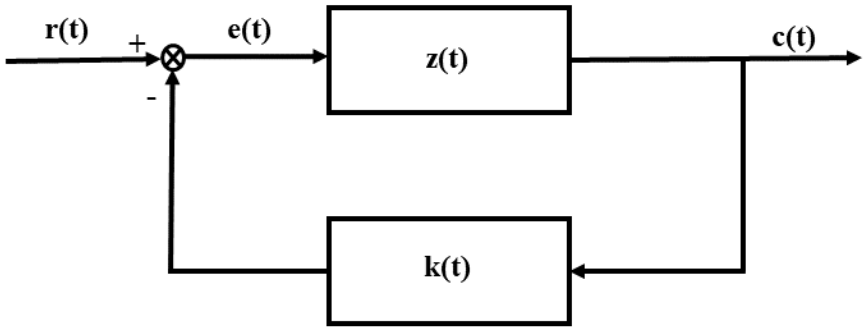

(a) Time domain

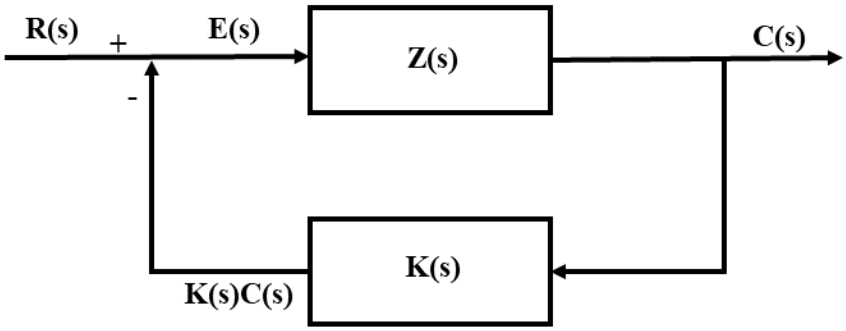

(b) Frequency domain

FIGURE 1.1: Block diagrams for a linear system with feedback.

is represented as error signal $e(t)$. $R(s), C(s)$ and $E(s)$ are the Laplace transforms of $r(t), c(t)$ and $e(t)$ respectively. The parameter $Z(s)$ is defined as $Z(s) = \dfrac{C(s)}{E(s)}$.

From Figure 1.1, we have

$$C(s) = Z(s)E(s) \tag{1.1}$$

and

$$E(s) = R(s) - K(s)C(s) \tag{1.2}$$

From Eqs. 1.1 and 1.2, we get,

$$C(s) = Z(s)R(s) - Z(s)K(s)C(s).$$

i.e., $$C(s)\left[1 + Z(s)K(s)\right] = Z(s)R(s)$$

The overall closed loop transfer function can be written as

$$H(s) = \frac{C(s)}{R(s)} = \frac{Z(s)}{[1 + Z(s)K(s)]}. \tag{1.3}$$

The product $Z(s)K(s)$ is usually called as open loop transfer function. The transient response of the system is defined by the poles of $H(s)$, which are the roots of the characteristics equation,

$$1 + Z(s)K(s) = 0. \tag{1.4}$$

If s_j's are the roots of the characteristic Eq. (1.4), the transient response of the system can be written as a linear combination of terms, $exp(s_j t)$. Linear stability of a system is assured if all the roots s_j have negative real part, that is all the roots of the characteristic equation are in the left half of s-plane. There are many methods to check whether the roots of the characteristic equation have any positive real part or not. The Root Locus method, Routh criterion and Nyquist criteria are the important methods.

The Routh-Hurwitz criteria: A method to identify the sign of the roots of the characteristic polynomial was developed by Routh and a detailed formulation was made later by Hurwitz. It is known as Routh- Hurwitz criteria or simply Routh criteria. In this method, an arrangement of numbers, named as Rouths array, is made from the coefficients of the characteristic polynomial. The condition for all the roots of the characteristic equation to be in the left half plane is that all entries in the first column (the Routh numbers) have the same sign. Using this method, it is able to predict whether the roots of the characteristics equation are in the left half or the right half of the s-plane or on the imaginary axis. The disadvantage of this method is that the nature of the system or the margin to instability cannot be determined.

Root Locus method: The root locus method is developed by Walter R. Evans [6]. In this method, the open loop transfer function is used to assess the stability of the closed loop system. The motion of roots of the characteristic equation in the s-plane is

investigated when the system gain is varied. Instability arises when the roots crosses the imaginary axis and enters the right half plane. By this method, we can find out range of gain in which the system is stable.

The Nyquist criteria: Harry Nyquist proposed a simple method [7] for determining the closed loop stability by studying the open-loop response to steady-state sinusoidal inputs. This is the most popular and effective method in linear stability analysis using transfer functions. If the real versus imaginary plot of open loop transfer function does not encircle the $(-1, i0)$ point, the system is said to be stable. The Nyquist criteria gives a measure of margin to instability in terms of gain and phase margins. Nyquist criteria is used in the present thesis for the stability assessment. More details about this criteria is discussed in Chapter 2.

In this thesis work, a detailed study of core stability is done in sodium cooled pool-type fast breeder reactors having different reactor powers, fuel compositions and sizes. So, before discussing them, a brief introduction about nuclear reactors and their important characteristics are outlined.

1.2 Basics of nuclear reactors

The discovery of nuclear fission in 1938 provided an alternate option of energy source much cleaner than the fossil fuel, which is depleting at an alarming rate. Hence, nuclear reactors are designed and built worldwide for energy production. Its design involves ensuring controlled fission chain reaction, and the removal of nuclear fission energy from the core and electricity generation using the conventional steam water system.

Safe and secure operation of reactors is of paramount importance in the nuclear industry. Many inherent and passive safety concepts are implemented in the design of current generation nuclear reactors for ensuring their safe operation. The physics of nuclear reactors depend significantly on core neutronics parameters such as energy

spectra of prompt and delayed neutrons, neutron life time, yield of delayed neutrons, power density, temperature and power coefficients of reactivities and other reactivity feedback coefficients. For a particular reactor design, these parameters can be optimised by proper selection of fuel, coolant and structural materials.

1.2.1 *Reactivity and its units*

In a reactor core, the neutrons are produced from nuclear fission reactions in fissionable nuclides. Each fission in U^{235} produces on an average 2.5 neutrons and about 3 neutrons from Pu^{239}. They continue to undergo fission in other nuclides in a controlled fashion in a nuclear reactor. The ratio of number of neutrons produced in one generation to that in the previous generation is called effective multiplication factor, k. It is represented as,

$$k = \frac{N_i}{N_{i-1}} \tag{1.5}$$

where N_i and N_{i-1} are the number of neutrons in i^{th} and $(i-1)^{th}$ generation respectively. It takes into account all loses of neutrons between each generation such as parasitic absorption in other materials and leakage from the core. The value of it measures the rate of change of neutron population (or power) in a nuclear reactor. If $k = 1$, the number of neutrons in any two consecutive fission generations will be the same, the reactor is said to be critical. The time dependence of neutron population arises when k is not equal to one. If $k < 1$, the total number of neutrons decreases after each generation and the reactor is said to be subcritical. If $k > 1$, the reactor is said to be supercritical, in which the neutron population increases continuously after each successive generation. A parameter, denoted by reactivity ρ, is often used to represent the fractional change of effective multiplication factor k as

$$\rho = \frac{k-1}{k} \tag{1.6}$$

Since it is a ratio, the reactivity is a dimensionless number. Nevertheless, there are certain terminologies in expressing it, which are often taken as its units. They are:

a)	Percent milli	(pcm)	$10^{-5}\frac{\Delta k}{k}$
b)	Percent	(cent)	$10^{-2}\frac{\Delta k}{k}$
c)	Milli-k	(millik)	$10^{-3}\frac{\Delta k}{k}$
d)	Dollar	($)	β (delayed neutron fraction)

1.2.2 *Prompt and delayed neutrons*

A nuclear fission is accompanied by the production of two fission fragments and 2-3 neutrons within $10^{-17}\ s$ of the fission event. These neutrons which constitute more than 99.3% of neutrons in a reactor are called prompt neutrons. Most of the fission fragments are neutron rich nuclei and they undergo $\beta-$ decay. In few cases, however, the daughter nuclei is produced in one of its excited states with energy greater than the last neutron binding energy, which emits a neutron immediately after it is formed. In effect, these neutrons are emitted with a delay depending upon the half-life of fission fragments (precursor nuclei). These neutrons, which are continuously produced but decreasing with certain half lives, are called delayed neutrons [8]. They are emitted with an energy distribution having an average value of 400 - 500 keV. The delayed neutron precursors are usually lumped into six groups based on half-lives, ranging from a fraction of a second to nearly a minute. The total delayed neutron fraction is denoted by β, which is the sum of their yield in each group, β_j. If the total number of neutrons is n, then the number of delayed neutrons is βn and the number prompt neutrons is $(1-\beta)n$. Though delayed neutrons in the reactor are about 0.7 % of the total, they significantly affect the kinetics of the nuclear reactors; the delay in delayed neutron production slows down the changes in neutron population under transient conditions.

1.2.3 *Reactor kinetics*

The time dependence of neutron population in a reactor core is governed by the neutron diffusion equation. The variation in power or neutron population (n) due to change in multiplication factor can be represented by the point kinetics model, in which the whole reactor is represented as a point and its kinetics behaviour is described by a set of differential equations (also called as point kinetics equation) as

$$\frac{dn\left(t\right)}{dt} = \frac{\rho\left(t\right) - \beta}{\Lambda} + \sum_{i=1}^{6} \lambda_i c_i \tag{1.7}$$

$$\frac{dc_i}{dt} = \frac{\beta_i}{\Lambda} n\left(t\right) - \lambda_i c_i \tag{1.8}$$

where, i, represents the delayed neutron precursor group and parameters λ_i, Λ, c_i and β_i represent the delayed neutron precursor decay constant, prompt neutron life time, precursor concentration and delayed neutron fraction respectively. Analytical solutions to point kinetics equations are extremely difficult because of their stiffness in nature, and numerical methods are often used for solving them.

In a nuclear reactor, different reactivity feedbacks become available due to power change. So the net reactivity ρ is the sum of external and the feedback reactivities which depends on the system temperature. It is to be noted that the power dependence of feedback reactivity makes the point kinetics equations nonlinear.

1.2.4 *Reactivity feedbacks*

The reactor core multiplication factor or reactivity depends on various core characteristics including the system temperature. All reactors are designed with a negative temperature and power coefficients of reactivities, which means that core reactivity decreases with rise in power or temperature. It has contributions from various reactivity components arising from temperature effects on fuel, clad, coolant, moderator and their geometrical arrangements. This property helps for the stable operation

of a nuclear reactor. In thermal reactors, moderator coefficient of reactivity is very important, which is usually negative. The most important prompt acting negative feedback is primarily due to Doppler effect in the neutron capture resonances of fertile nuclides (e.g. U^{238}, Pu^{240} etc.). This feedback acts as one of the important prompt inherent safety characteristics during a power (or temperature) transient. It depends on neutron spectrum which in turn depends on reactor size, type of fuel, coolant and moderator used; thermal reactors have higher Doppler reactivity feedback compared to fast reactors. More details of feedback reactivity in fast reactors are discussed in Chapter 2.

1.2.5 *Classification of nuclear reactors*

Nuclear reactors are broadly classified into thermal and fast reactors based on the energy of neutrons causing fission reaction. As the name indicates, in a thermal reactor, majority of fission reaction takes place with thermal neutrons whereas fast neutrons ($> 100keV$) undergo majority of fission reactions in a fast reactor. Moderators are essential in thermal reactors, but no specific moderators are provided in fast reactors. Thermal reactors are further categorized as Light Water Reactors (LWR) and Pressurized Heavy Water Reactors (PHWR) based on the primary coolant system used for heat removal [9]. The neutron flux spectrum is highly thermalized in thermal reactors which permits to use natural uranium as the fuel in PHWRs or slightly enriched (2-4 %) uranium in LWRs. A unique feature of thermal reactors is that they are designed in a state of most reactive configuration [10]. They have larger core size (lower power density) and hence less coupled neutronically. The most common coolant currently used is the light water; two types of water-cooled reactors are Pressurized Water-cooled Reactors (PWRs) and Boiling Water Reactors (BWRs). In PWRs, coolant is maintained at high pressure in order to avoid coolant boiling at a high temperature while in BWRs the coolant pressure is maintained low to allow steam production within the reactor core [11]. Both these reactors have large pressure vessel to contain the reactor core and

coolant at high pressures. Light water is used as moderator in both BWRs and PWRs. Another class of thermal reactor called as RBMK reactor uses graphite as moderator [12]. In such reactors pressure tubes are used for coolant channels housed inside large graphite stack. In PHWRs, heavy water is used as both coolant and moderator [13]. The lower neutron absorption cross section of D_2O compared to H_2O helps to use natural uranium as the fuel in PHWRs. The liquid metal coolant such as sodium is used in fast reactors due to their high heat transfer properties with low moderating properties. Sodium cooled fast reactors (SFRs) are usually designed in two types such as pool-type and loop-type. Since the present thesis focuses on stability and safety studies in sodium cooled fast reactors, more details of these reactors are given in the following sub-section.

1.2.6 *Characteristics of fast reactors*

The absence of moderators in fast reactors results harder neutron spectrum. But, little moderation do exist mainly by in-elastic scattering collision of neutrons in fuel, structural materials and sodium. The neutron flux spectrum is generally peaked in the energy range of few tens of keV to MeV (Figure 1.2). Such a hard neutron spectrum has an advantage of higher value of η (average number of neutrons produced per neutron absorbed in fuel), and lower parasitic absorption in structural materials and fission products [14]. In effect, more neutrons can be produced in a fast reactor than it consumes. These extra neutrons can be used for converting fertile nuclides to fissile nuclides. Therefore, fast reactors can be designed such a way that it produce more fissile material than it consumes, thus breeding fuel. Hence, they are called 'Fast Breeders'. Further the best utilization of nuclear fuel is found to be possible with a breeder reactor. The η value of Pu^{239} is found to be sufficiently high to give neutrons for sustaining chain reaction and also for breeding. Fuel cycle studies show that with the concept of multiple recycling of refueled fuel, natural uranium utilization up to 60-80% is possible in fast reactors. For higher breeding, radial blanket made of $DDUO_2$ (deeply

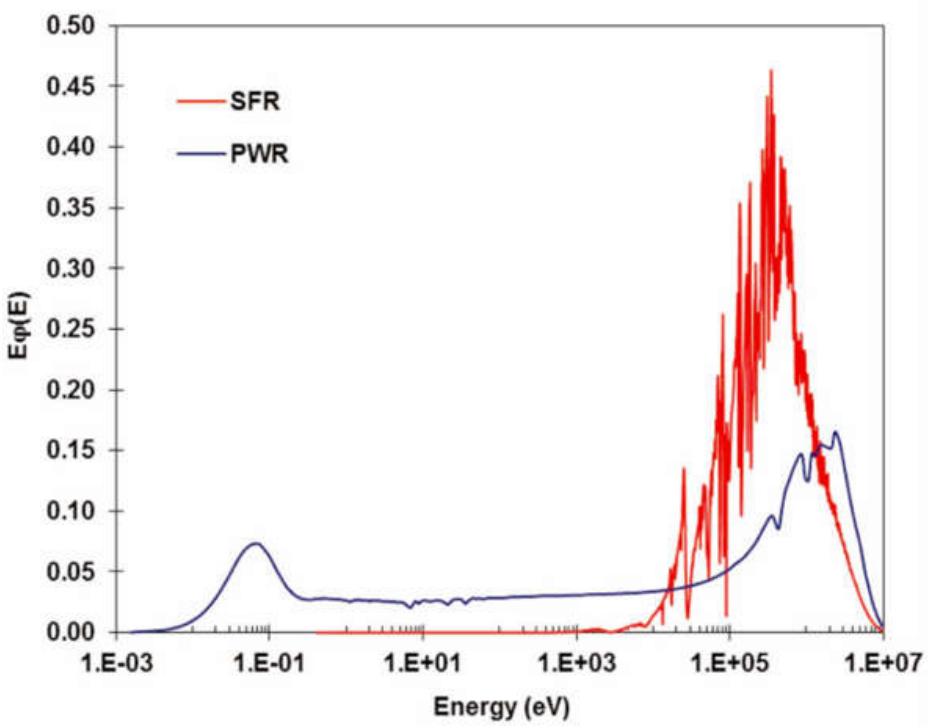

FIGURE 1.2: Comparison of a typical SFR and PWR flux spectra.

depleted UO_2) is provided around the active core, by which leaking neutrons from the core can be used for breeding more fissile fuel. Based on the primary coolant system design, it can be either pool-type or loop-type. In the pool-type design, reactor core is immersed in a pool of primary sodium in the reactor vessel. The primary sodium is circulated through the core by using sodium pumps kept inside the vessel, whereas in the loop type design, heat from the core is removed by circulating primary sodium with the help of sodium pumps kept outside the reactor vessel. The primary sodium circuit removes the nuclear heat generated in the core and transfers to the secondary system through intermediate heat exchangers (IHXs). The secondary system transfers this heat to steam/water system through steam generators. The heat transport systems in a typical pool type SFR is given in Figure 1.3 [15].

The reactor core is the source of heat due to nuclear fission. Schematically, the core consists of central fuel region enveloped by blanket region. This, in turn, is surrounded by neutron reflectors (Figure 1.4).

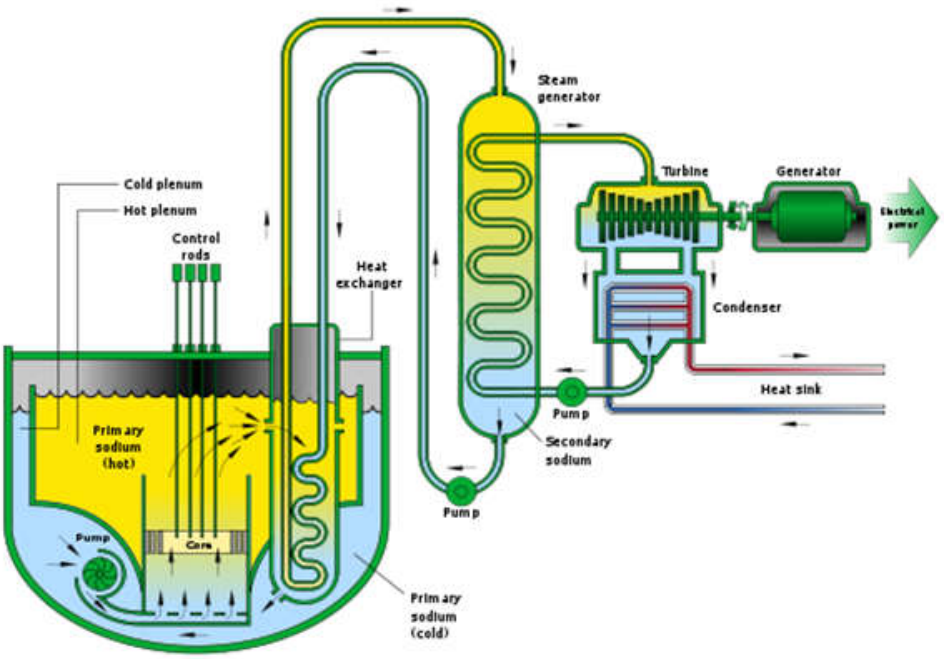

FIGURE 1.3: Typical SFR Heat Transport System (Pool-Type).

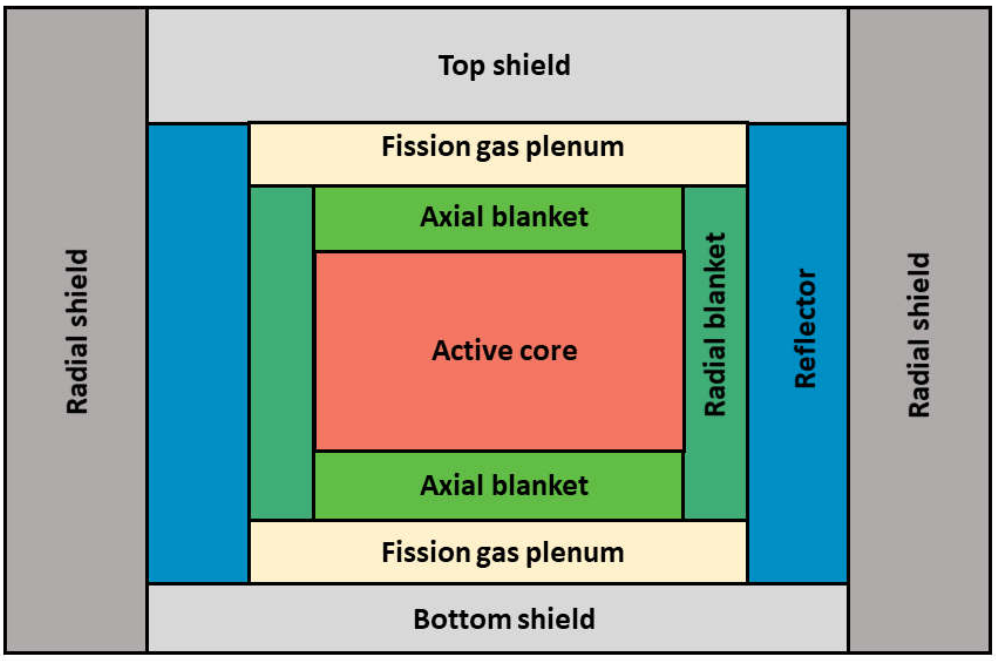

FIGURE 1.4: R-Z view of an SFR core (axial plane through core center).

Important core neutronics characteristics of fast reactors are summarized below:

- Higher capture in fertile nuclides but lower fission in fissile nuclides necessitates fuel enrichment (10 - 30%) in fast reactors.
- The combination of increased fission to capture ratio, and increase in the number of neutron yield by fission (ν), gives higher value of η, which decides the breeding potential of fuels. The minimum condition for breeding is $\eta > 2$.
- In harder neutron energy spectrum, parasitic neutron capture is less and it leads to better neutron economy. In addition, the effect of fission product poisoning is found to be less significant in fast reactors.
- The average neutron mean free path is about 10 - 20 cm in FBRs compared to $\sim$ 2 cm in LWRs. It means the reactor core is tightly-coupled. Further, the heterogeneity effects are relatively less in fast reactors.
- Larger mean free path of fast neutrons lead to increased neutron leakage. These neutrons are used for fissile breeding by using external radial and axial blankets.
- The critical mass of fuel is generally high in fast spectrum. So, the reactor core size is generally made very small with higher power density.
- Fast reactors have lower effective delayed neutron fraction (β_{eff}) and shorter prompt neutron life time. It leads to faster response to external reactivity perturbations.
- Prompt inherent Doppler feedback from U^{238} capture resonances is always negative. The expansion feedbacks (axial and radial) are generally negative. In small SFRs, sodium void reactivity coefficient is negative, whereas in medium and large reactors, sodium void coefficient could be positive and would result in net positive reactivity addition when coolant starts boiling.

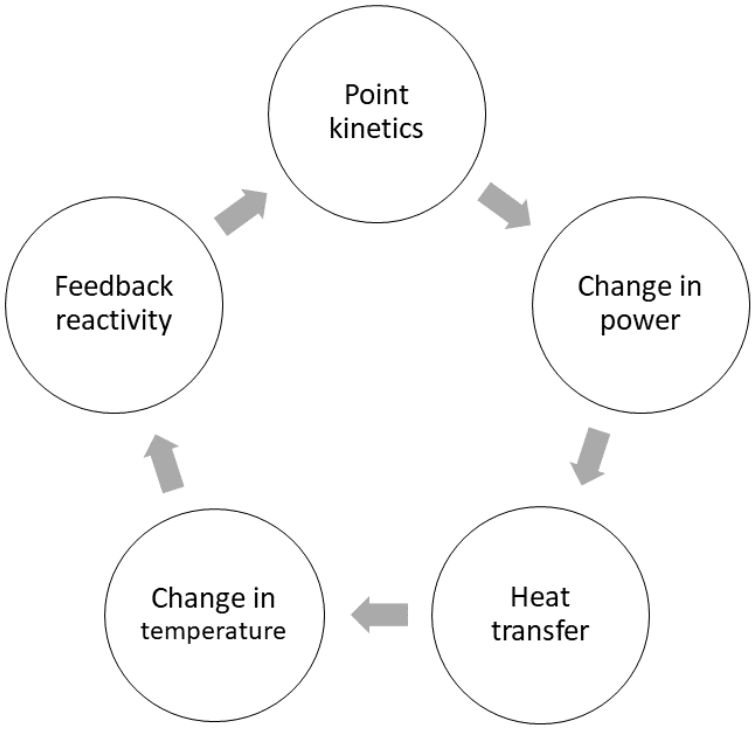

FIGURE 1.5: Representation of reactor dynamics in a fast reactor.

1.3 Fast reactor core as a feedback system

As discussed earlier, point kinetics approximations are usually used to obtain power evolution in a nuclear reactor due to reactivity perturbations. When there is a power change, the system temperatures also change, which alter all reactivity feedbacks. It has the overall effect on the net reactivity as it is the sum of both external and feedback reactivities. It is to be noted that the heat transfer equations are solved for obtaining the fuel, clad and coolant temperatures. This feedback loop in an FBR is represented in Figure 1.5. Further, thermo-mechanical re-adjustments in the core region during operation may introduce some positive reactivity depending on core subassembly support and restraint design. It is to be noted that, bowing of fuel rods also introduces non-linear feedback effects. It is observed that core expansion in a fast reactor leads to decrease in reactivity (negative reactivity feedback) while core compaction results positive reactivity feedback. A description about each feedback mechanisms and its calculation are detailed in section 2.3.2 of Chapter 2.

1.4 A short survey of stability analysis in nuclear reactors

Stability issues are more prominent in thermal reactors compared to fast reactors. Few experiments performed in nuclear reactors were limited only to special conditions because of the dangers involved in doing such experiments. However, many theoretical studies were done to assess the dynamic and safety characteristics in nuclear reactors. The theory of linear stability analysis for reactor systems having reactivity feedbacks is explained in detail at Ref. [16]. Stability analysis for different reactor systems like Molten salt reactor [17], boiling water reactor [18] advanced heavy water reactor [19] were studied with various methods.

The behavior of BWRs in the nonlinear regime is described in Ref.[20] and it is observed from stability tests that the boiling water reactors are susceptible to reactivity instabilities under low flow conditions. March-Leuba [21] developed a phenomenological model to simulate the qualitative behaviour of BWRs in the nonlinear regime. Limit cycle oscillations were predicted due to interactions between two unstable equilibrium points, once the linear stability threshold is crossed. The feedback from moderator density changes results in limit cycle behaviour in such reactors. The existence of limit cycles in BWR was experimentally verified by Turso [22] using a hybrid reactor simulation testing arrangement in the TRIGA reactor at Pennsylvania State University, USA. Stability of BWR is investigated with sub-diffusive effects and thermal-hydraulics feedback, using frequency domain method by Vyavahare in [23].

Linear stability for nuclear reactor dynamics is investigated using root locus, bode plot and unit step response for fractional-space neutron point kinetics models. Results of such studies were compared to classical point kinetics equations by Vyawahare in Ref. [24].

For PWR, a simple model was reported [25] to study Xe spatial oscillations in load following conditions. In this study, one group neutron diffusion equation with temperature and Xenon feedbacks, Iodine-Xenon dynamics equations and the energy balance relation for the core represented the state equations. Similar methodology was

used to study the problem of Xe oscillations in the axial direction under load following conditions by Ukai [26]. They have found that steady state distribution of neutron flux shape did not get altered with power change. Li discusses the use of T-S fuzzy model and Lyapunov theory for the nonlinear stability analysis of PWR in [27].

A linear stability analysis on all Gen-IV reactor concepts using root locus method was reported recently in Ref. [28] by considering a zero dimensional model. Results showed that all the systems are stable with large margins.

In 1970, Yu [29] investigated the stability of a fast reactor by assuming a positive Doppler feedback. The study was essentially carried out to check whether the negative fuel expansion feedback acts fast enough to compensate the positive feedback from Doppler.

Stability characteristics of metal cooled fast reactor along with the primary heat transport system is discussed in Ref [30]. Mathematical stability behavior of general point reactor model is analyzed using comparison theorems for nonlinear voltera integral equations in Ref. [31]. Stability domain estimation for nonlinear point kinetics model with linear temperature and power coefficient is reported in Ref. [32]. Nonlinear stability topological method and Liapunov second method is applied to point kinetics model with reactivity feedbacks [33], [34]. An analytical model for fast reactor stability analysis and comparison of results with EBR-1 experiment is discussed in Ref. [35]. A review of reactivity feedback, stability and related operating experience in fast power reactors from EBR-I to BN 800 is available in [36]

The EBR experience The Experimental Breeder Reactor (EBR-I & II) are metal fueled fast breeder reactors operated at Argonne National Laboratory. The stability analysis studies on EBR-I reactor and modifications made in the core to improve the stability characteristics shows light on the importance of the problem [37], [38]. A partial meltdown accident occurred in EBR-I during a transient test by stopping the main coolant flow. A series of tests were conducted to measure the transfer function under various power and flow conditions. Possibility of resonant oscillations were

demonstrated at certain frequencies. Detailed analysis revealed that a prompt positive power coefficient of reactivity existed even if the delayed coefficient is negative. The unstable behaviour observed in EBR-I Mark -II core (a small, highly enriched metal fueled core) was studied in detail and was attributed to, negligible prompt negative feedback contribution from Doppler effect, a prompt positive feedback due to bowing of fuel rods and delayed negative feedback involving convective heat transfer to structural materials. The Mark-III core of EBR-I had modifications to address the source of reactivity feedbacks causing oscillations and the stability is ensured. From the Mark III (EBR-I) stability studies it is concluded that there is nothing intrinsic in the mechanical or neutronic features of a fast reactor which would cause it to be unstable. It is demonstrated that the stability can be ensured by careful planning and proper mechanical design.

1.5 Objectives of the thesis

The literature survey showed that plenty of studies have been carried out in the domain of stability for thermal reactors. The instability issues are significant in BWRs due to coolant boiling and Xe oscillations. Both these issues are absent in fast reactors. The instability observed in EBR-I and the results of few experiments carried out as part of its investigation are available in the literature. However, limited studies have been reported in the area of nonlinear stability analysis in fast power reactor systems. The studies reported have used very simplified models with point kinetics approximation and lumped reactivity feedback coefficients. A multichannel approach for heat transfer with spatial dependent temperature distribution and corresponding reactivity feedbacks is found to be lacking in the area of fast reactor stability analysis. Further, computational tools required to perform such a study are very limited but they are not licensed to all users.

Fast reactors are not in the most reactive configuration and hence the potential for core disruptive accidents is a major concern regarding the safety of any fast reactor.

Efforts are all made to have a design which is inherently safe against catastrophic accidents. One of the promising option is the use of metal fuel for Fast Breeder Reactors (FBRs). Recent studies demonstrated that metal FBRs have higher inherent safety characteristics [39]. At the same time the eutectic alloy formation in metal fuel pins and the limited operating experience with such fuel made the European Fast Reactor project to continue with oxide fuel, and the studies showed the advantages in safety by using metal fuel is marginal in comparison to oxide fuel type [40]. The lower Doppler feedbacks and higher positive sodium void reactivity compared to oxide cores made metal fueled FBRs unattractive. But studies conducted on the transient response to various initiating events have demonstrated the safety characteristics of metal FBRs. There are research articles preferring a metal fueled FBR over an oxide fueled one [39], [41]. Another study comparing the performance fo metal and oxide fuels during various accident situations is reported by Cahalan [42], in which it is shown that the advantage of metal fuel core is limited to certain accidents only and more detailed analysis are required to have a complete picture.

The better breeding potential and improved safety characteristics of metal FBRs have favored them for next generation fast reactors. With respect to MOX fuels, Doppler feedback is relatively lower in metal FBRs. The physics design of future metal FBR cores for power generation requires the characterisation of their core stability, which in turn has large dependence on neutron spectrum, fuel composition, core size and power etc. In this context, a detailed study is necessary to investigate the above aspects in the various fast reactor systems.

A nuclear reactor is a typical example of a non-linear system and the degree of non-linearity depends on its system parameters. Since fast reactor cores are tightly coupled, possibility of spatial oscillations of neutron flux is relatively less in a medium sized reactor. But the degree of neutronics coupling reduces as the core size increases. The eigen value separation between fundamental and next higher mode measures the coupling nature of the core. Though various methods of non-linear stability analysis such as bifurcation analysis and Liapunov function approach exist, a detailed study

is not performed so far towards investigating a safe operating domain in fast power reactors.

The reactor response to oscillating reactivity perturbations under a seismic event is of interest, as it may trigger instability in the reactor core. It is very challenging to simulate the reactivity fluctuations in the core by taking the exact core vibration pattern. The power and temperature oscillations under an earthquake is to be studied to ensure the stable nature of operation of the core under severe reactivity oscillations.

1.6 Works performed and organization of the thesis

The present thesis focuses mainly to address various objectives and the associated challenges involved to perform stability analysis in fast reactors. Following important works are performed to address these objectives:

(a) ***Development of a new computer code, DYNRCO.***

An indigenous computational tool, DYNRCO, is developed for the first time to perform stability analysis in fast reactor cores using point kinetics approximation for neutron kinetics and multichannel approach for heat transfer and feedback reactivity calculations. To perform the simulations in the frequency domain, a Laplace transform has been performed on the linearized dynamic equations. A multichannel 2-D model for heat transfer and feedback reactivity effects are used in it. This code has been used extensively for studying the stability characteristics of both MOX and metal FBR cores. The theory and methodology used in DYNRCO are explained in Chapter 2.

(b) ***Validation of computer code PREDIS against Phenix EOL test***

The transient analysis code PREDIS, which is used for the time domain analysis is validated with Phenix End of Life test. In this test, the inlet temperature of the core increases with time due to reduced heat removal from secondary. Time evolution of reactor power and reactivity is simulated using PREDIS code and compared with the experimental results.

(c) ***Linear stability analysis in oxide and metal FBRs***

The code DYNRCO has been applied to quantify the stability characteristics of three pool-type SFR cores having different core sizes and neutron spectrum. The reactors considered include a 500 MWe MOX core (PFBR)[43] and 3 metal FBRs having 120, 500 and 1000 MWe power levels. The stability margins in these reactors are quantified for the first time. This study shows that the stability margin in a metal FBR is greater than that of MOX core. Results of these studies are given in Chapter 3.

(d) ***Nonlinear stability analysis***

Nonlinear stability analysis has been carried out for a typical medium sized oxide SFR core (PFBR) using bifurcation method and its characteristics are compared with that of a thermal reactor in Chapter 4. The nonlinear stability assessment is also carried out using transient analysis code PREDIS by studying the core response to various reactivity perturbations. The study has shown that under these perturbations the reactor power is not diverging with time, indicating the stale nature of the core.

(e) ***Investigations of core stability and design safety limits of core components in a medium sized oxide SFR core under a seismic event***

Stability in PFBR core under seismic conditions are investigated in the time domain and the results are discussed in Chapter 5. The methodology has been developed to simulate core reactivity fluctuation under a seismic event by considering the relative motion between control rods and the core. The stability characteristics and the safety of the core under such reactivity oscillations are studied. The horizontal motion of sub-assemblies and vertical motion of the core are simulated to estimate the net reactivity changes during a seismic event. Transient analysis code PREDIS is used to study the reactor power and temperature evolution. This study helped to ascertain PFBR core stability under

seismic conditions and has shown that there is no diverging oscillations and the system temperatures are within design safe limits.

Finally, the summary, conclusions and the scope for future works are given in Chapter 6.

Chapter 3

Linear Stability Analysis of MOX and Metal Fueled FBRs

3.1 Introduction

The development of computer code DYNRCO for performing linear stability analysis in SFRs is discussed in chapter 2. It is applied to a medium sized MOX fueled fast reactor core and the results are discussed in this chapter. The 500 MWe PFBR is chosen for the analysis. The dynamic power coefficient and associated time constant are estimated and the stability of the core is demonstrated using Nyquist criteria. In the second part of this chapter, the analysis is repeated for metal fueled cores of three different sizes and the results are compared.

Metal fuel is used in many reactors during initial days of technology development. Low melting point and high void swelling [57] in metal fuel forced to look for alternate ceramic fuel choices. Oxide fuel become the most popular choice while carbide and nitride are considered as advanced fuel types for the future. Even though carbide and nitride have many advantages, they are yet to be proven commercially. The ULOF (Unprotected Loss of Flow) transient behavior of the three metal cores are compared in an earlier study and it was found that the smaller metal cores are safer than larger cores [58], [59]. Another study by Harish et.al [60] compares oxide and metal core response under an unprotected loss of flow event. The possibility of higher breeding and enhanced feedbacks in a metal fueled fast reactor is investigated by Merk in [61].

The stability characteristics of a medium sized MOX fueled FBR is studied first, the initial core configuration of PFBR (175 FSA) is chosen for the study. In later part the equilibrium core configuration of PFBR (181 FSA)is analyzed along with the metal cores for comparison. The results of these studies are discussed in this chapter.

3.2 Stability analysis of a medium sized FBR MOX core

The computer code DYNRCO is used to establish stable behavior of the 500 MWe MOX fueled PFBR initial core with 175 FSAs. The reactor core is divided into 12 radial and 14 axial meshes. The important physical data used in the calculations are given in Table 3.1 .

Stability of the reactor has been studied with respect to perturbations in reactivity of the system. A necessary but not sufficient condition for stability is that $K_p(0) < 0$, *i.e.* the static power coefficient of the reactor must be negative. The static power coefficient of reactivity is found to be $-0.62pcm/MWt$. Thus the necessary condition of stability is satisfied. The dynamic power coefficient is estimated as a function of frequency, from which the open loop transfer function and Nyquist plot is generated.

The magnitude of $K_p(i\omega)$ is given in Figure 3.1 as the dotted line. These values are fitted with Eq. 2.27, to determine the time constant of the feedback. The solid line in Figure 3.1 gives the fitting of this analytical expression 2.27 with feedback transfer function, by the method of least squares. The time constant of dynamic power coefficient of reactivity for the core is 2.9 s. The magnitude of dynamic power coefficient at zero frequency corresponds to static power coefficient. The value as per Figure 3.1 is $0.6208pcm/MWt$. The important estimate in the present study is the time constant. Figure 3.2 depicts the variation of phase with frequency in reactivity feedback. It can be seen that, for high frequencies, reactivity lags power but for low frequencies, lag between reactivity and power is zero. In other words as the feedback approaches saturation value, the power and reactivity are in phase.

TABLE 3.1: Kinetics and thermo physical parameters- PFBR initial core.

Group index		1	2	3	4	5	6
Decay constant	λ_i	0.0129	0.0312	0.1344	0.3448	1.3927	3.755
Delayed neutron fraction	β_i	8.336	77.618	67.854	130.94	58.974	17.549

Effective delayed neutron fraction, β (pcm) = 361.27

Prompt neutron life time l (s) = 4.72×10^{-7}

Thermal expansion coefficient of fuel (K^{-1}) = 11.2

Thermal expansion coefficient of clad (K^{-1}) = 20

Thermal expansion coefficient of coolant (K^{-1}) = 95

Thermal conductivity of fuel $(Wcm^{-1}K^{-1})$ = 0.022

Thermal conductivity of clad $(Wcm^{-1}K^{-1})$ = 0.21

Thermal conductivity of coolant $(Wcm^{-1}K^{-1})$ = 0.59

Heat transfer coefficient over fuel pellet $(Wcm^{-1}K^{-1})$ = 0.2764

Heat transfer coefficient over gap $(Wcm^{-1}K^{-1})$ = 0.8796

Heat transfer coefficient over clad $(Wcm^{-1}K^{-1})$ = 8.031

Heat transfer coefficient over sodium $(Wcm^{-1}K^{-1})$ = 24.88

Fuel specific heat $(Jg^{-1}K^{-1})$ = 0.325

Steel specific heat $(Jg^{-1}K^{-1})$ = 0.569

Coolant specific heat $(Jg^{-1}K^{-1})$ = 1.268

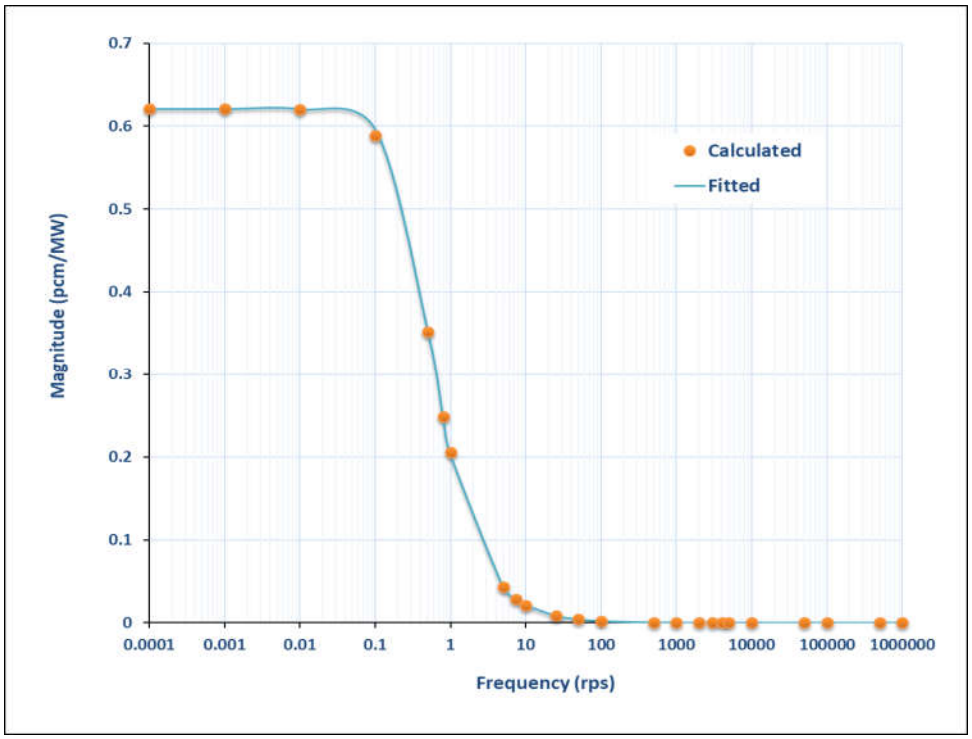

FIGURE 3.1: Magnitude of feedback transfer function: PFBR.

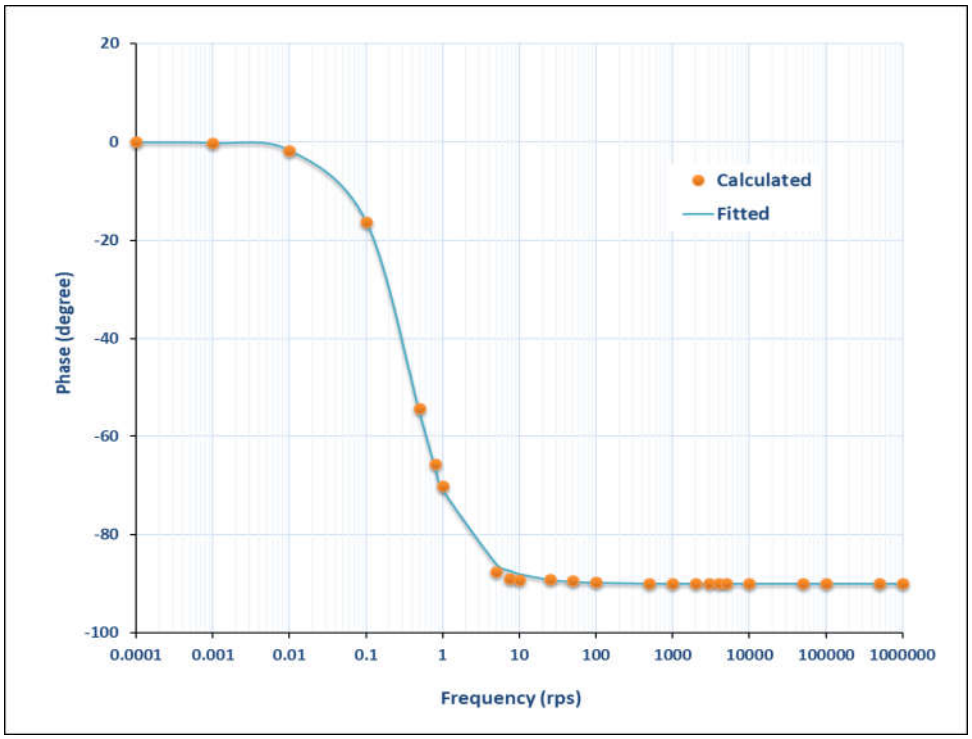

FIGURE 3.2: Phase of feedback transfer function: PFBR.

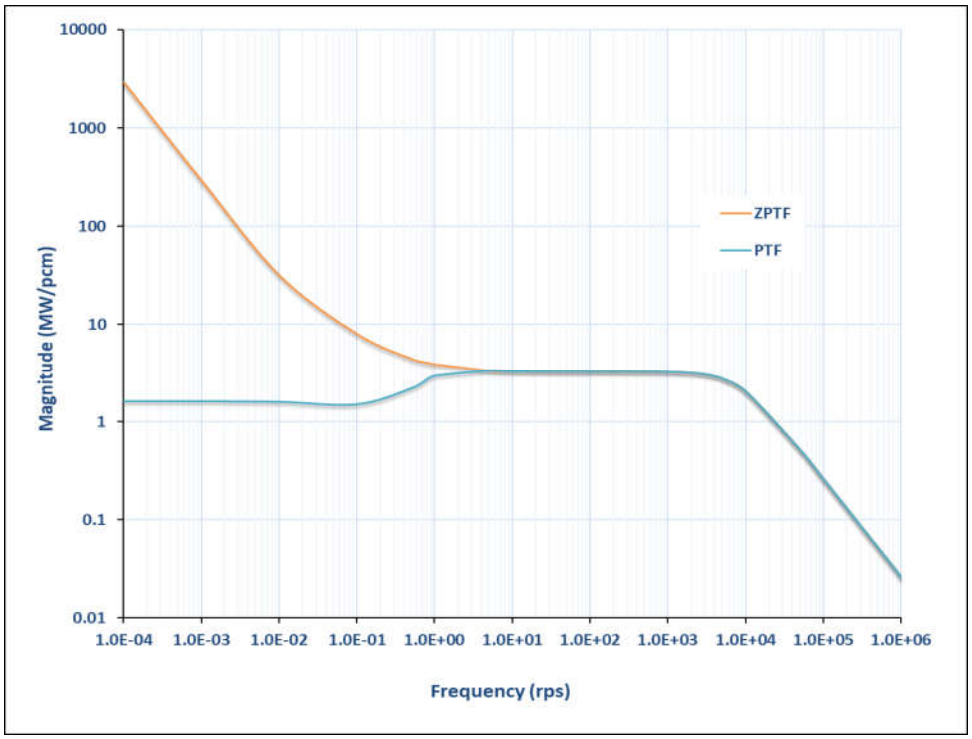

FIGURE 3.3: Magnitude of zero power and power transfer function: PFBR.

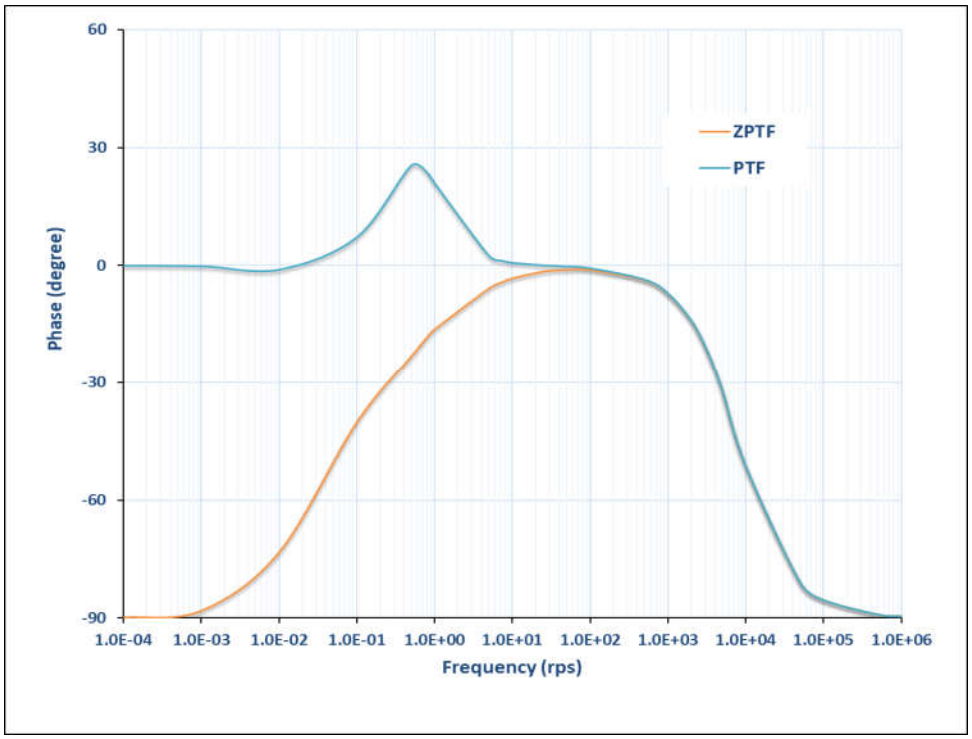

FIGURE 3.4: Phase of zero power and power transfer functions: PFBR.

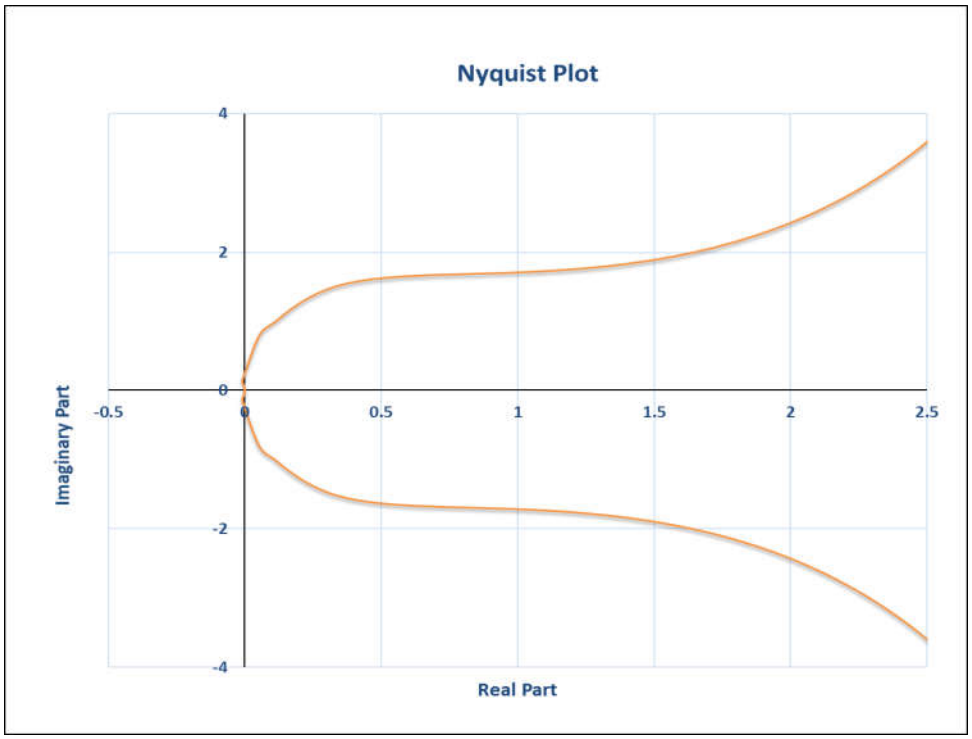

FIGURE 3.5: Nyquist Plot: PFBR.

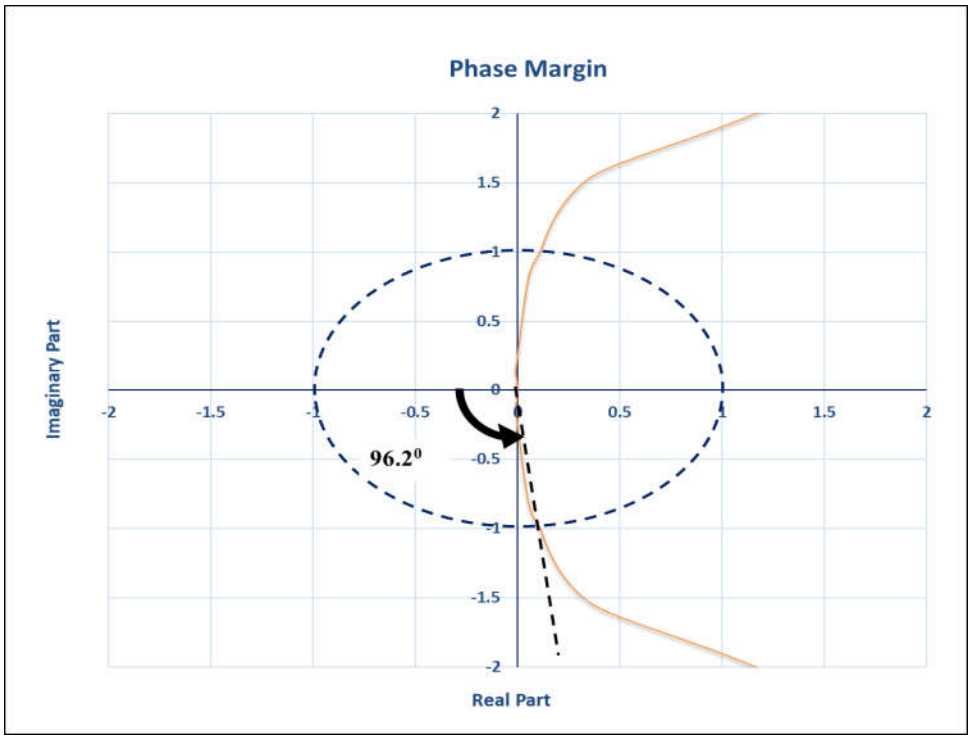

FIGURE 3.6: Phase margin from Nyquist plot: PFBR.

The magnitude and phase of zero power transfer function and power transfer function are plotted in Figure 3.3 and 3.4. No poles or impulse is observed at any frequency of the power frequency response function. It is seen that at low frequencies gain is high for zero power transfer function, indicating absence of feedbacks, and low for power transfer function, suggesting that reactor is safe. The Nyquist plot for PFBR initial core is given in Figure 3.5. It can be seen that the curve is far away from $(-1, i0)$ point and this confirms that the reactor is stable.

Stability margin: The gain margin and phase margin are estimated from the Nyquist diagram as a measure of stability margin. It is found that the gain margin is infinite (the Nyquist plot is not intersecting the negative x-axis, but at origin). The phase margin is calculated to be 96.2^0 as shown in Figure 3.6.

3.3 Stability analysis of metal fueled FBR

Various studies are being conducted to asses the safety characteristics of metal FBRs. In the present study three metal cores of different core size and power rating are considered. Other than the transient response to severe accidents the stability characteristics of the metal FBR against reactivity perturbations is to be studied to have a complete understanding about their performance safety.

The space dependence of power density, temperatures and reactivity feedbacks are accounted by dividing the core into various axial and radial meshes assuming azimuthal symmetry. The material removal worth of each mesh is calculated by a first order perturbation code [62]. The details of the basic theory and the calculation methodology are discussed in Chapter 2. The linear stability analysis is carried out for three metal cores and one MOX fueled core. In addition, the neutronic coupling of the two 500 MWe oxide and metal fueled cores are compared in terms of Eigen Value Separation (EVS). The reactor response to 100 pcm step reactivity insertion is also studied to check for the occurrence of any power oscillations. The description

about each core is given in section 3.3.1. The results of the analysis and the comparative stability characteristics of these cores are discussed in section 3.4.

3.3.1 *Important characteristics of MOX and metal FBRs considered*

Three metal fueled reactors at power ratings of 120MWe, 500MWe and 1000MWe and one Oxide core of 500 MWe power are studied. Metallic ternary alloy of U-Pu-Zr is the fuel chosen for all the three metal cores while MOX fuel is taken for the oxide core. The equilibrium core of PFBR is chosen as the oxide core. Fuel pin radius of 120 MWe and 500 MWe cores are chosen as 6.6mm while that of the 1000 MWe metal core is chosen 8mm. Number of enrichment zones is one for small core, two for medium sized core and three for the large core. The core configurations of metal and MOX cores are given in Figures 3.7 - 3.10, and the details are given in Table 3.2. The kinetics parameters and thermo-physical properties of the four reactors are given in Table 3.3. Delayed neutron parameters for the three metal core are given in Table 3.4 and that of MOX core is given in Table 3.5.

TABLE 3.2: Core design parameters.

	Oxide	Metal		
Parameter	Medium	Small	Medium	Large
Reactor power (electric/thermal)	500/1250	120/320	500/1250	1000/2630
Peak heat rating (W/cm)	450	450	450	500
Cycle length ($days$)	180	180	180	240
Number of core enrichments	2	1	2	3
Number of fuel sub-assembly	85/96	72	85/96	79/96/72
Fuel pin radius (mm)	6.6	6.6	6.6	8
SA pitch (cm)	13.5	13.5	13.5	16.8

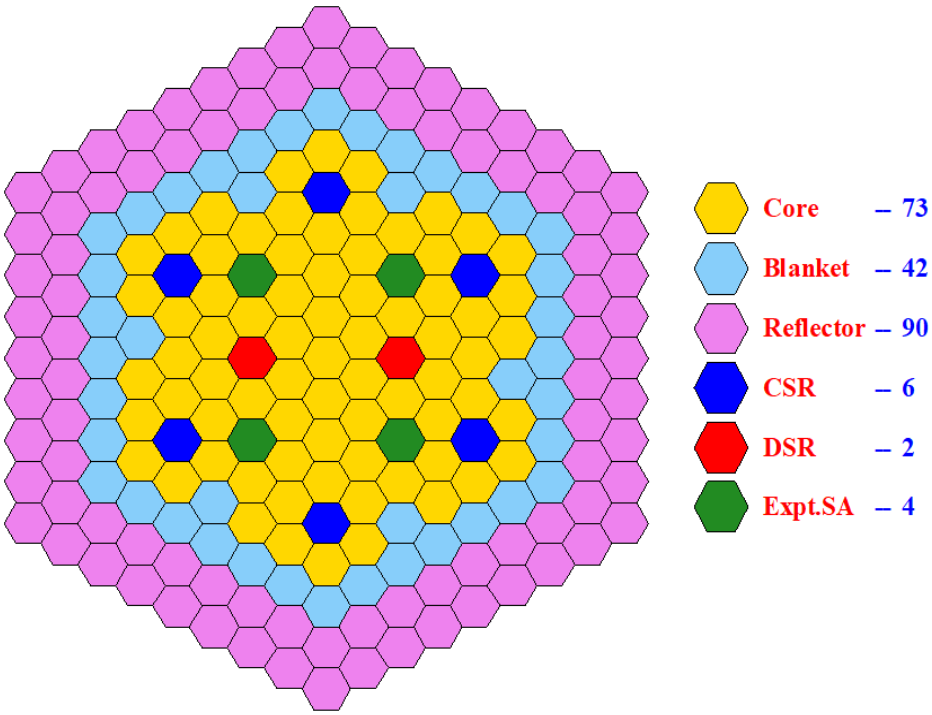

FIGURE 3.7: Core configuration of 120 MWe metal core.

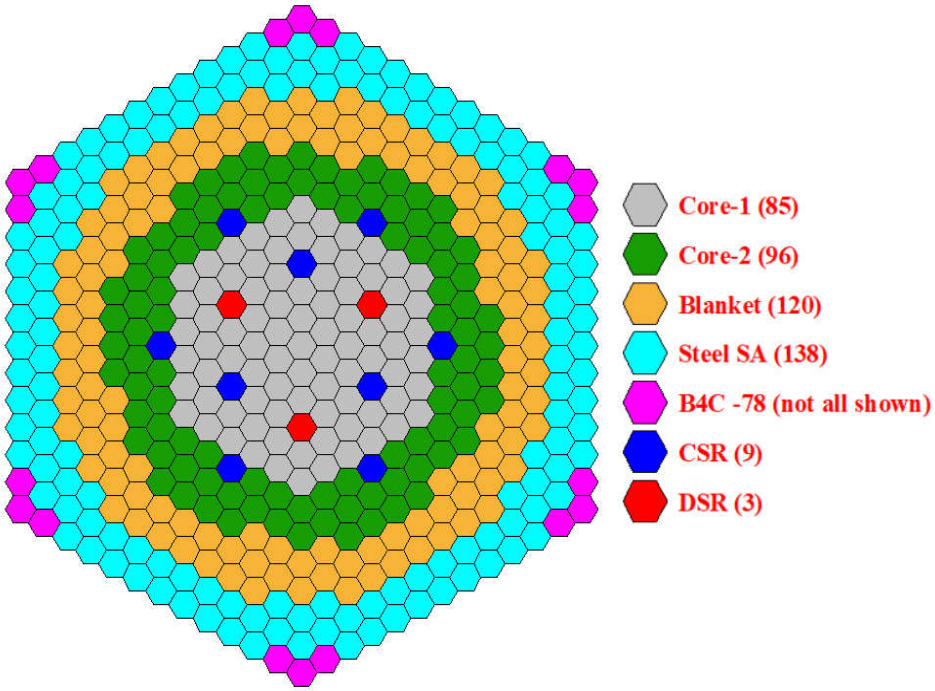

FIGURE 3.8: Core configuration of 500 MWe metal core.

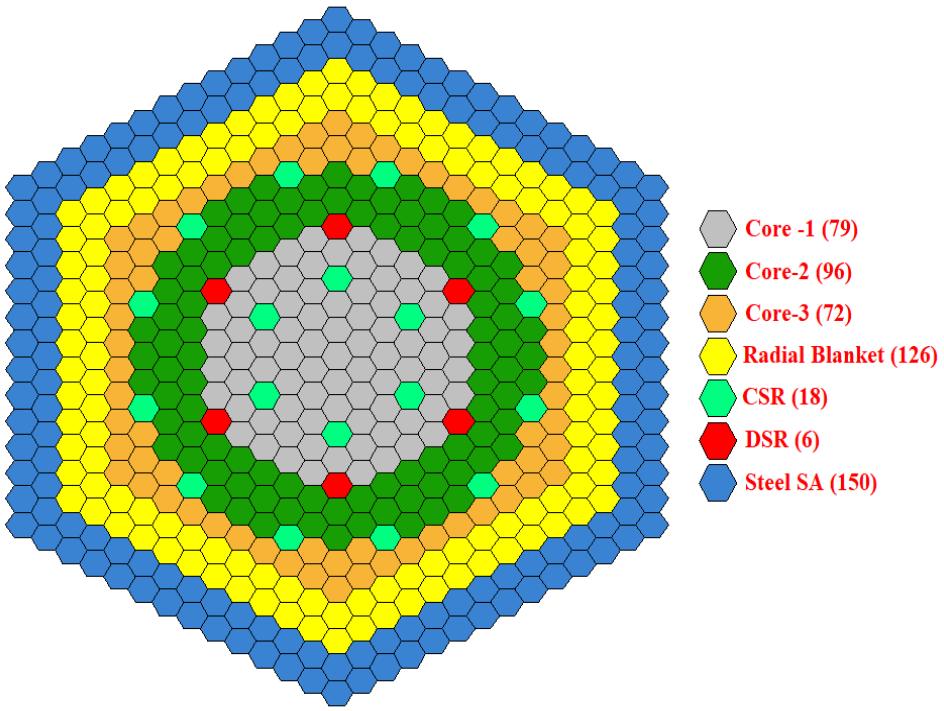

FIGURE 3.9: Core configuration of 1000 MWe metal core.

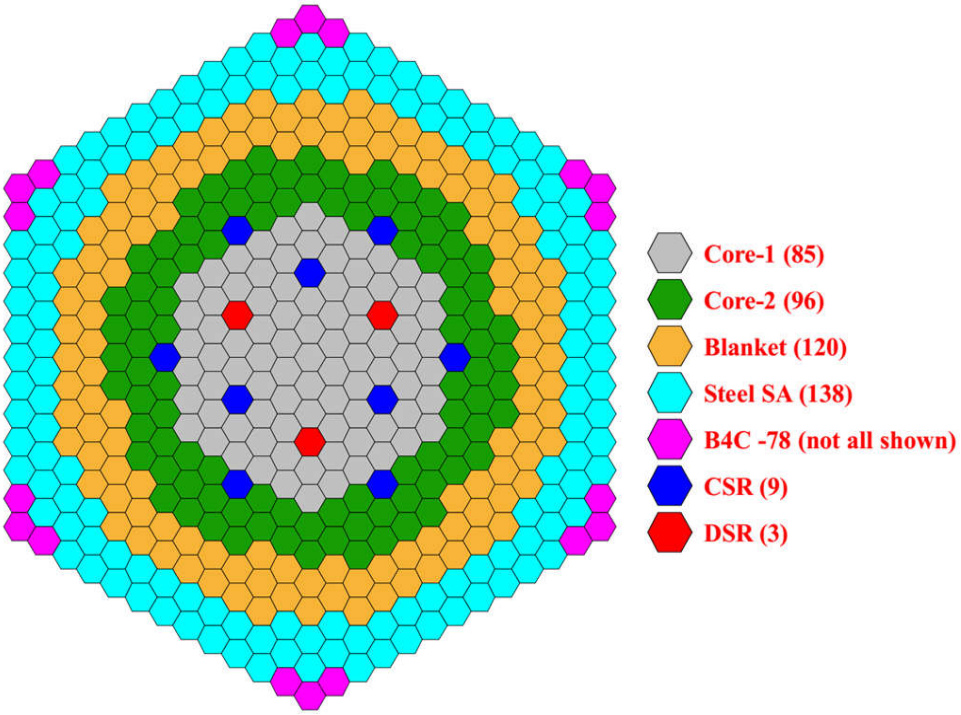

FIGURE 3.10: Core configuration of 500 MWe MOX core.

TABLE 3.3: Kinetics and thermo physical parameters of MOX and metal cores.

Parameter	Oxide	Metal		
	Medium	Small	Medium	Large
(MWe)	(500)	(120)	(500)	(1000)
Effective delayed neutron fraction, (pcm)	363	385	401	419
Prompt neutron life time (μs)	0.452	0.248	0.278	0.264
Effective delayed neutron decay constant (s^{-1})	0.0893	0.0921	0.0941	0.0965
Effective delayed neutron life time (s)	11.19	10.86	10.63	10.36
Effective neutron life time (s)	0.041	0.041	0.043	0.044
Fuel to clad heat transfer coeff. ($W/cm/K$)	0.4241	4.0842	4.1448	4.2989
Clad to coolant heat transfer coeff. ($W/cm/K$)	10.444	10.444	9.7607	11.492

TABLE 3.4: Delayed neutron parameters of metal cores.

120 MWe	λ_i	0.0129	0.0313	0.1349	0.3462	1.3930	3.799
	β_i	8.433	79.549	71.250	140.39	65.270	19.848
500 MWe	λ_i	0.0129	0.0313	0.1350	0.3469	1.3949	3.819
	β_i	8.437	81.078	73.721	147.24	69.569	21.304
1000 MWe	λ_i	0.0129	0.0314	0.1352	0.3477	1.3965	3.841
	β_i	8.459	82.596	76.345	154.69	74.378	22.962

TABLE 3.5: Delayed neutron parameters for the oxide core.

500 MWe	λ_i	0.0129	0.0313	0.1344	0.3449	1.3927	3.759
	β_i	8.3122	77.646	68.08	131.57	59.453	17.732

3.4 Results and Analysis

3.4.1 *Linear Stability Analysis Using Nyquist Criteria*

The calculation requires kinetics parameters of the core, power density, material removal worths and Doppler constants as inputs. The variation of reactivity perturbation worths as a function of reactor size is studied and the static power coefficient and isothermal temperature coefficient are estimated in an earlier study [58]. In the present study, the dynamic power coefficient of reactivity is estimated.

Frequency response of a reactor core is usually expressed as magnitude and phase plots with respect to frequency. Magnitude of zero power transfer function varies inversely with frequency at both lower and higher limits and phase approaches -90 as $\omega \longrightarrow 0$ and $\omega \longrightarrow \infty$ (Figures 3.11 and 3.12). The lower value of neutron generation time in fast reactors makes the wider flat region in the magnitude plot. In Figure 3.12 it is clear that in 500 MWe oxide core, phase starts decreasing from zero at a lower frequency compared to the metal cores. This is because the oxide core is having maximum neutron generation time.

The static power coefficient and its components along with feedback time constants are compared in Table 3.6. The three metal cores have comparable time constant while the MOX fueled core has a much higher value. This can be attributed to the better heat transfer properties of the metal fueled core. The heat transfer properties of each core is given in Table 3.3. The metal cores have lower Doppler feedback coefficients and better fuel expansion feedback coefficients compared to a MOX core. Out of the three metal fueled cores the 120 MWe core is having maximum value for negative power

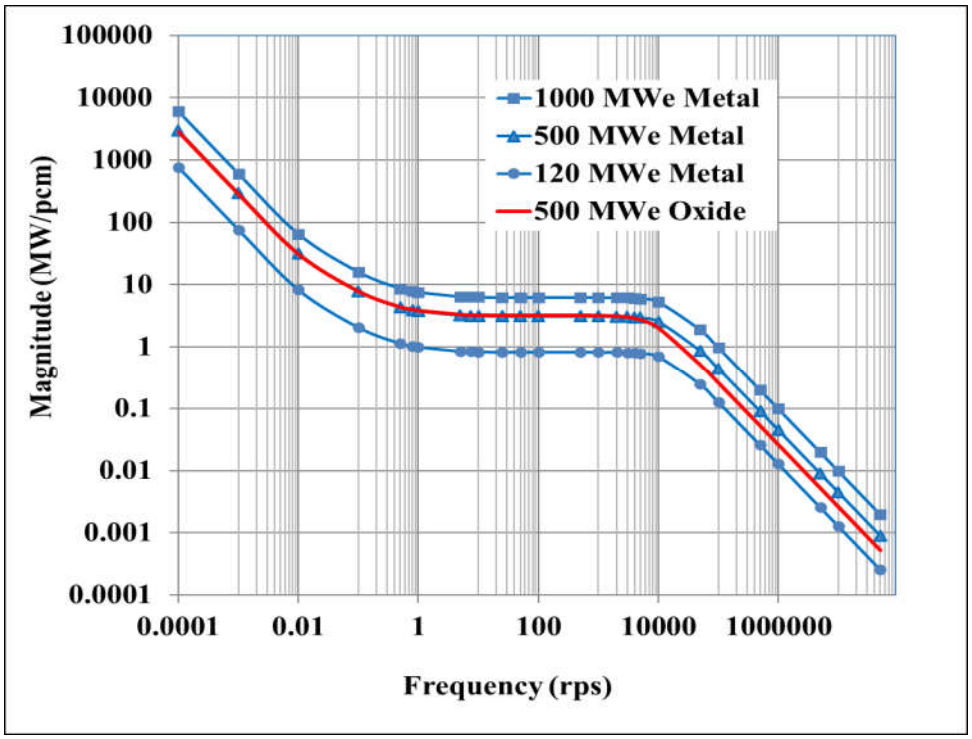

FIGURE 3.11: Magnitude of zero power transfer function.

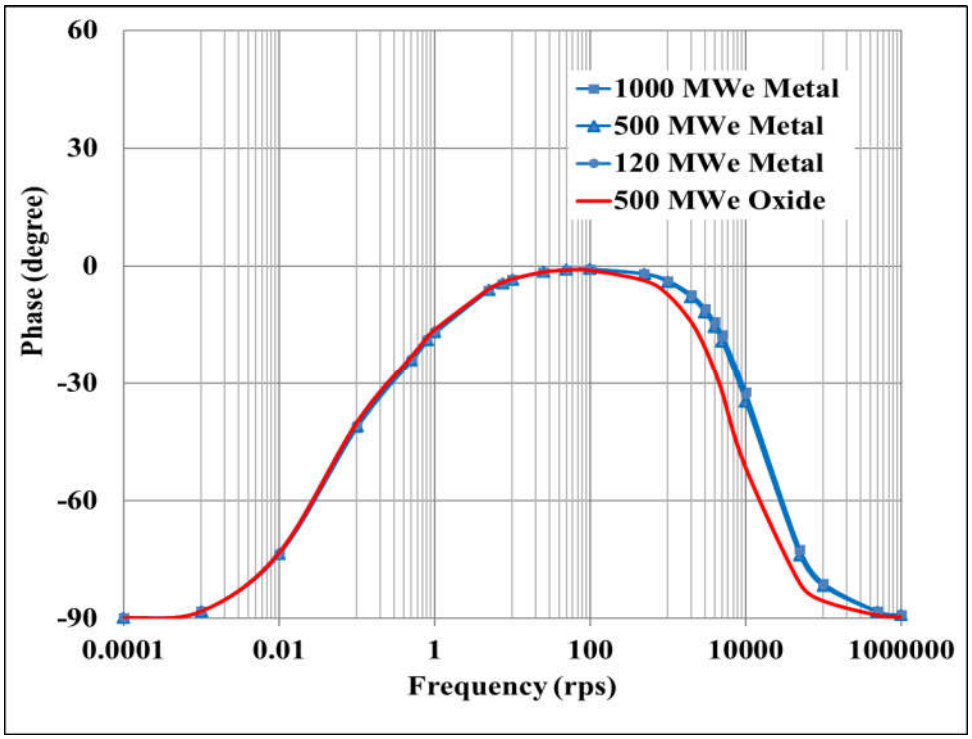

FIGURE 3.12: Phase of zero power transfer function.

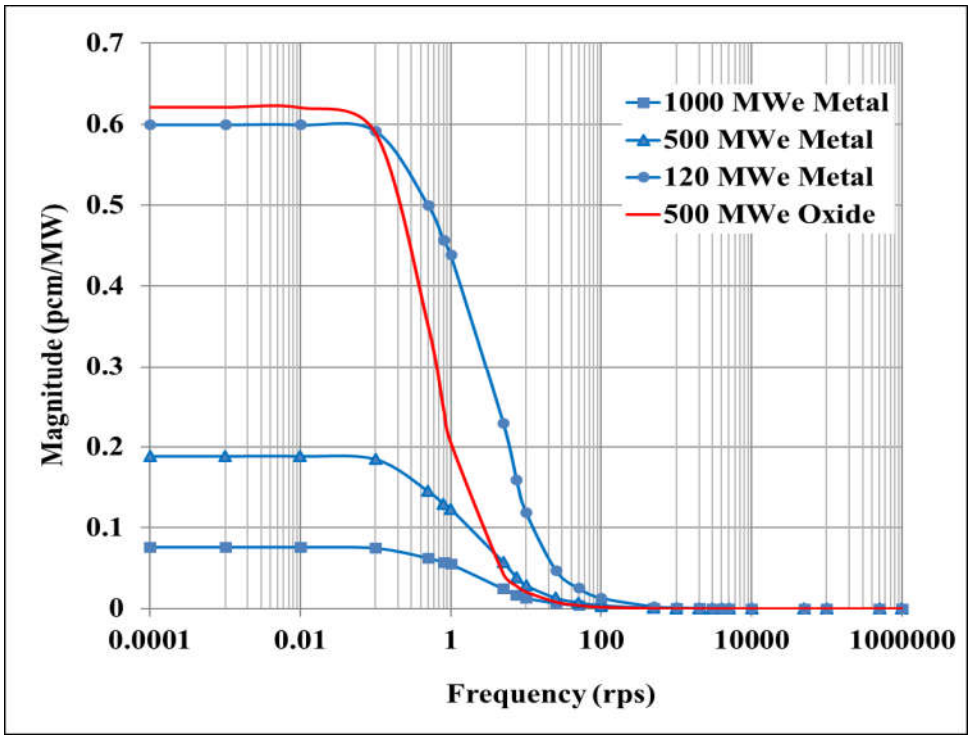

FIGURE 3.13: Magnitude of feedback transfer function.

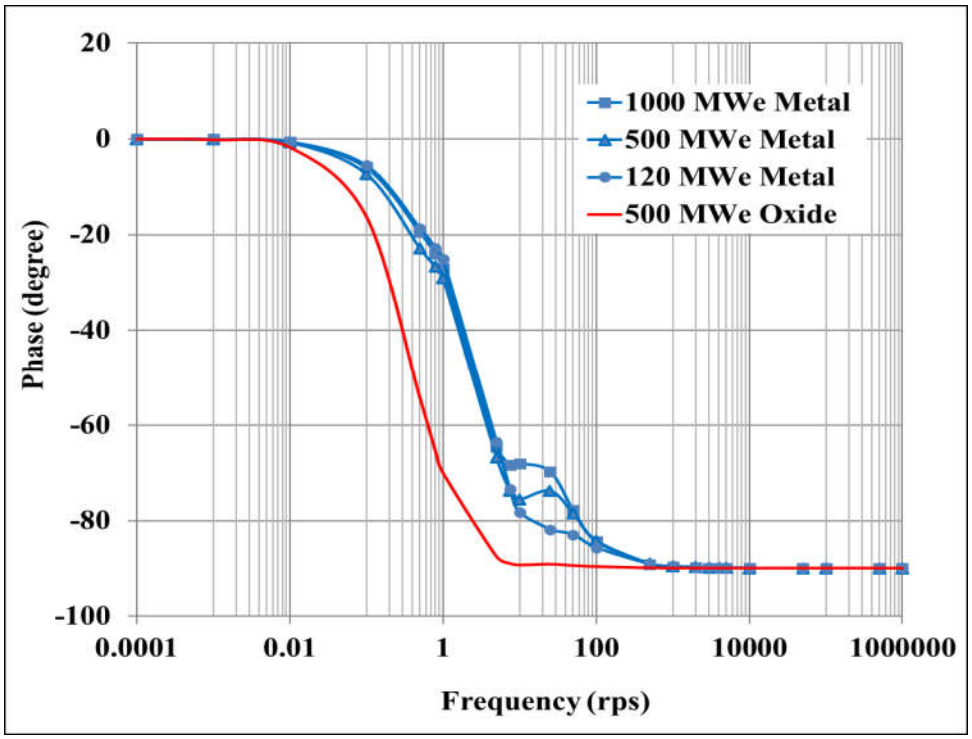

FIGURE 3.14: Phase of feedback transfer function

TABLE 3.6: Components of static power coefficient and time constants.

Parameter	Oxide	Metal		
	Medium	Small	Medium	Large
(MW)	(500)	(120)	(500)	(1000)
Fuel expansion feedback (pcm/MW)	-0.1785	-0.2439	-0.0737	-0.0329
Steel expansion feedback (pcm/MW)	0.0070	0.0087	0.0081	0.0050
Sodium expansion feedback (pcm/MW)	0.0139	0.0206	0.0377	0.0231
Doppler feedback (pcm/MW)	-0.3471	-0.1477	-0.0738	-0.0467
Core radial expansion feedback (pcm/MW)	-0.1162	-0.2373	-0.0869	-0.0247
Static power coeff.of reactivity (pcm/MW)	-0.6208	-0.5996	-0.1886	-0.0762
Feedback reactivity time constant (s)	2.9	1.051	1.301	1.051

coefficient, due to better feedbacks from core expansion. As the core size increases the power coefficient decreases; the leakage effect in a larger core is lower than a small core, and hence reduced core expansion feedbacks.

Magnitude of feedback transfer function is plotted in Figure 3.13, in which the y-intersect in each curve represents the static power coefficient. Figure 3.14 shows the phase of feedback transfer function variation with frequency. The magnitude and phase plots for the power transfer function $H(s)$ are given in Figure 3.15 and 3.16 respectively. At very low frequencies the dip in magnitude of power transfer function in case of oxide core can be attributed to the strong negative reactivity feedback of the core.

Nyquist plot for all the four cores are made by plotting the imaginary part of open loop transfer function against real part. Figure 3.17 shows the Nyquist plot for metal and the oxide cores. In all cases, the plot is confined to the right hand side of the imaginary axis and the curve is not encircling the $(-1, i0)$ point ensuring stability of all reactor cores.

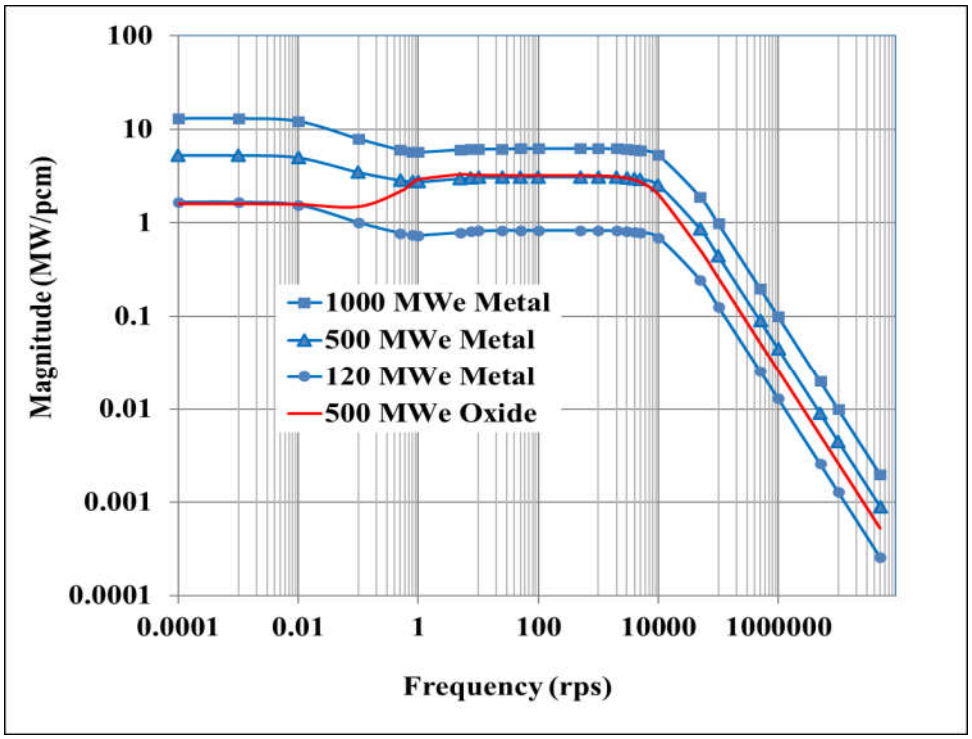

FIGURE 3.15: Magnitude of power transfer function.

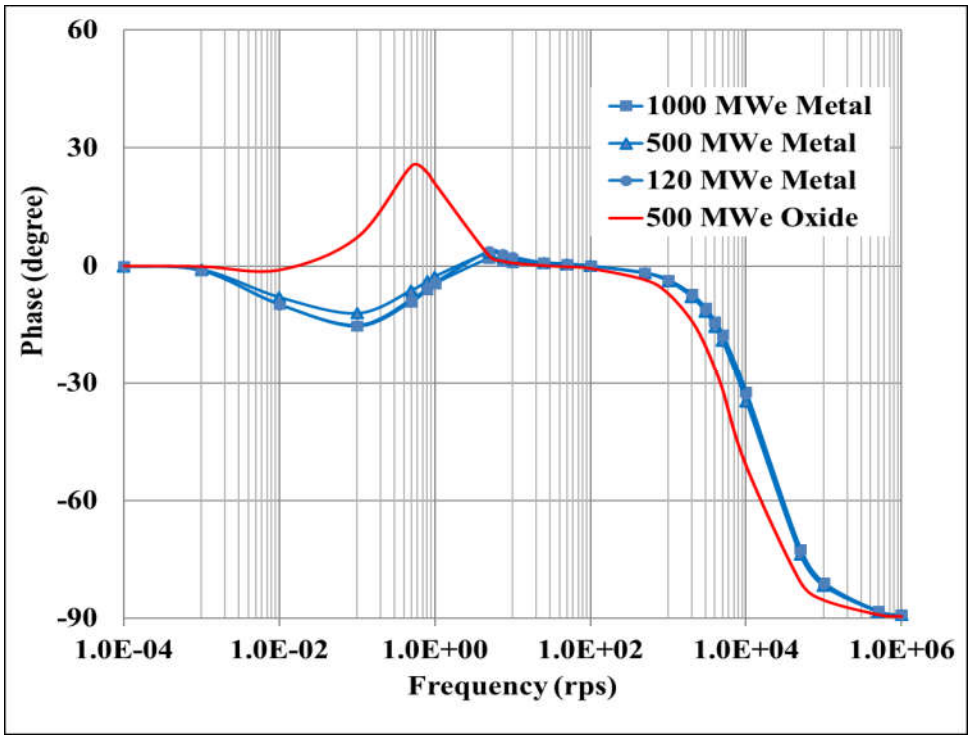

FIGURE 3.16: Phase of power transfer function.

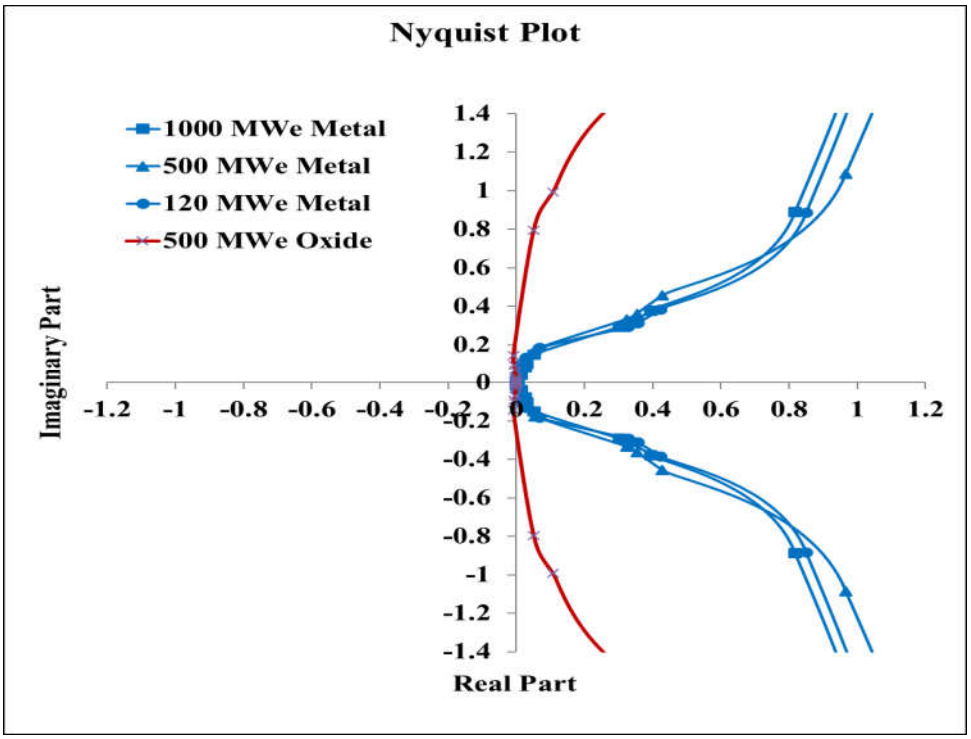

FIGURE 3.17: Nyquist diagram.

Stability margins are used as a measure of how far the reactor is from instability. In the closed loop model of the reactor core, gain margin is infinite for all the cores considered. The phase margin in case of the metal cores are comparable while the MOX fueled core is having a lower phase margin to instability, as given in Table 3.7. Even though the feedback power coefficient is larger in case of a MOX core, its stability margin is lower compared to the metal cores considered.

TABLE 3.7: Stability margin.

Reactor	Phase margin	Gain margin
500 MOX	97	Infinity
120 Metal	138	Infinity
500 Metal	136	Infinity
1000 Metal	136	Infinity

3.4.2 *Eigen Value Separation*

The Eigen Value Separation (EVS) is a measure of core neutronic coupling and the stability of the reactor. A larger EVS between the fundamental mode and higher mode in a reactor indicates the core is tightly coupled and the spatial instabilities are less probable. The EVS values are calculated for 500 MW metal and 500 MW oxide cores and are compared. The physical dimensions, and the height to diameter ratios of the two cores are identical. The neutron energy spectrum in the two cores are different; oxide core has a softer spectrum. The EVS are estimated using mode subtraction method with a four group calculation model. The EVS between the fundamental mode and the first azimuthal mode are estimated to be 11044 pcm for oxide core and 11190 pcm for the metal core. The EVS is found to be slightly higher for the metal fueled core indicating the better neutronic coupling.

3.4.3 *Step Reactivity Insertions*

The time evolution of the normalized reactor power against step reactivity insertions gives an indication of the stability characteristics of the reactor core. A step reactivity of 100 pcm is applied to the four reactor cores considered and the normalized power evolution is found out using PREDIS. The normalized power evolution for the step reactivity insertion are compared in Figure. 3.18. The net reactivity change after the insertion of external reactivity is depicted in Figure 3.19. In metal cores, no power oscillations are observed and the power reached stationary values very smoothly. In case of 500 MWe oxide core, the normalized power increases to 1.23 within one second and then decreases to 1.13 and later stabilize at 1.14 times the initial value. The oscillation in power is due to the delay in feedback reactivity to act after a power change. This can be attributed to the higher reactivity feedback time constant in case of the oxide core as given in Table 3.6. The rise in power level in metal cores are much higher, around 50%, compared to that of oxide core. The final steady state power level depends on the magnitude of step reactivity and also the static power coefficient of the core. In

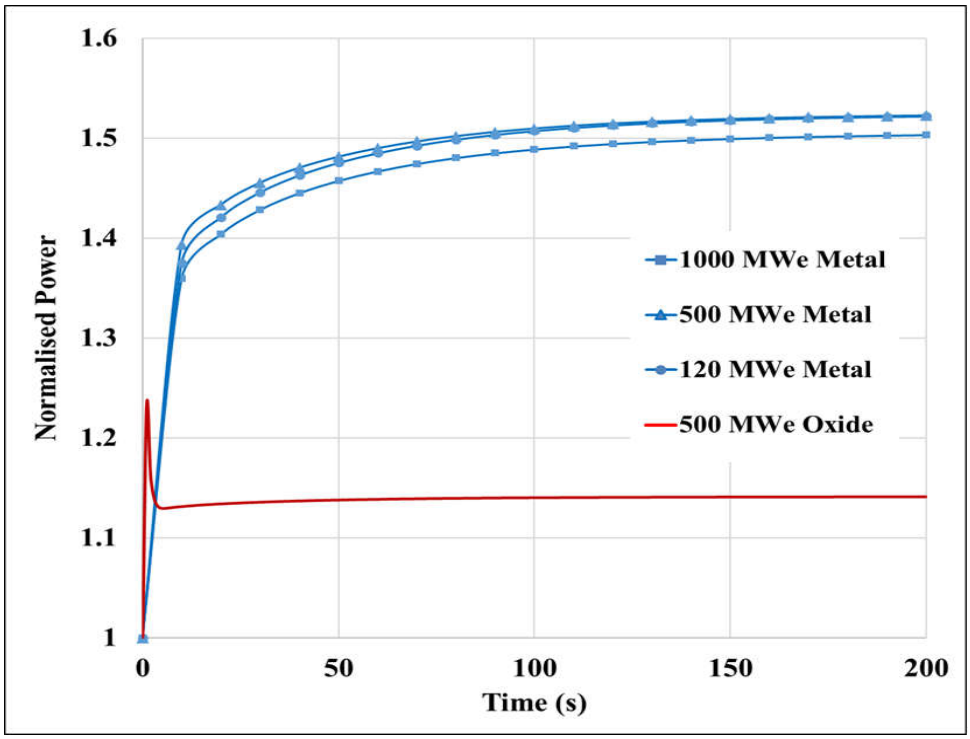

FIGURE 3.18: Normalised power variation due to reactivity insertion of 100 pcm.

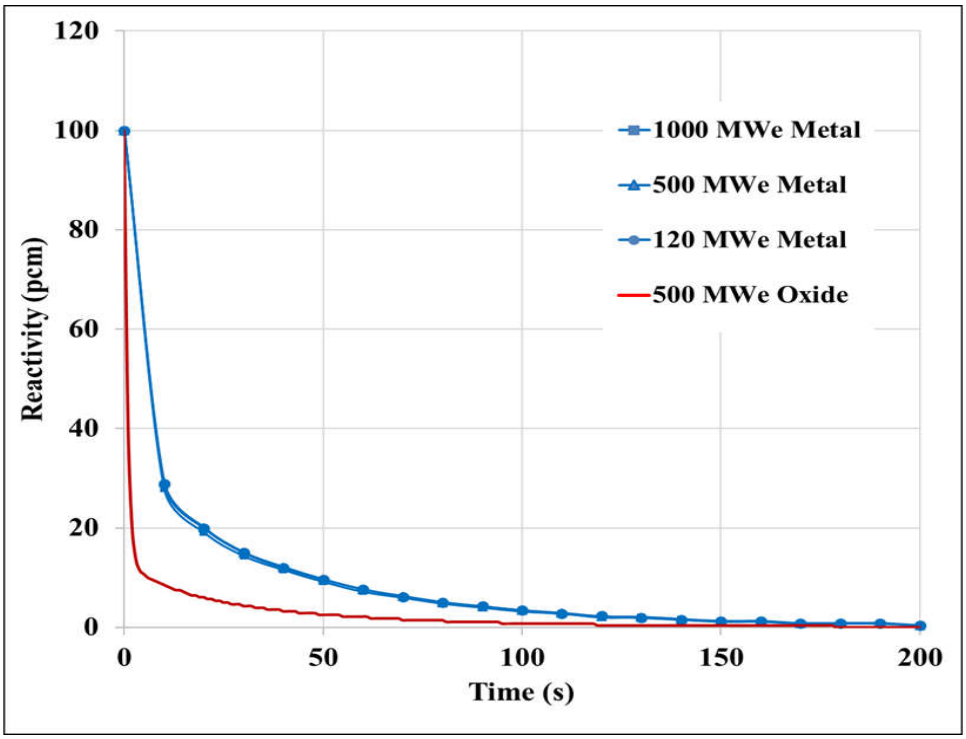

FIGURE 3.19: Net reactivity variation after reactivity insertion of 100 pcm.

case of metal cores the magnitude of static power coefficient is less, resulting in a higher final power level at the end of the transient. The metal cores stabilize at higher power levels smoothly, but the relative rise in power is much higher compared to the oxide core. The smooth variation in power as seen in metal cores is a desired property for power rising operations.

3.5 Summary

The stability characteristics of a medium sized 500 MWe MOX and three metal fueled cores having different power and core sizes are studied and compared. The well known transfer function method and Nyquist criteria are used for establishing the stability of the cores. For all the three metal fueled FBR cores, the closed-loop stability of the core is demonstrated. The feedbacks are stronger in the MOX fueled core compared to similar sized metal core, but the metal core has lower time constant resulting prompt feedback. The smaller time constant due to better heat transfer properties of the metal core gives a higher stability margin for the metal fueled FBRs. The eigen value separation for metal cores are found to be little higher compared to an oxide core of same size. The response of various cores to a step reactivity insertion indicated that the metal cores have smoother response without oscillations due to their shorter feedback reactivity time constant. From all these studies, the metal fueled cores are found to be marginally better in stability compared to an oxide core.

Chapter 4

Nonlinear Stability Analysis in SFRs

4.1 Introduction

In chapter 3, it is shown that FBR cores are linearly stable based on linear stability analysis using Nyquist stability criteria. However, to study the system behavior for larger perturbations, nonlinear stability analysis is to be carried out with all reactivity feedbacks. Here nonlinear stability analysis of FBR is addressed using two methods i) Bifurcation theory and ii) Time domain numerical integration method. The first method is used to examine the bifurcation of stable power distribution to multiple possibly unstable distributions, and in the time domain analysis the reactor response to perturbations are studied.

Many articles are available in the literature on nonlinear stability analysis of thermal reactors but limited papers on fast reactor stability. BWR stability analysis using bifurcation method is reported in [63]–[65]. The multiplicity of power distribution in PWR systems is studied by both Yang and Lavande [66], [67], considering a nonlinear reactor model, and it is shown through bifurcation theory that multiple steady-state solutions are possible for a range of parameters that correspond to various design and operating conditions. The same formalism is followed for the analysis of PFBR with suitable modifications, and checked for the existence of multiplicity in steady-state solutions[1], [68]. Feedback components from Xe and soluble Boron poison are absent in fast reactor systems. The moderator expansion feedback which is negative

in PWR, is replaced with coolant expansion feedback in this study. The continuation code MATCONT is used for bifurcation analysis.

Another method used to assess the stability of the reactor is studying its time response to reactivity perturbations directly. The transient analysis code PREDIS is used for such a time domain analysis. The details about these two studies are discussed in this chapter.

4.2 Nonlinear model of a nuclear reactor with feedback

In large power reactors, the spatial effects in the dynamic behavior of neutron population is very important. The point kinetics approximation is not enough to analyze such systems and time dependent neutron diffusion equation or transport equation is necessary. The approach followed by N. Z. Cho [25] is used in the analysis. First the method is used in a PWR system with boron and Xenon equations and the emergence of instability is demonstrated, then the equations are suitably modified for a fast reactor and the stable nature of solution is shown. The non linear one-group neutron diffusion equation describing a PWR core with feedbacks is as follows.

$$\frac{1}{v}\frac{\partial\phi\left(r,\theta,z,t\right)}{\partial t} = \nabla D\nabla\phi - \Sigma_a\phi + \nu\Sigma_f\phi + \alpha_m\nu\Sigma_f\left[T_m\left(r,\theta,z,t\right) - \bar{T}_m\right]\phi + \alpha_f\nu\Sigma_f\left[T_f\left(r,\theta,z,t\right) - \bar{T}_f\right]\phi - \sigma_x X\left(r,\theta,z,t\right)\phi - \sigma_b c_b b N_w\left(r,\theta,z,t\right)\phi \quad (4.1)$$

ϕ $\Rightarrow$ Neutron flux

v $\Rightarrow$ Velocity of neutron

D $\Rightarrow$ Diffusion coefficient

Σ_a $\Rightarrow$ Macroscopic absorption cross section

Σ_f $\Rightarrow$ Macroscopic fission cross section

ν $\Rightarrow$ Number of neutrons produced per fission

σ_x $\Rightarrow$ Absorption cross section of Xe

σ_b $\Rightarrow$ Absorption cross section of boron

T_m $\Rightarrow$ Moderator temperature

T_f $\Rightarrow$ Fuel temperature

$\bar{T}_m$ $\Rightarrow$ Reference moderator temperature

$\bar{T}_f$ $\Rightarrow$ Reference fuel temperature

X $\Rightarrow$ Xe_{135} concentration

N_w $\Rightarrow$ Moderator molecular density

b $\Rightarrow$ Boron concentration

c_b $\Rightarrow$ Conversion factor for boron concentration from parts per million to atoms of B^{10} per molecule of water

α_m $\Rightarrow$ thermal expansion coefficient of moderator

α_f $\Rightarrow$ thermal expansion coefficient of fuel

Boundary conditions applicable to a bare reactor core are

$$\begin{aligned} \phi(R,\theta,z,t) &= 0 \\ \phi(r,\theta,0,t) &= 0 \\ \phi(r,\theta,H,t) &= 0 \end{aligned} \tag{4.2}$$

where R and H are the radius and height of the reactor respectively.

Using first order perturbation theory approximation, feedback reactivity can be expressed in terms of changes in absorption cross section due to temperature changes. Moderator and fuel temperature feedbacks are represented as,

$$\Delta\Sigma_{\mathrm{a}} \approx -\alpha_{\mathrm{m}}\nu\Sigma_{\mathrm{f}}\Delta\mathrm{T}_{\mathrm{m}} \tag{4.3}$$

$$\Delta\Sigma_{\mathrm{a}} \approx -\alpha_{\mathrm{f}}\nu\Sigma_{\mathrm{f}}\Delta\mathrm{T}_{\mathrm{f}} \tag{4.4}$$

For a single channel moderator, the energy balance equations can be written as:

$$\rho_m C_{pm} dV_{ch} \frac{\partial T_m(r,\theta,z,t)}{\partial t} + C_{pm} w_c(r,\theta,z,t)\, dz \frac{\partial T_m(r,\theta,z,t)}{\partial z} = 2\pi r_f dz h_0 [T_f(r,\theta,z,t) - T_m(r,\theta,z,t)] \quad (4.5)$$

Two terms on the left hand side of Eq. 4.5 represents the moderator internal energy change and the heat removal by flow and the term on the right hand side gives the heat transfer from fuel to moderator.

Similarly the energy balance equation for fuel in small core volume :

$$\rho_f C_{pf} dV_f \frac{\partial T_f(r,\theta,z,t)}{\partial t} = \varepsilon \Sigma_f \phi s^2 dz - 2\pi r_f dz h_0 [T_f(r,\theta,z,t) - T_m(r,\theta,z,t)] \quad (4.6)$$

Left hand side of Eq. 4.6 is for the internal energy change while the first term on the right hand side is heat source from fission and the second term corresponds to heat transfer from fuel to moderator.

Here

ρ_m	$\Rightarrow$	Moderator density
ρ_f	$\Rightarrow$	Fuel density
C_{pm}	$\Rightarrow$	Moderator specific heat
C_{pf}	$\Rightarrow$	Fuel specific heat
V_{ch}	$\Rightarrow$	Control volume around the single channel
V_f	$\Rightarrow$	Control volume of the fuel
w_c	$\Rightarrow$	coolant mass flow rate
r_f	$\Rightarrow$	Radius of fuel rod
h_0	$\Rightarrow$	Fuel to moderator heat transfer coefficient
ε	$\Rightarrow$	Energy per fission
s	$\Rightarrow$	Fuel pin pitch

Xenon and iodine dynamics equations for a PWR system as,

$$\frac{\partial I\left(r,\theta,z,t\right)}{\partial t}=\gamma_I\Sigma_f\phi-\lambda_I I \tag{4.7}$$

$$\frac{\partial X\left(r,\theta,z,t\right)}{\partial t}=\gamma_X\Sigma_f\phi+\lambda_I I-\lambda_x X-\sigma_x X\phi \tag{4.8}$$

where

$I \Rightarrow I_{135}$ concentration

$\gamma_I \Rightarrow$ Fission yield of I_{135}

$\lambda_I \Rightarrow$ Decay constant of I_{135}

$\gamma_X \Rightarrow$ Fission yield of Xe_{135}

$\lambda_x \Rightarrow$ Decay constant of Xe_{135}

Steady state equations are obtained by setting the time derivative terms in the above expressions equal to zero. By solving them, the steady state temperatures are found out to be,

$$T_{m,0}\left(r,\theta,z\right)=\frac{s^2}{C_{mc}}\varepsilon\Sigma_f\int_0^z\frac{\phi_0\left(r,\theta,z'\right)}{w_c\left(r,\theta,z'\right)}dz'+T_{m,in,0} \tag{4.9}$$

$$T_{f,0}\left(r,\theta,z\right)=\frac{s^2}{2\pi r_f h_0}\varepsilon\Sigma_f\phi_0\left(r,\theta,z'\right)+\frac{s^2}{C_{pm}}\varepsilon\Sigma_f\int_0^z\frac{\phi_0\left(r,\theta,z'\right)}{w_c\left(r,\theta,z'\right)}dz'+T_{m,in,0} \tag{4.10}$$

where $T_{m,in,0}$ is the moderator (coolant) inlet temperature at steady state.

The dependent variables ϕ_0, I_0, X_0 are assumed to be separable in the radial and axial directions. There radial dependence are described by the zero-order Bessel function. Due to symmetric core configuration, they are independent of the azimuthal direction.

$$\begin{aligned} \phi_0(r,\theta,z) &= J_0(B_r r)\,\phi(z) \\ I_0(r,\theta,z) &= J_0(B_r r)\,I(z) \\ X_0(r,\theta,z) &= J_0(B_r r)\,X(z) \end{aligned} \tag{4.11}$$

Further, with appropriate control of the mass flow rate, the moderator temperature distribution is assumed flat in the radial direction. Feedback variables can be finally combined into the steady state flux distribution equation for $\phi_0(z)$

$$\begin{aligned} 0 = \nabla D\nabla\phi_0 - \Sigma_a\phi_0 + \nu\Sigma_f\phi_0 + \alpha_m\nu\Sigma_f\left[T_{m,0}(r,\theta,z) - \bar{T}_m\right]\phi_0 \\ + \alpha_f\nu\Sigma_f\left[T_{f,0}(r,\theta,z) - \bar{T}_f\right]\phi_0 \\ - \sigma_x X_0(r,\theta,z)\,\phi_0 - \sigma_b c_b b_0 N_{w,0}(r,\theta,z)\,\phi_0 \end{aligned} \tag{4.12}$$

Integration over r and θ distributions gives :

$$\frac{d^2u(x)}{dx^2} + \lambda u = Au\int_0^x u(x')\,dx' + Bu^2 + C\frac{u^2}{1+u} \tag{4.13}$$

$0 < x < 1, \qquad u(0) = u(1) = 0$

Dimensionless flux $u(x) = \frac{\bar{\sigma}_x}{\lambda_x}\phi(x)$, Dimensionless height : $x = \frac{z}{H}$ where,

$$\bar{\sigma}_x = \frac{\bar{\bar{J}}_0}{\bar{J}_0}\sigma_x, with \tag{4.14}$$

$$\bar{J}_0 = \int_0^R r J_0(B_r r)\,dr$$

$$\bar{\bar{J}}_0 = \int_0^R r J_0^2(B_r r)\,dr$$

It may be noted that all terms on right hand side of Eq. 4.13 are nonlinear. Constant A is mainly dependent on the moderator and fuel temperature coefficients and the concentration of boron. The second term is a nonlinear term due to fuel temperature feedback. The third nonlinear term is due to Xenon and C is always a constant.

The feedback constants A, B and C as defined in ref [66] are given by :

$$A = -\left[\frac{H^3}{D}\frac{2N\bar{J}_0 s^2 \nu\Sigma_f \varepsilon\Sigma_f}{WC_{pm}R^2}\frac{\lambda_x}{\bar{\sigma}_x}\right](\alpha_m + \alpha_f) - \left[\frac{H^3}{D}c_b\sigma_b N_{w,0}(0)\,\beta\frac{2N\bar{J}_0 s^2\varepsilon\Sigma_f}{WC_{pm}R^2}\frac{\lambda_x}{\bar{\sigma}_x}\right] b_0 \quad (4.15)$$

$$B = -\left[\frac{H^2}{D}\frac{\nu\Sigma_f s^2\varepsilon\Sigma_f \bar{\bar{J}}_0}{2\pi r_f h_0 \bar{J}_0}\frac{\lambda_x}{\bar{\sigma}_x}\right]\alpha_f \quad (4.16)$$

$$C = \frac{H^2}{D}(\gamma_x + \gamma_I)\,\Sigma_f \quad (4.17)$$

$$\lambda = \frac{H^2}{D}\left[\nu\Sigma_f - \Sigma_a - DB_r^2 + \alpha_m\nu\Sigma_f\left(T_{m,in,0} - \bar{T}_m\right) + \alpha_f\nu\Sigma_f\left(T_{m,in,0} - \bar{T}_f\right)\right] - \frac{H^2}{D}\left[c_b\sigma_b b_0 N_{w,0}(0)\right] \quad (4.18)$$

Parameter λ is determined by various feedback coefficients and reactor parameters, in particular the macroscopic parameter Σ_a. Once the constants A, B, and C are fixed, λ can be considered as a convenient parameter in examining the behavior of flux distribution.

4.2.1 *Reactor dynamics equations for FBR*

Expressions discussed above describes the PWR system, while in a fast reactor there is no Boron and Xenon terms and the moderator term is to be replaced by coolant. Hence Eq. 4.12 becomes,

$$0 = \nabla D\nabla\phi_0 - \Sigma_a\phi_0 + \nu\Sigma_f\phi_0 + \alpha_c\nu\Sigma_f\left[T_{c,0}(r,\theta,z) - \bar{T}_c\right]\phi_0 + \alpha_f\nu\Sigma_f\left[T_{f,0}(r,\theta,z) - \bar{T}_f\right]\phi_0 \quad (4.19)$$

The expressions for coolant and fuel temperature remain as,

$$T_{c,0}\left(r,\theta,z\right)=\frac{s^{2}}{C_{pc}}\varepsilon\Sigma_{f}\int_{0}^{z}\frac{\phi_{0}\left(r,\theta,z'\right)}{w_{c}\left(r,\theta,z'\right)}dz'+T_{c,in,0} \tag{4.20}$$

$$T_{f,0}\left(r,\theta,z\right) \;=\; \frac{s^{2}}{2\pi r_{f}h_{0}}\varepsilon\Sigma_{f}\phi_{0}\left(r,\theta,z'\right) \;+\; \frac{s^{2}}{C_{pc}}\varepsilon\Sigma_{f}\int_{0}^{z}\frac{\phi_{0}\left(r,\theta,z'\right)}{w_{c}\left(r,\theta,z'\right)}dz' \;+\; T_{c,in,0} \tag{4.21}$$

After separation of variables and assuming independence in the θ direction,

$$T_{c,0}\left(z\right)=\frac{2N\bar{J}_{0}s^{2}}{WC_{pc}R^{2}}\varepsilon\Sigma_{f}\int_{0}^{z}\phi\left(z'\right)dz'+T_{c,in,0} \tag{4.22}$$

$$T_{f,0}\left(r,z\right) \;=\; \frac{s^{2}}{2\pi r_{f}h_{0}}\varepsilon\Sigma_{f}J_{0}\left(B_{r}r\right)\phi\left(z\right) \;+\; \frac{2N\bar{J}_{0}s^{2}}{WC_{pc}R^{2}}\varepsilon\Sigma_{f}\int_{0}^{z}\phi\left(z'\right)dz' \;+\; T_{c,in,0} \tag{4.23}$$

where,

$$W=\int_{0}^{R}w_{c}\left(r\right)2\pi rdrN_{d} \tag{4.24}$$

$$N=\int_{0}^{R}2\pi rdrN_{d} \tag{4.25}$$

where

$N \;\Rightarrow$ Total number of channels

$W \;\Rightarrow$ Total mass flow rate

$N_d \;\Rightarrow$ Number of channels per unit cross sectional area of the core

With the assumption of a flat radial temperature distribution in core and non-dimensional parameters defined as,

$$u\left(x\right)=\frac{\sigma_{a}}{\beta^{2}\bar{\lambda}}\phi\left(x\right) \tag{4.26}$$

where $x = z/H$, the dimensionless height,

$\beta \Rightarrow$ Delayed neutron fraction

$\bar{\lambda} \Rightarrow$ One group delayed neutron decay constant

The dynamics equation in non dimensional form is,

$$\frac{d^2u\left(x\right)}{dx^2} + \lambda u = Au\int_0^x u\left(x'\right)dx' + Bu^2 \tag{4.27}$$

where $0 < x < 1$ and $u(\theta) = u(1) = 0$. Corresponding expressions for A, B and λ in this case are

$$A = -\left[\frac{H^3}{D}\frac{2N\bar{J}_0 s^2 \nu\Sigma_f \varepsilon\Sigma_f}{WC_{pc}R^2}\frac{\beta\bar{\lambda}}{\sigma_a}\right](\alpha_c + \alpha_f) \tag{4.28}$$

$$B = -\left[\frac{H^2}{D}\frac{\nu\Sigma_f s^2 \varepsilon\Sigma_f \bar{\bar{J}}_0}{2\pi r_f h_0 \bar{J}_0}\frac{\beta\bar{\lambda}}{\sigma_a}\right]\alpha_f \tag{4.29}$$

$$\lambda = \frac{H^2}{D}\left[\nu\Sigma_f - \Sigma_a - DB_r^2 + \alpha_c\nu\Sigma_f\left(T_{c,in,0} - \bar{T}_c\right) + \alpha_f\nu\Sigma_f\left(T_{c,in,0} - \bar{T}_f\right)\right] \tag{4.30}$$

where

$$\bar{J}_0 = \int_0^R rJ_0\left(B_r r\right)dr \tag{4.31}$$

$$\bar{\bar{J}}_0 = \frac{1}{R}\int_0^R J_0\left(B_r r\right)dr \tag{4.32}$$

4.2.2 *Bifurcation theory and analysis*

Eq. 4.13 in the following form describes a distributed parameter system [DPS].

$$\frac{d^2u\left(x\right)}{dx^2} + \lambda u = g\left(x, u\right) \tag{4.33}$$

with $g\left(x,u\right) = Au\int_0^x u\left(x'\right)dx' + Bu^2$ and $u(0) = u(1) = 0$

As per a theorem [25] for $g(x,u)$ strictly increasing, the equation admits only one stable solution for all $\lambda's$. Reactors with parameters A, B, C contributing to this condition is always stable. For $g(x,u)$ not strictly increasing, the equation admits more solution for some $\lambda's$. Parameter C is always positive while B is normally positive [-ve Doppler coefficient]. Thus, A must be negative for investigating multiplicity and stability of solutions as a function of λ. Therefore a necessary condition for reactor instability is that $A < 0$.

Multiplicity and stability are two related aspects in a nonlinear analysis. In this context, one converts the DPS Eq. 4.33 into a set of lumped parameter system [LPS] equations using finite difference approximation.

$$f_i\left(u_1, u_2, \cdots, u_n, \lambda\right) = \frac{u_{i+1} - 2u_i + u_{i-1}}{\Delta x^2} + \lambda u_i - A u_i \Delta x \left[\frac{u_0 + u_1}{2} + \frac{u_1 + u_2}{2} + \cdots + \frac{u_{i-1} + u_i}{2}\right] - B u_i^2 - C\frac{u_i^2}{1 + u_i} = 0 \quad (4.34)$$

with $i = 1, ..., n$; and $u_0 = u_{n+1} = 0$

Following the requirements of continuation algorithm and to get the solution, we differentiate Eq. 4.33 with respect to λ leading to a set of equations:

$$\frac{d\mathbf{u}}{d\lambda} = -\mathbf{J}^{-1}\left(\mathbf{u}, \lambda\right)\frac{\partial \mathbf{f}}{\partial \lambda} \quad (4.35)$$

$$\mathbf{u}\left(\lambda_\mathbf{0}\right) = \mathbf{u_0}$$

$$\mathbf{u} = \left[u_1, u_2, \cdots, u_n\right]^T$$

$$\mathbf{J} = \left\{\frac{\partial f_i}{\partial u_j}\right\} \quad (4.36)$$

$$\frac{\partial \mathbf{f}}{\partial \lambda} = \left[\frac{\partial f_1}{\partial \lambda}, \frac{\partial f_2}{\partial \lambda}, \cdots, \frac{\partial f_n}{\partial \lambda}\right]^T$$

$$\mathbf{f}\left(\mathbf{u}_0, \lambda_0\right) = \mathbf{0}$$

Continuation of solution amounts to finding steady state solutions under variation of parameter λ. If Jacobian matrix is regular, for then the solution can be obtained using natural continuation method. However the method fails when matrix becomes singular at a branch point. This problem is circumvented using (n+1) dimensional space and is achieved by differentiating the equilibrium system with respect to arc-length s of solution in the extended space (u, λ). Thus s becomes an independent variable and λ becomes dependent variable u_{n+1}. Applying Newton Raphson's techniques to our linear equations and using differential equation solver one gets solutions for different values of λ.

4.2.3 *Multiplicity and stability of solutions*

The solution diagrams are classified into three types:

- Type 1: one bifurcation point and two limit points. It is possible to have 1 to 3 solutions depending on the value of λ.
- Type 2: one bifurcation point and one limit point. It is possible to have 2 solutions up to the limit point and no solutions above the limit point.
- Type 3: exhibits only one bifurcation point and it always has one solution which is stable.

The solution curves for a range of parameters A and B while C is fixed at 509 is shown in Figures 4.1 to 4.4. A is varied from 0 to -90 and B=0.1 and -90, in the range applicable for LWRs. When $A = 0, B = 0.1, C = 509$, there is one stable solution (Figure 4.1) when λ is varied over a wide range. The number of possible solutions becomes two for the case $A = -5.0, B = 0.1, C = 509$, (Figure 4.2) and three for the case of $A = -90.0, B = 10, C = 509$ (Figure 4.4). For PFBR model, the solution curve is of type three, with one stable solution. This can be seen from the numerical solution curve obtained with A, B values applicable for PFBR as shown in Figures 4.5 and 4.6. The numerical results are justified by positivity of parameter 'A' leading to

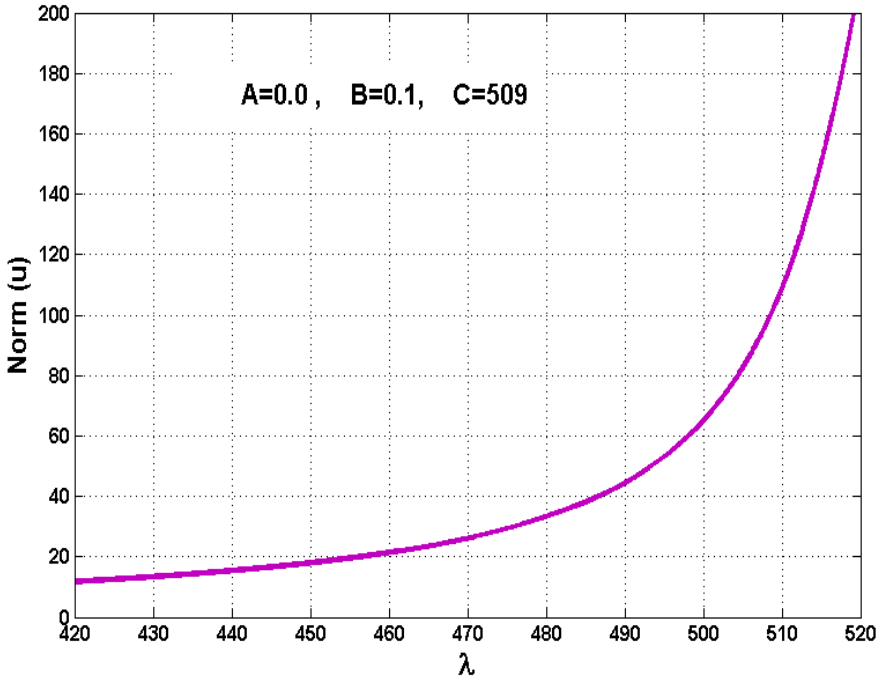

FIGURE 4.1: A single stable solution.

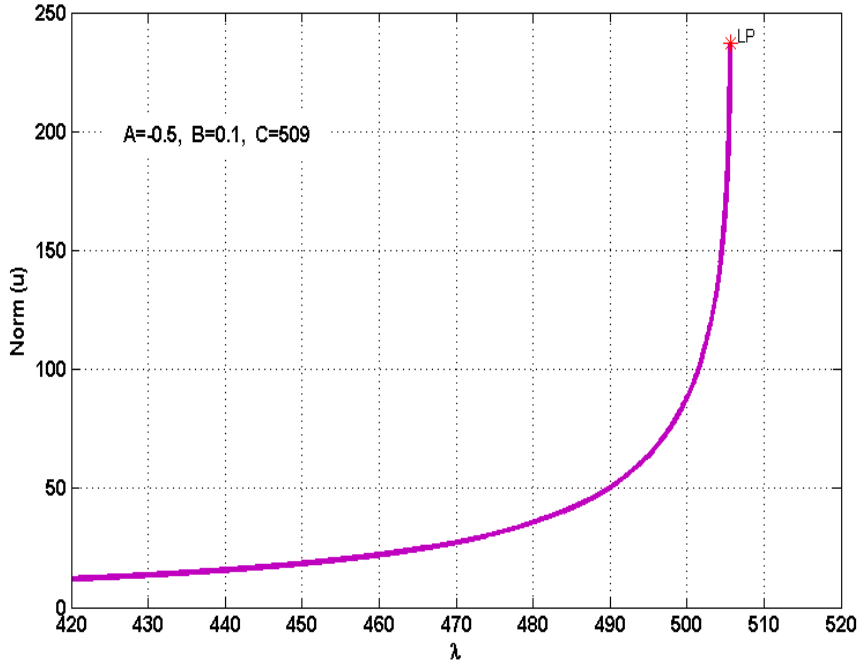

FIGURE 4.2: The emergence of instability.

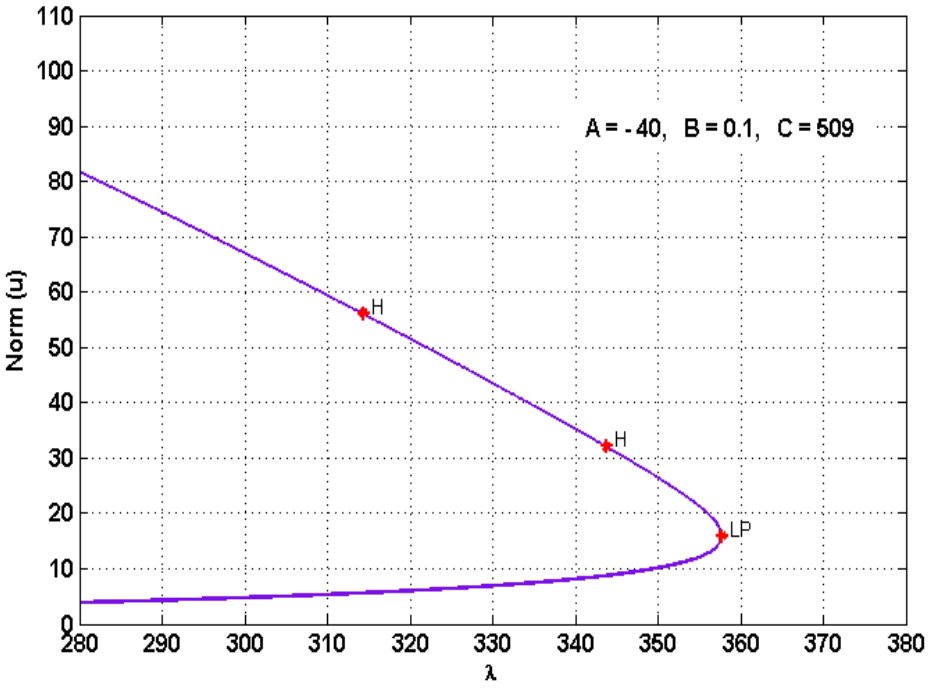

FIGURE 4.3: One limit point.

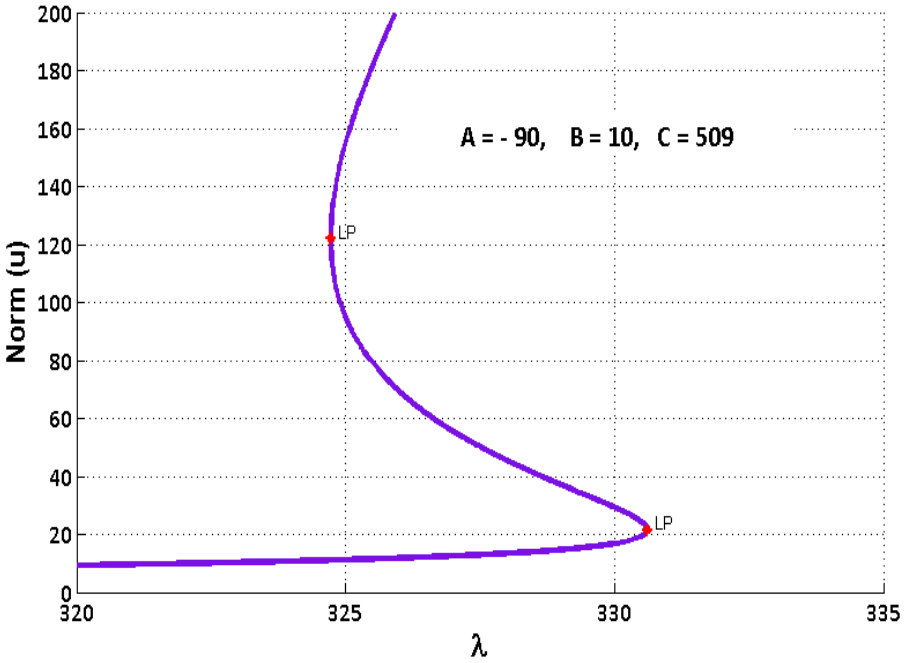

FIGURE 4.4: Two limit point.

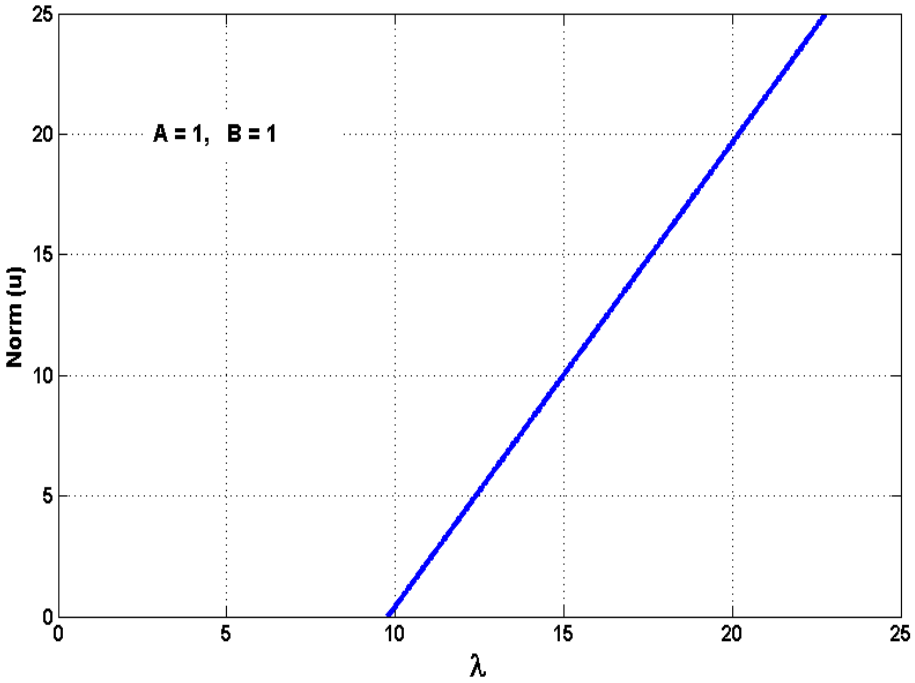

FIGURE 4.5: Single stable solution, A=1, B=1 (PFBR).

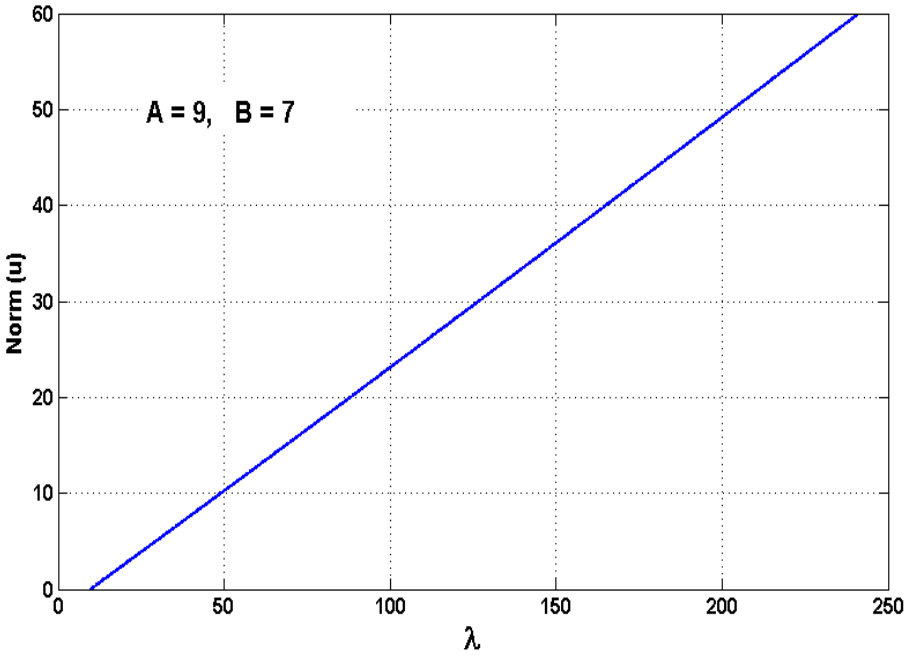

FIGURE 4.6: Single stable solution, A=9, B=7 (PFBR).

strictly increasing function $g(x,u)$ in Eq. 4.33. Negative A is a necessary condition for instability [67]. The analysis uses averaged fuel, steel and coolant temperature coefficients $-1.2pcm/K$ (for fuel), $+0.24pcm/K$ (for coolant+steel)). Radially averaged reactivity coefficients considering axial variation also gives rise to strictly increasing $g(x,u)$, permitting only stable solutions.

4.3 Stability assessment using pulsed and sinusoidal reactivity insertions

The stability of PFBR 175 FSA Initial Core is also assessed by reactivity perturbations in the form of pulses and sine wave reactivity inputs. The perturbations considered are reactivity pulses of amplitudes 0.1, 0.3, and 0.5 $ of 1 s duration at full power and it is found that for all these cases the power converged smoothly without any oscillation confirming the stability of the reactor. A flow perturbation of 10 % has also been considered and found that the power converges smoothly. Sinusoidal reactivity perturbations of amplitude 0.5 $ and frequencies 0.01, 0.1, 1 and 10 Hz are applied and the power oscillations are found to be non-diverging. Analysis with sinusoidal pulses of various frequencies indicates that the reactor is stable even when Doppler feedback alone is considered.

4.3.1 *Reactor stability assessment with step reactivity perturbations*

Stability assessment of PFBR initial core is carried out at its nominal power by reactivity input in the form of pulses and sine waves. In the present study, the exact model of heat transfer is employed. The reactor does not SCRAM when the reactivity perturbation is input and thus the PPS (Plant Protection System) is assumed not to be functional. Pulse inputs of one second duration and amplitudes 0.1, 0.3, 0.5 and 0.95 $ were used. The reactivity pulse is input between 10 s and 11 s, and it is zero at all

other times. This is appropriate in this analysis since the time constant of reactivity feedback for the core is 2.9 s and the duration of 1 s is a good compromise to study feedback reactivity and power evolution. A shorter perturbation will give a benign effect and longer duration will be a problem for safety analysis (not a perturbation). The reactivity values are chosen to represent small and large values. 0.1 \$ is considered a small pulse, though it is conservative in that. For sake of illustration, large perturbation leading to near prompt critical (0.95 \$) has also been considered. The range of reactivity perturbations considers the entire possible range and this analysis is adequate to establish the stability of the reactor.

The results of analysis of the various reactivity perturbations are given graphically for the various cases. Figures 4.7 - 4.9 give the evolution of net reactivity and normalized power for reactor operating at full power and full flow conditions, and for the reactivity perturbation inputs of 0.1, 0.3 and 0.5 \$. Similar reactivity perturbations are considered for two more reactor operation conditions one with 40% power and 60% flow and another with 20% power and 50% flow. The results are given in Figures 4.10 to 4.15. The evolution of net reactivity and normalized power for near prompt critical (0.95 \$) perturbation for full power is given in Figure 4.16. A careful observation for reactivity inputs of 0.1, 0.3 and 0.5 \$ brings out the fact that power converges to original steady state value in few seconds without any oscillation in all the three operating conditions considered. The power is steady after reaching its original value. As the value of reactivity perturbation is more, the peak power reached is also more, as is expected.

Apart from this, a flow perturbation of 10% (increase) has also been assessed. The power increase is very small, and also it converges with time. Figure 4.17 shows the evolution of normalized power and net reactivity. Power goes up by 3% and reactivity 0.02\$. The power and reactivity evolutions are smooth without any oscillation. The various feedback reactivity components are shown in Figure 4.18. Thus the stability of PFBR core is established with range of reactivity pulse perturbations.

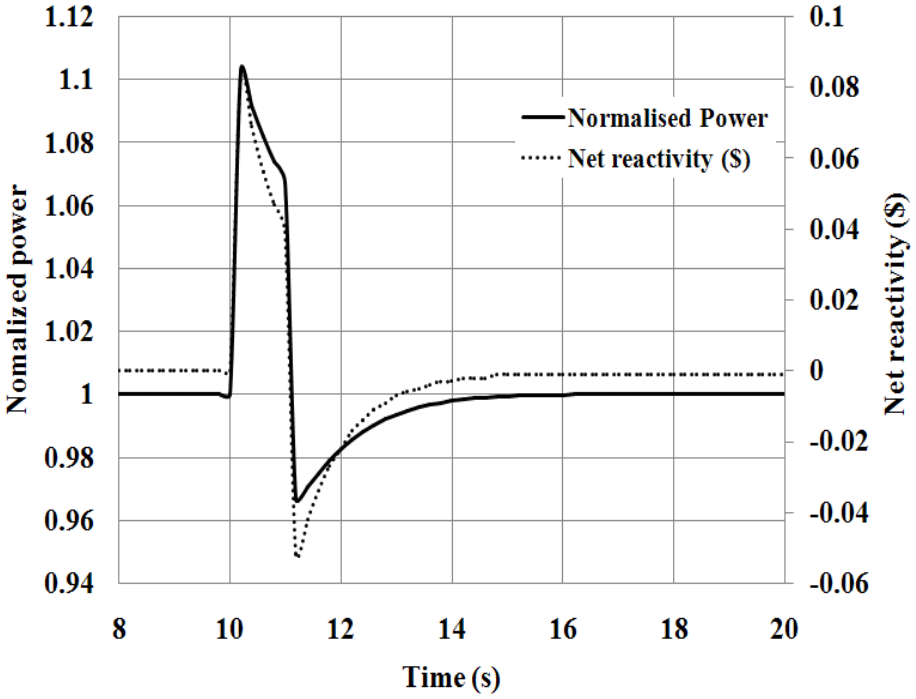

FIGURE 4.7: Initial power 100% and flow 100%, reactivity perturbation 0.1$.

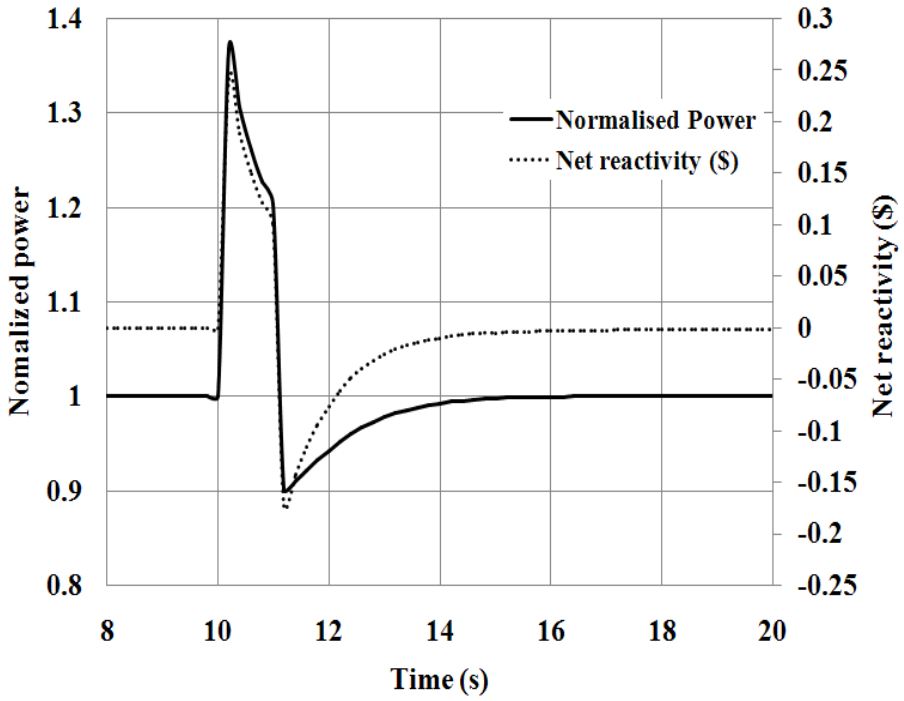

FIGURE 4.8: Initial power 100% and flow 100%, reactivity perturbation 0.3$.

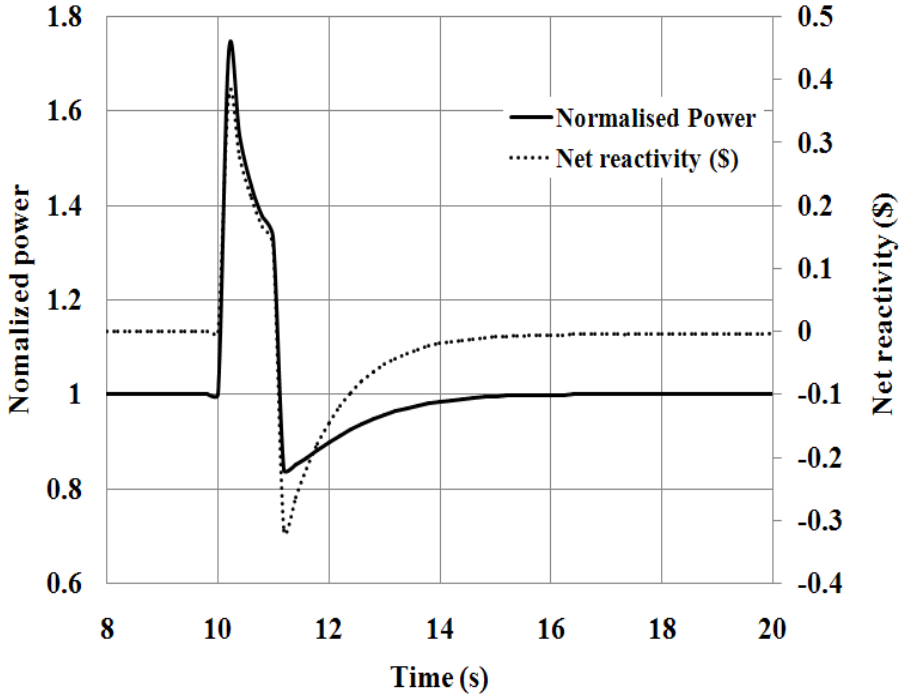

FIGURE 4.9: Initial power 100% and flow 100%, reactivity perturbation 0.5$.

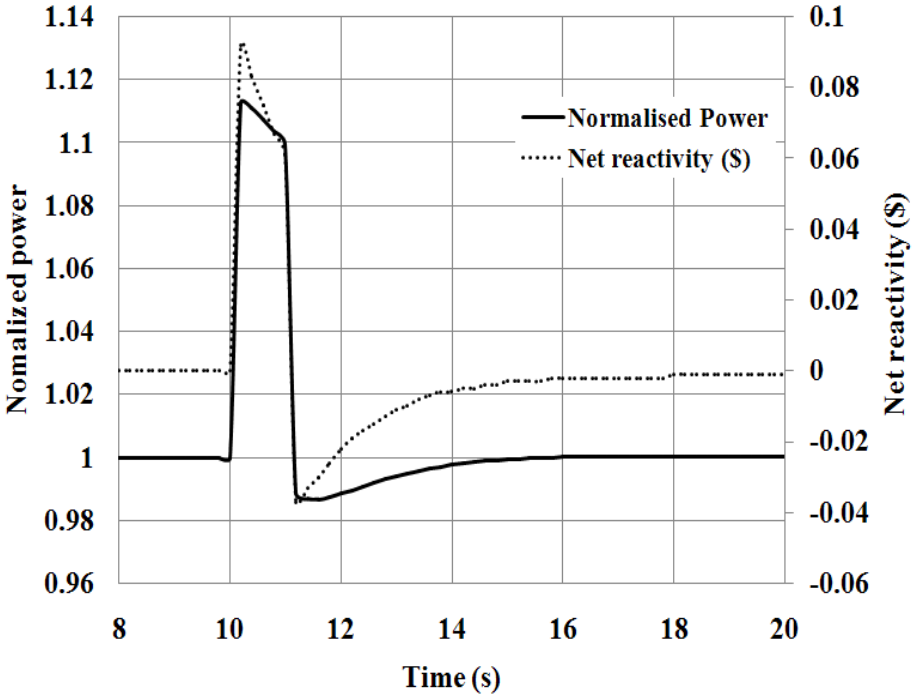

FIGURE 4.10: Initial power 40% and flow 60%, reactivity perturbation 0.1$.

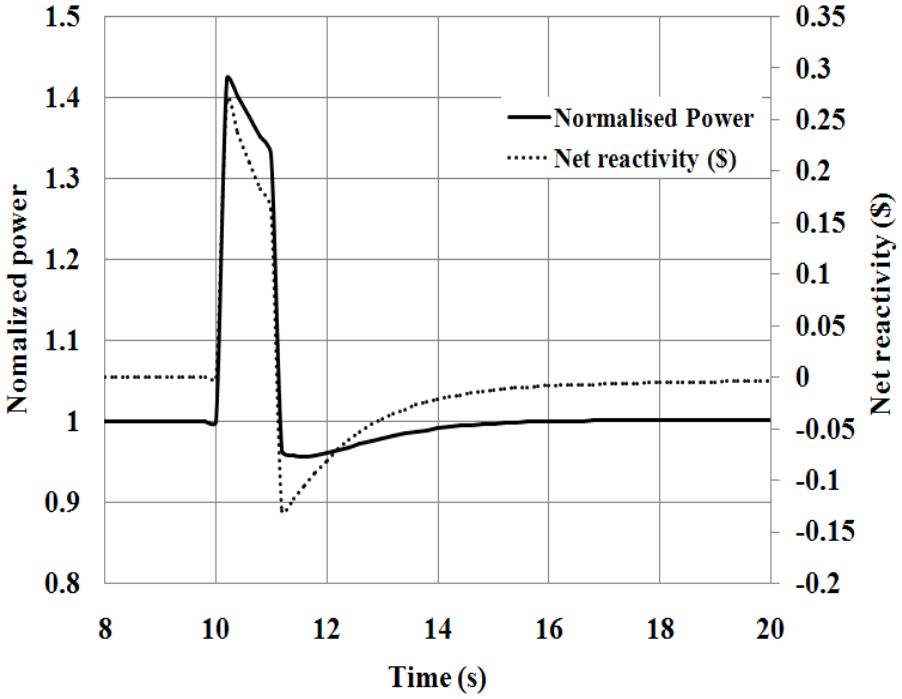

FIGURE 4.11: Initial power 40% and flow 60%, reactivity perturbation 0.3$.

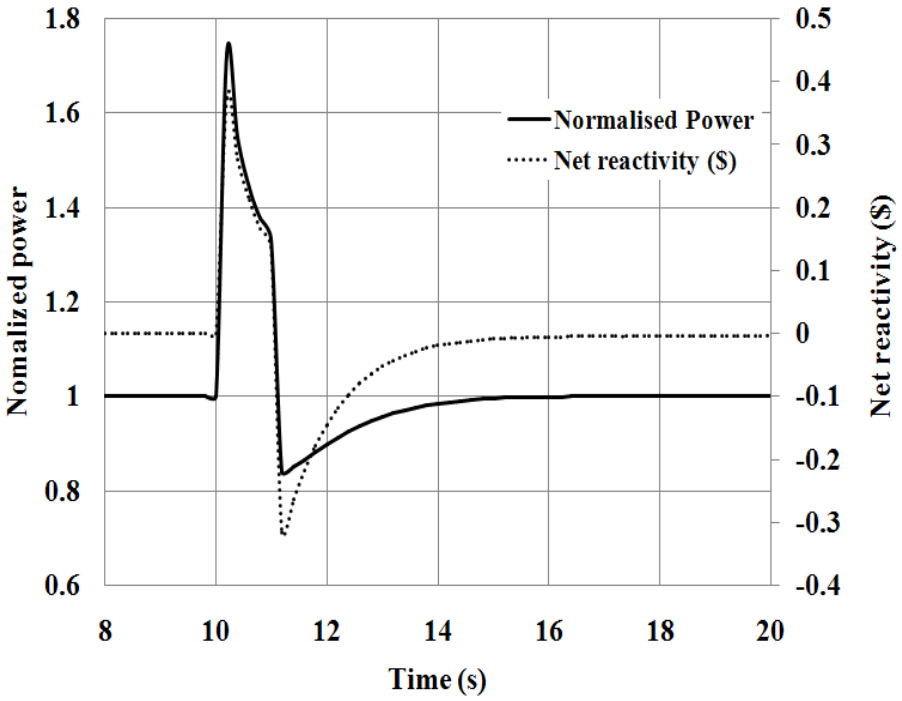

FIGURE 4.12: Initial power 40% and flow 60%,reactivity perturbation 0.5$

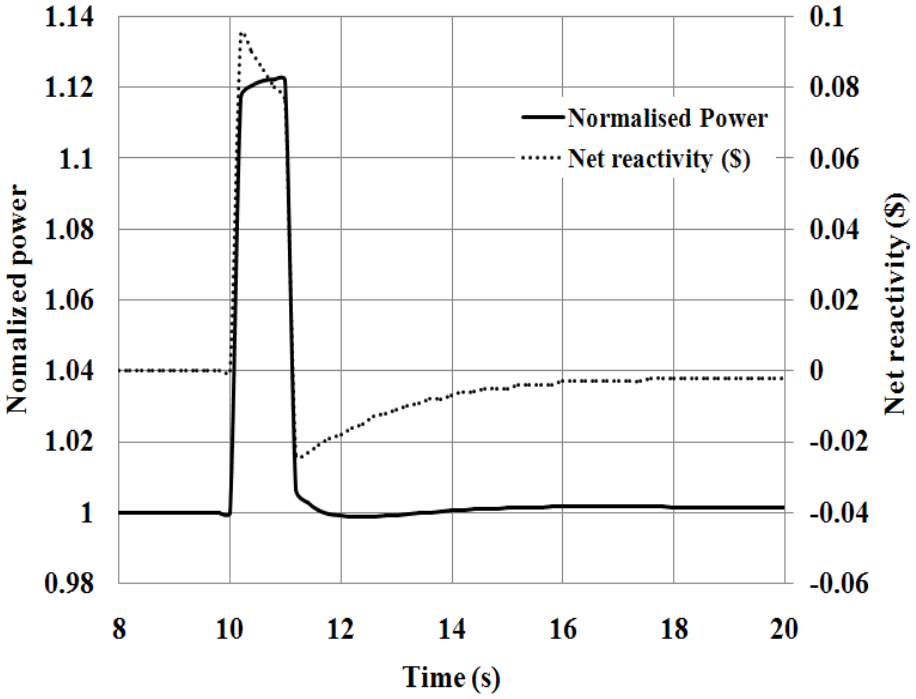

FIGURE 4.13: Initial power 20% and flow 50%, reactivity perturbation 0.1$.

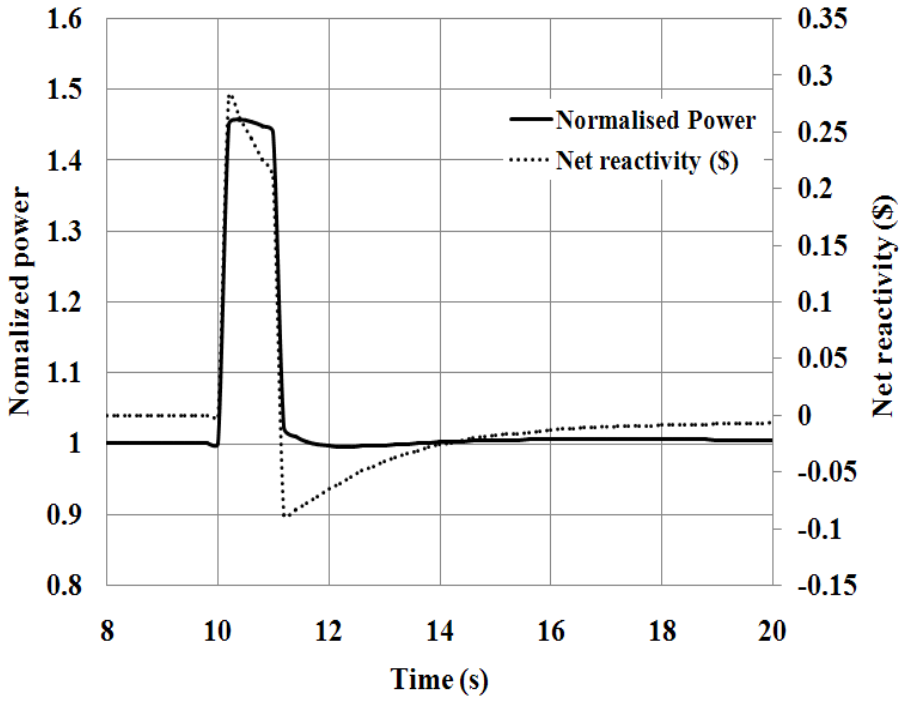

FIGURE 4.14: Initial power 20% and flow 50%, reactivity perturbation 0.3$.

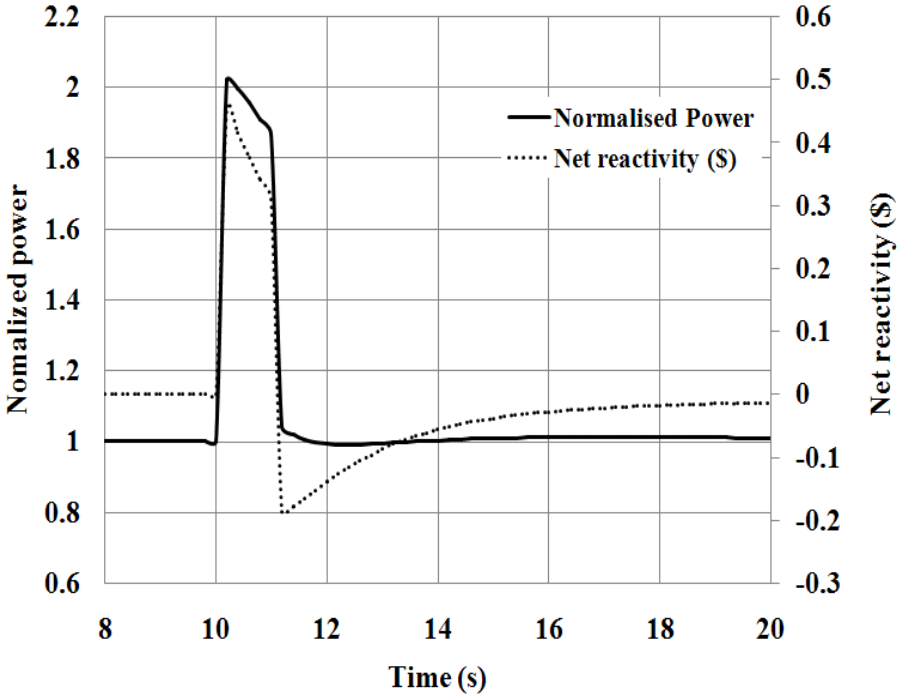

FIGURE 4.15: Initial power 20% and flow 50%, reactivity perturbation 0.5$.

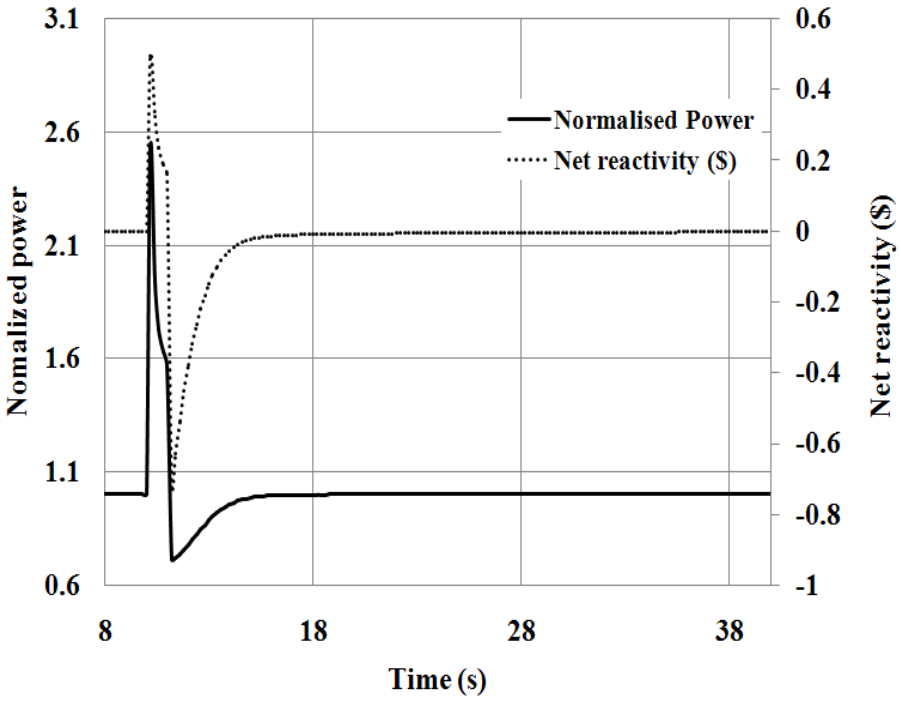

FIGURE 4.16: Initial power 100% and flow 100%, reactivity perturbation 0.95$.

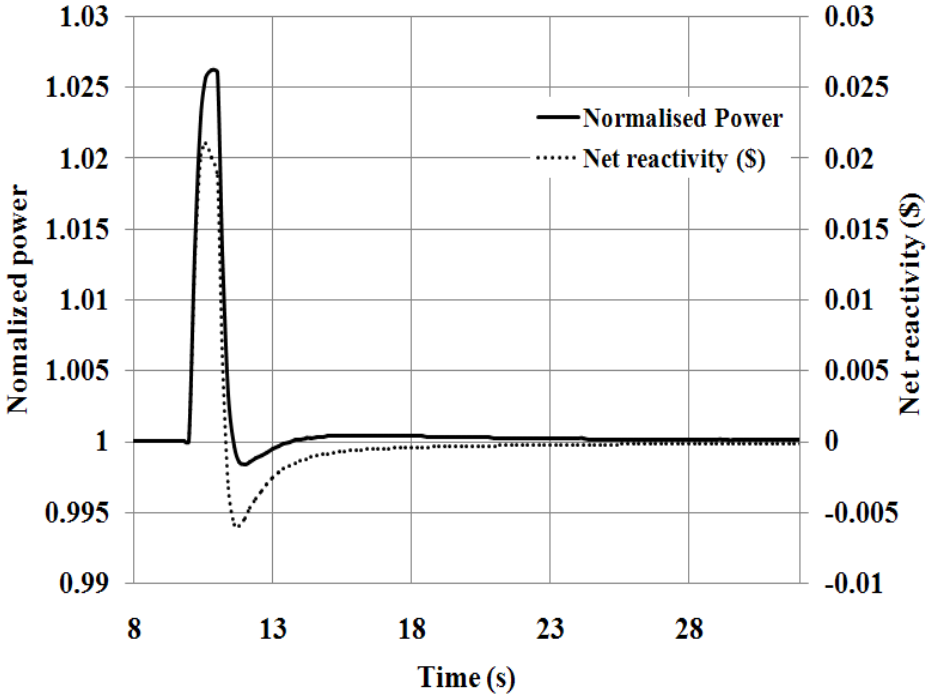

FIGURE 4.17: Initial power 100% and flow perturbation 10% increase.

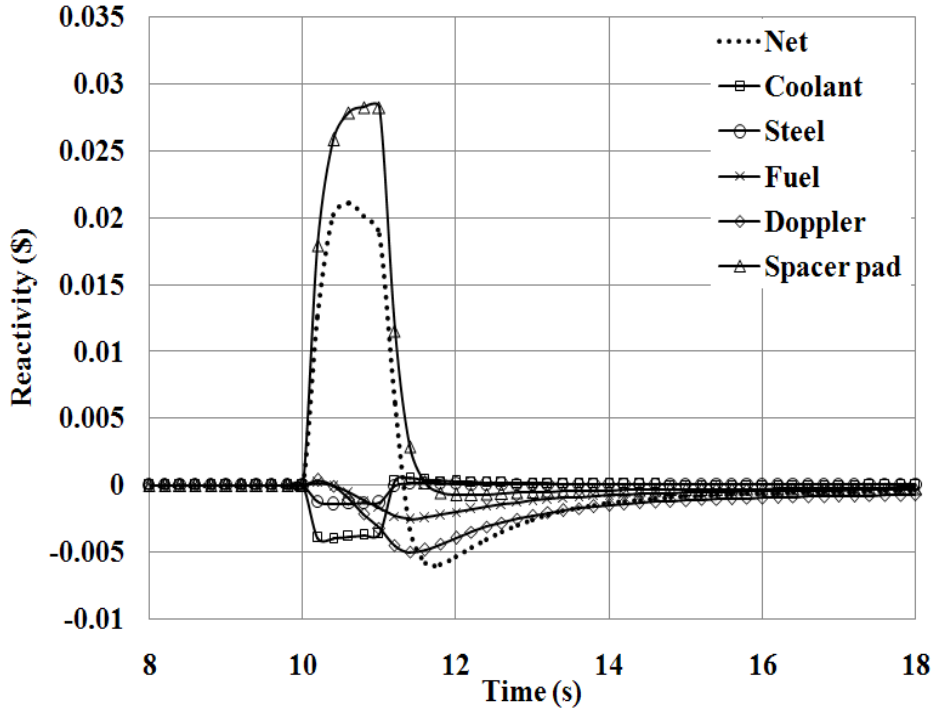

FIGURE 4.18: Components of reactivity feedbacks in case of flow perturbation.

4.3.2 *Assessment of core stability with sinusoidal reactivity perturbations*

It is also important to check reactor stability when the reactivity input is oscillatory in nature. Hence the reactor power, fuel temperature and coolant temperature evolution has been checked for various frequencies and with different reactivity feedback conditions.

A sinusoidal reactivity $\rho(t)$ expressed as, $\rho(t) = A\sin(\omega t)$ where, A is the amplitude and ω is the frequency. The consequence of sinusoidal reactivity input to reactor without feedbacks will be a constant increase of power. This is due to the absence of prompt neutrons when reactivity is negative. While when reactivity is positive, the reactor is controlled by both prompt and delayed neutrons, and when reactivity is negative, the reactor is controlled only by delayed neutrons (0.359%). The normalized power varies as

$$\rho_0 \left[|Z\left(i\omega\right)| Sin\left(\omega t + \phi\right) + \frac{1}{\omega\Lambda} \right]$$

where ρ_0 is the reactivity amplitude, Λ is the neutron generation time and ω is the frequency, $Z\left(i\omega\right)$ is the zero power transfer function. $Z\left(i\omega\right)$ is higher for low frequencies, and also in second term ω is in the denominator. Thus, increase is more for lower value of frequency, and also prompt neutron generation time. The increase is thus higher in case of fast reactors. However, in case of PFBR, we have negative reactivity feedbacks from Doppler fuel expansion and spacer pad expansion. Hence, the power increases for some time and then it saturates. Similarly, the fuel and clad temperatures also increase and then saturate.

The analysis had been carried out for frequencies 10, 1, 0.1 and 0.01 Hz and amplitude 0.5 \$. Reactivity amplitude of 0.5\$ has been chosen because seismic oscillations fall within maximum reactivity pulse of 0.3 \$. The computer code PREDIS has been used for the transient analysis with sinusoidal reactivity input. The calculations are performed with and without reactivity feedbacks. The reactor was stable when all the reactivity feedbacks were included. When all feedbacks were excluded, the power

increases with time and fuel temperature reaches melting point. The increase was more for lower frequencies. The study was carried out with perturbation worths based on ABBN – 93 cross section set.

The results of the present analysis are depicted in the form of graphs which give the variation of normalized power, peak fuel temperature and peak clad (steel) temperature with time. In all cases duration for 50 cycles of sine wave has been considered to precisely check the dependence on frequency. Hence, for each frequency duration of the plot is different.

Figure 4.19 gives the variation of normalized power, peak fuel temperature and peak clad (steel) temperature with time for $10Hz$ frequency with reactivity feedbacks and without reactivity feedbacks. Duration for 50 cycles (5 s) has been shown. It is seen that when all reactivities are considered, the trend of mean normalized power is uniform. In the beginning it goes down a little over small duration because fuel and steel temperatures have a small buildup time and hence the associated reactivity feedbacks. The fuel and clad temperatures saturate around 1420^0C and 607^0C, and remain well below their melting points (2750^0C for fuel and 1427^0C for clad). When the reactivity feedbacks are suppressed, we see a monotonically increasing trend for normalized power, fuel temperature and steel temperature. A more continuous evolution will lead to fuel and clad melting. Within first 50 cycles (5 s), they remain below melting points.

The variation of normalized power and peak fuel and clad temperatures with time are given in Figure 4.20, for a sinusoidal reactivity perturbation of frequency $1Hz$. The fuel and clad temperatures saturate around 1420^0C and 607^0C. Without reactivity feedbacks, normalised power continuously increases, fuel temperature and steel temperature follows that. Fuel temperature touches melting point at 35 s.

In case of input reactivity fluctuations of $0.1Hz$ the normalised power variation is similar to that with $10Hz$ and $1Hz$ perturbations. Figure 4.21 gives the variation of normalized power, peak fuel temperature and peak clad temperature with time, with and without reactivity feedbacks, for a duration of 50 cycles (500 s). The fuel and clad

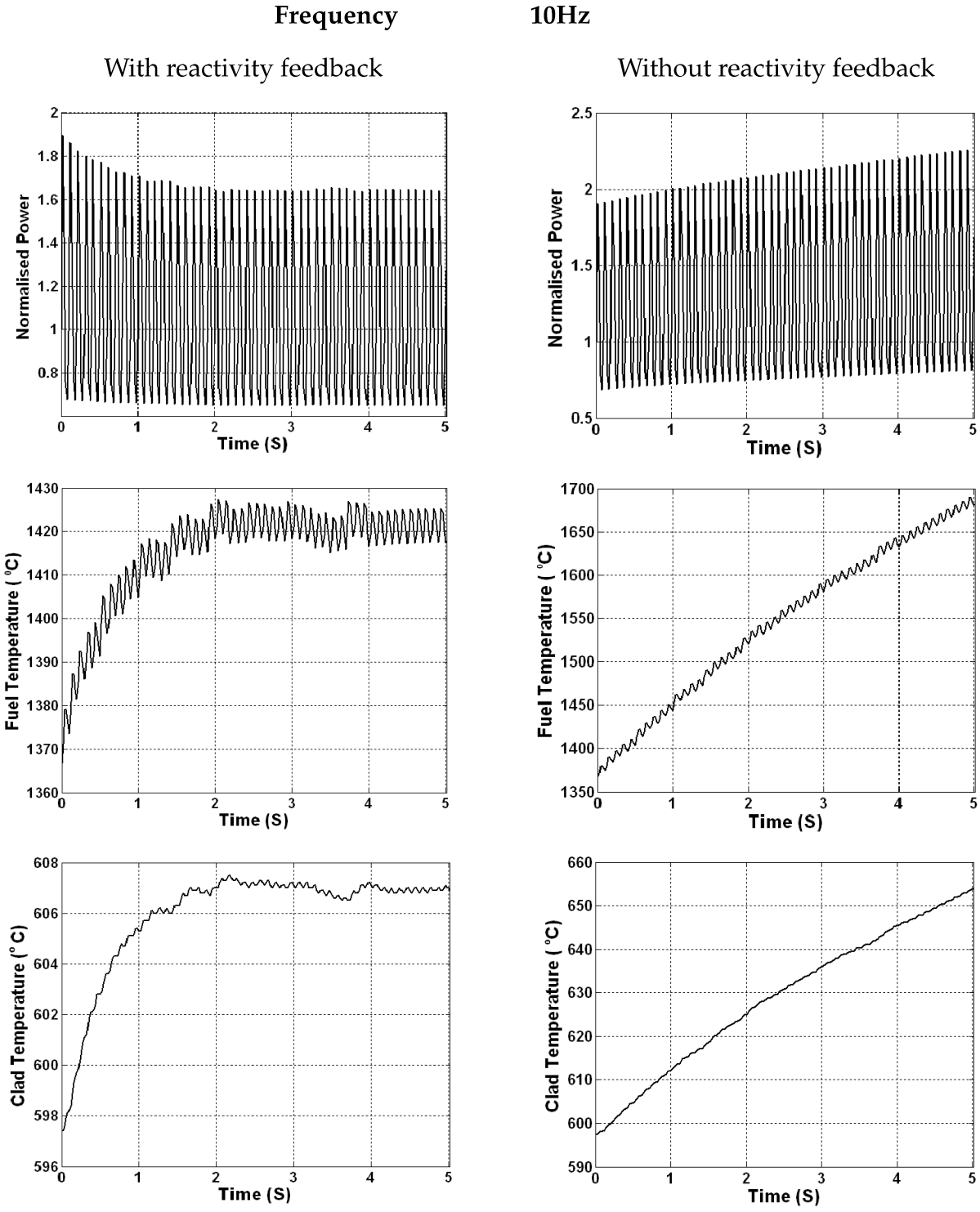

FIGURE 4.19: Variation of normalized power, fuel temperature and clad temperature with time for frequency 10 Hz, with and without feedback.

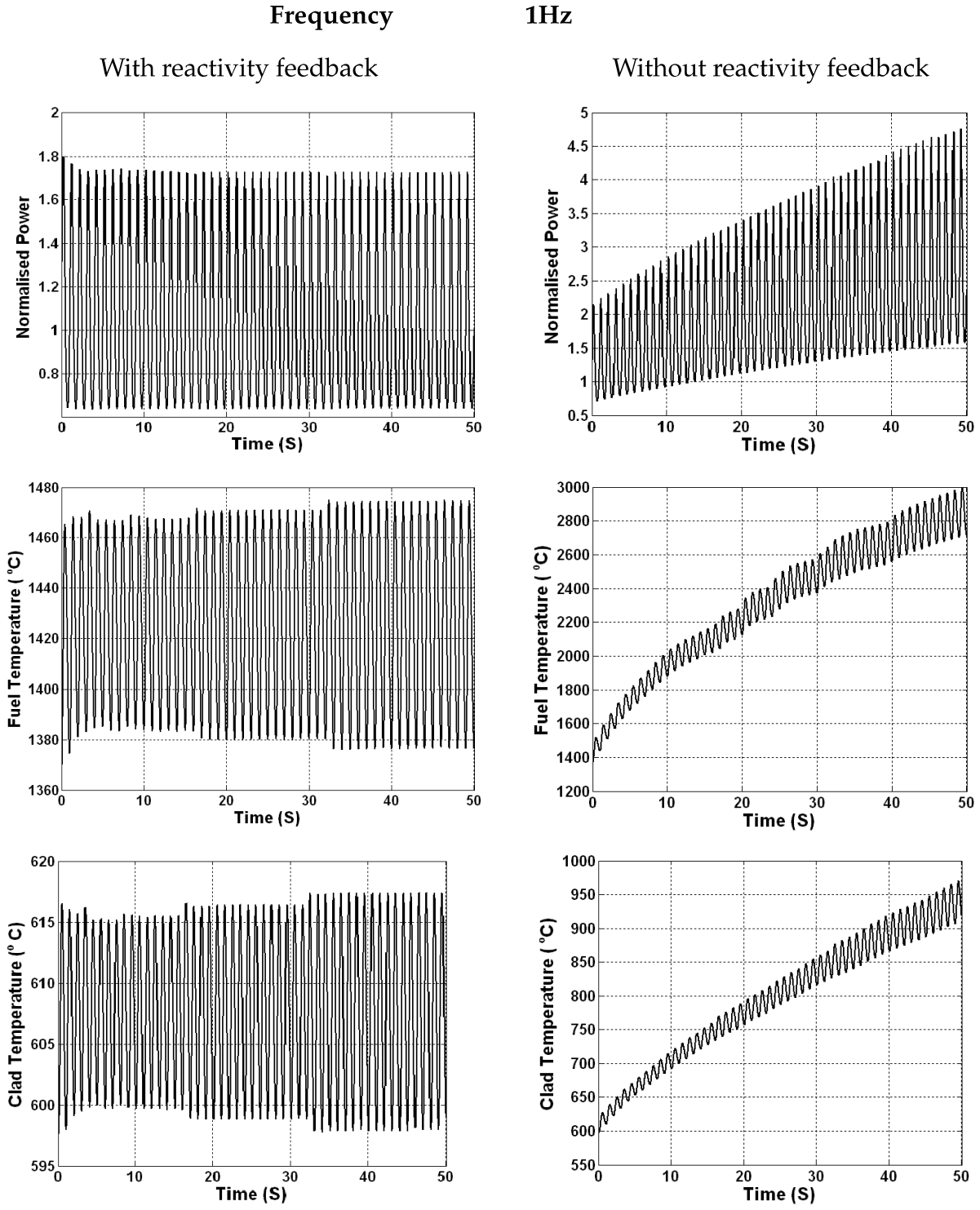

FIGURE 4.20: Variation of normalized power, fuel temperature and clad temperature with time for frequency 1 Hz, with and without feedback.

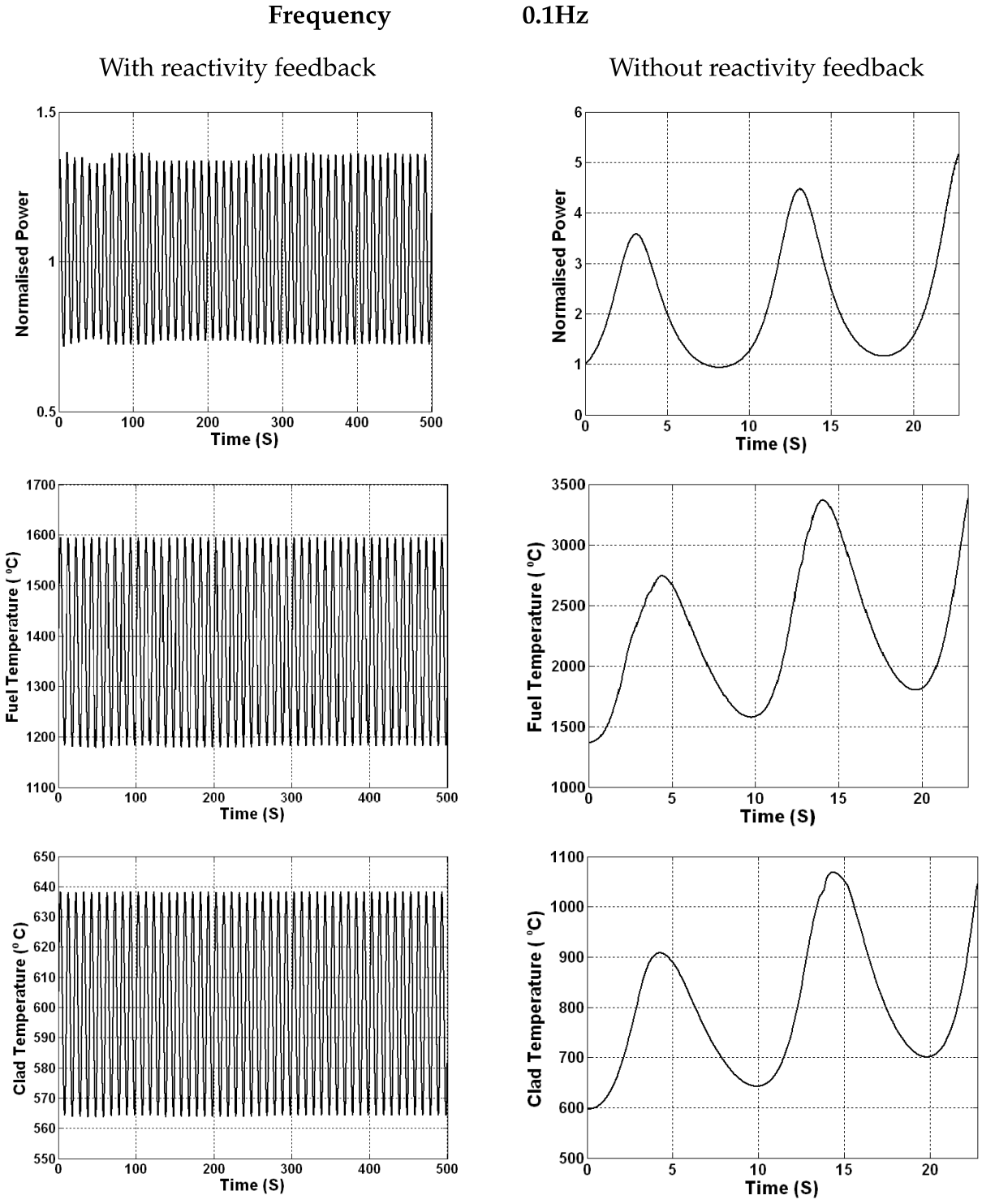

FIGURE 4.21: Variation of normalized power, fuel temperature and clad temperature with time for frequency 0.1 Hz, with and without feedback.

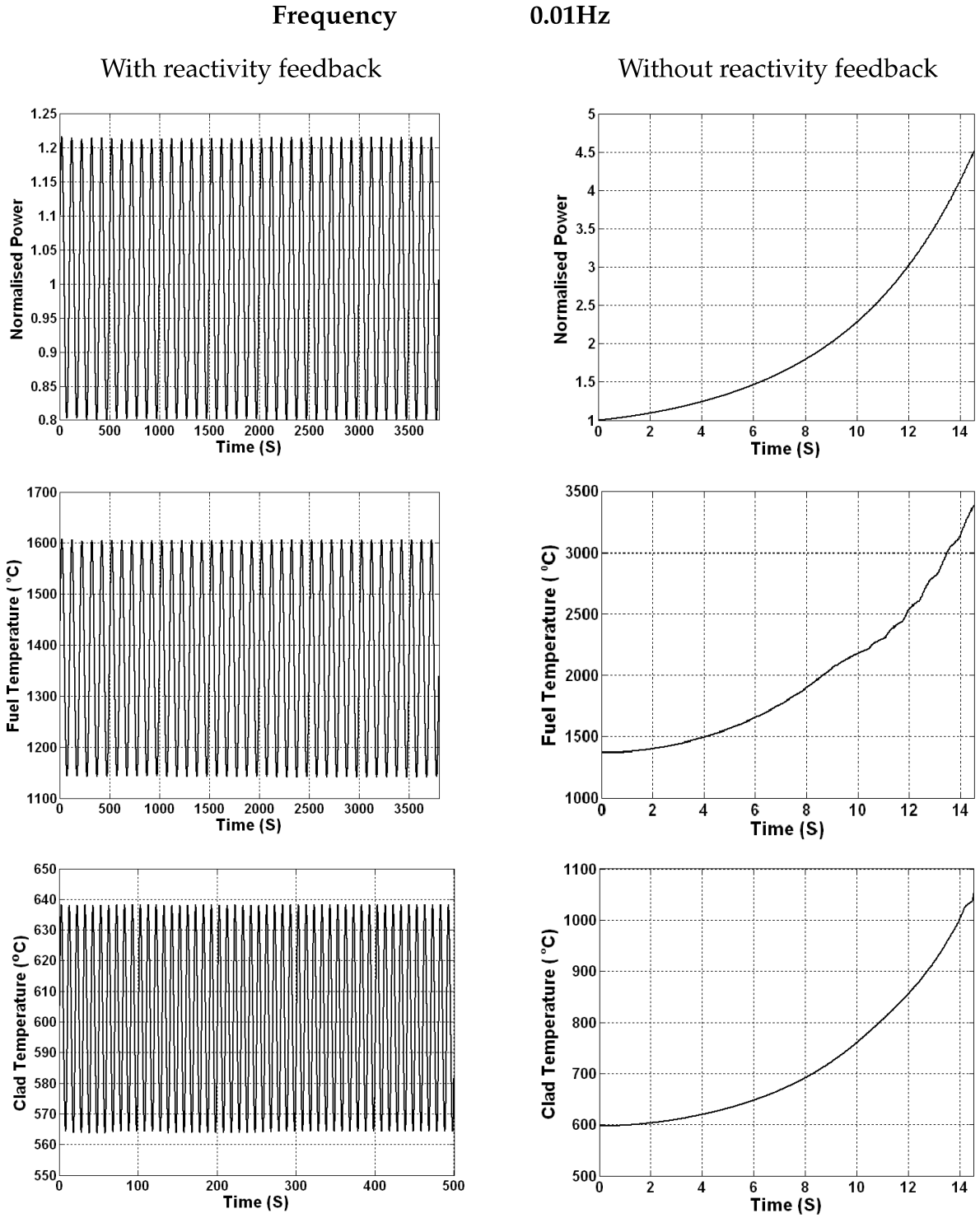

FIGURE 4.22: Variation of normalized power, fuel temperature and clad temperature with time for frequency 0.01 Hz, with and without feedback.

temperatures saturate around 1400^0C and 600^0C, which are well below their melting points. When the reactivity feedbacks are suppressed, reactor power and temperatures increases and fuel reaches melting point at 12 s.

Figure 4.22 gives the variation of normalized power, peak fuel temperature and peak clad temperature with time for a sinusoidal reactivity perturbation of frequency $0.01Hz$ with and without reactivity feedbacks. Duration for 50 cycles (5000 s) has been shown. When all reactivities are considered, in the beginning the normalised power goes down a little over small duration because expansion feedbacks have a buildup time. But this is not visible in the picture because it has been plotted for long duration (5000 s). The fuel and clad temperatures saturate around 1350^0C and 600^0C.

4.4 Summary

- One group space dependent non-linear reactor dynamics equation for a typical FBR with fuel, steel and coolant temperature feedbacks is studied using bifurcation theory for stability. It is concluded from this study that FBR has unique stable solution within the operating regime without any non-trivial bifurcations.

- The nonlinear stability analysis is carried out for PFBR core by studying step and sinusoidal reactivity perturbations. It is established that reactivity feedbacks in PFBR assure the safety and stability of the reactor. When the reactivity feedbacks are suppressed, the fuel temperature goes up, reaches melting point after few power cycles when frequency is not very low (case of 1 Hz) and within the first cycle when reactivity is building up (case of 0.1 Hz and 0.01 Hz).

- In all cases of sinusoidal reactivity input, the reactor is stable with fuel and steel temperatures saturating far below their melting point when feedbacks are included.

Chapter 5

Response of SFR Core to Reactivity Oscillations Due to Seismic Events

5.1 Introduction

In this chapter, reactivity oscillations in a nuclear reactor due to seismic events are studied. Seismic vibrations can cause significant reactivity oscillations in an SFR core and its impact has to be studied. The stability of the core against such reactivity oscillations is to be ensured. The stability in the mathematical sense may not be adequate to ensure the safety of the core, because even in a stable core the system temperatures may cross the allowed limits under severe reactivity oscillations. To address this issue detailed safety analysis is essential and it is a major requirement in the design of nuclear reactors. The seismic analysis has been considered as one of Design Basis Events (DBEs) and Design Extension Conditions (DECs). DBEs are those events for which there are design provisions to arrest the consequences and the Plant Protection System (PPS) is functional. Integrity of core components are retained for DBE. DECs are those events in which PPS fails on demand and can result in severe consequences.

DBEs fall in 4 categories; normal, upset, emergency and faulted events. These are also referred as Category I, II, III and IV events with associated probability ranges for occurrence (Table 5.1) [49], [69]. Seismic events are one class of many events, that lead to DBEs. Seismic events arise due to natural consequences. It is very essential to assess

TABLE 5.1: Categorization of Design Basis Events.

Event Category	Frequency of occurrence per reactor year (ry)
I (Normal Operation)	$f > 1/ry$
II (Upset)	$10^{-2} < f \leq 1/ry$
III (Emergecy)	$10^{-4} < f \leq 10^{-2}/ry$
IV (Faulted)	$10^{-6} < f \leq 10^{-4}/ry$

the safety potential of the reactor under seismic conditions and affirm that the reactor is completely safe.

In the event of an earthquake, vibrations will be caused in the main vessel and internals of LMFBR [70]–[72]. Under vertical excitation, reactivity changes occur due to relative motion between Control and Safety Rods (CSRs) and core [73], [74]. It is essential to establish that the fuel clad and coolant hot spot temperatures fall within safe limits due to power fluctuations because of reactivity fluctuations. Two reference earthquakes are addressed. They are, (a) Operating Basis Earthquake (OBE) and (b) Safe Shutdown Earthquake (SSE) [75]. OBE is the earthquake that could be expected to affect the site of a nuclear reactor, but for which the plant's power production equipment is designed to remain functional without undue risk to public health and safety. This is categorized as an emergency event. SSE is the maximum earthquake potential for which certain structures, systems, and components, important to safety, are designed to sustain and remain functional. This event is more severe and less probable than OBE and categorized as faulted event. Hence, under SSE conditions some systems can fail, but shutdown shall be possible.

For PEC (Prova Elementi Combustibile) experimental reactor core (118 MWth) reactivity oscillations with peak amplitude of 0.64 $ face to face and 0.67 $ corner to corner has been considered in design, with a limiting value of 0.79 $. The fuel temperature

remains below melting point [73]. For SNR-2 loop type power reactor core (3420 MWth) the peak reactivity reaches up to 0.1 $ and varies with a basic frequency of 7.5 Hz. Fuel temperature is well below its melting point, and it reaches the melting point only for peak reactivity amplitude of 1.02 $ [74].

In the present study, the safety aspect of a SSE has been analyzed for PFBR equilibrium core. The core configuration is given in Figure 3.10 and the salient aspects of the core can be found in Table 3.2. The stability of the core is demonstrated using Nyquist criteria and the results are discussed in section 3.4. Here the seismic safety analysis is carried out for the same core. The calculations are carried out considering it in the seismic zone II; seismic intensity VI on Modified Mercalli Intensity scale, Ritcher Magnitude 5.0 to 5.9. The ground acceleration for SSE and OBE for PFBR are 0.156 g and 0.076 g. The peak magnitude of the reactivity oscillations is estimated to be below 0.4 $ and the frequency spectrum is dominant in the range of 7 to 10 Hz. The safety credential established by SSE analysis will also form an envelope to OBE, which is a less severe event. In section 5.2 the analysis methodology used is described. The transient analysis carried out with reactivity fluctuations is described in section 5.3.

5.2 Analysis methodology

The transient analysis of the reactivity fluctuations has been carried out by using the computer code PREDIS. The processes modeled in the code are neutronics, transient thermal hydraulics, reactivity feedbacks. The net reactivity ρ is the sum of both external and feedback reactivities.

$$\rho(t) = \rho_{ext}(t) - \rho_{fb}(t) \tag{5.1}$$

The 500 MWe FBR core consists of 181 fuel sub-assemblies of two different enrichments, 85 sub-assemblies in the inner core are of lower enrichment and 96 in the outer core are of a higher enrichment. There are nine control and safety rods (CSR) and three

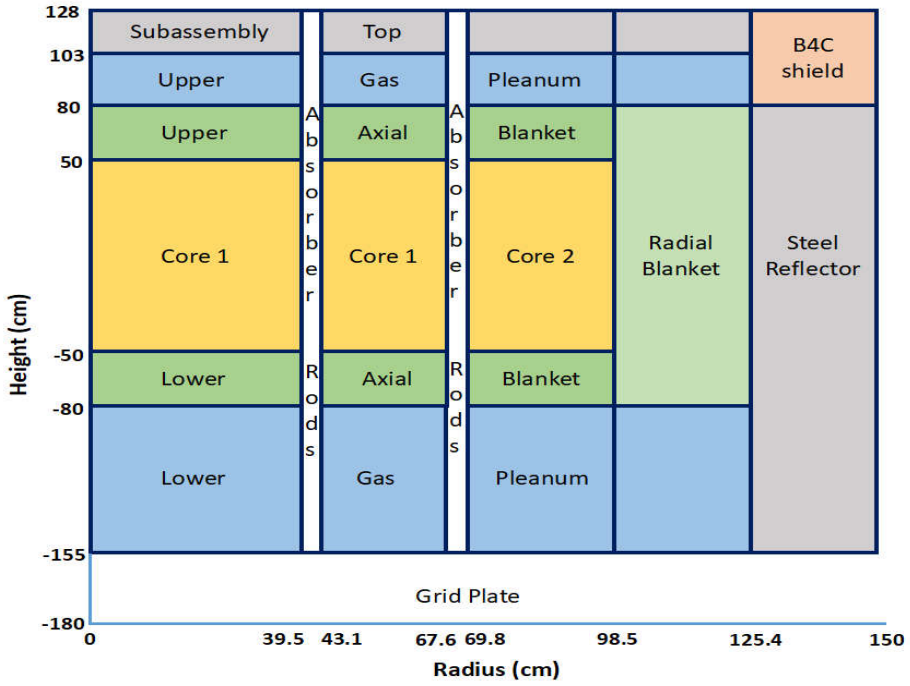

FIGURE 5.1: R-Z model of PFBR core.

diverse safety rods (DSR). The R-Z view of the reactor is shown in Figure 5.1. The cylindrical core is divided into 10 radial channels and 14 axial rows for the analysis. The first four radial channels correspond to inner core, next three for outer core, and the last three for radial blanket. The upper and the lower two axial rows correspond to Upper Axial Blanket and Lower Axial Blanket. The ten rows between the UAB and LAB correspond to active core. Each radial channel is represented by a pin.

The reactivity worths data used for the calculations are computed using ABBN-93 cross section set. Table 5.2 gives integral reactivity worths for fuel, steel (clad and wrapper), coolant and Doppler constant. Reactivity worth of fuel is the amount of reactivity added into the core due to removal of fuel. The reactivity worths are given for both core alone (fissile region) and whole core (fissile + radial and axial blanket) cases separately.

TABLE 5.2: Reactivity worths for PFBR.

Parameter	Core alone	Whole reactor
Fuel worth (pcm)	-35530	-35778
Steel worth (pcm)	4015	3162
Coolant worth (pcm)	888	604
Doppler constant (pcm)	-639	-746

5.3 Transient analyses

Two sets of calculations have been done for the transient analysis. In both cases the reactor is assumed to be operating at full power.

- First, response of the reactor is studied to the sinusoidal reactivity input with 0.5 $ amplitude and frequencies of 7 Hz and 10 Hz to understand the behavior of reactivity oscillation. The reactivity oscillate between a minimum value of - 0.5 $ and a maximum value of + 0.5 $
- Secondly, response of the reactor to seismic excitation is analyzed. The reactivity oscillations in case of SSE are obtained using the perturbation theory based boundary movement worths and SA movements with CORESEIS [76], [77] code.

5.3.1 *Simulation of reactivity fluctuations due to SSE*

CORESEIS is a 3D code capable of modeling the full reactor core under seismic conditions. Each sub-assembly is modeled as a 3D beam with pinned boundary conditions at the bottom and top plates of grid plate. Fluid structure interaction is considered by lumping the added mass at the beams. In CORESEIS, the load pad impact is modeled by linear spring and dash-pot along with the required gap. The reactivity oscillations due to seismic vibrations are estimated using the sub assembly reactivity

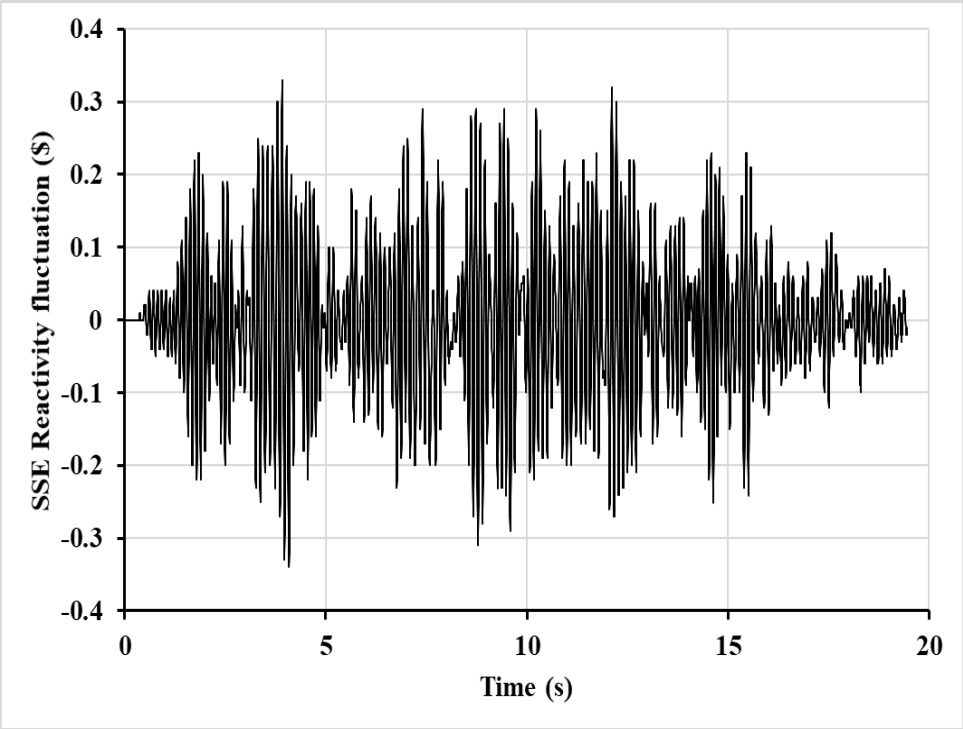

FIGURE 5.2: Input reactivity fluctuations for SSE.

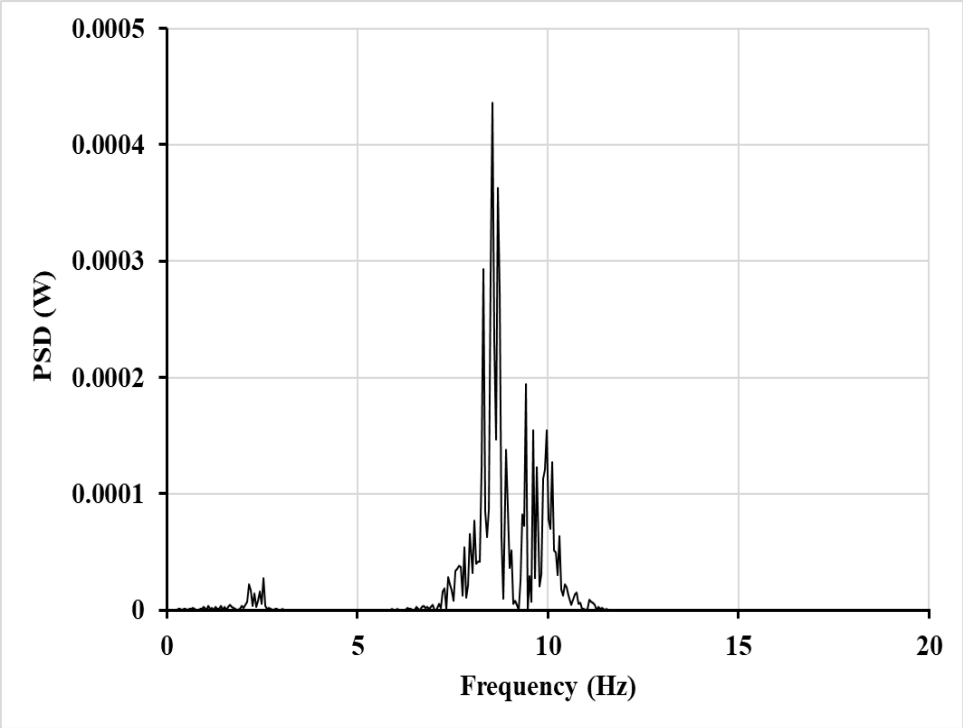

FIGURE 5.3: Spectrum of SSE reactivity fluctuations.

worth data and the relative motion of sub-assemblies. These oscillations in case of SSE as calculated using CORESEIS is given in Figure 5.2 [78]. The frequency spectrum of the above oscillation is given in Figure 5.3. It is found that the magnitude of the reactivity oscillations are below 0.4 $ and the frequency spectrum is in the range of $7Hz$ to $10Hz$, the Power Spectral Density (PDS) outside this range being negligible.

5.3.2 *Analysis with sinusoidal reactivity*

A study of sinusoidal reactivity input with higher amplitude compared to seismic reactivity input, and frequencies in the sensitive frequency range of SSE spectrum is of interest. The SSE reactivity fluctuations are to a great extent less than 0.2 $. Hence, reactivity amplitude of 0.5 $ has been studied, with frequencies 7 Hz and 10 Hz.

A sinusoidal reactivity, $\rho(t)$ is expressed as,

$$\rho(t) = \rho_0 Sin(\omega t) \tag{5.2}$$

where ρ_0 is the reactivity amplitude and ω is the frequency. The power evolves with time as [8], [79]

$$P(t) = P_0 \left[1 + A_1(\omega)\, Sin(\omega t) + \frac{\omega \rho_0}{\Lambda}\right] \tag{5.3}$$

where ω is the frequency, Λ is the neutron generation time and A_1 is a function of ω, $P(t)$ is the power at time t, and P_0 is the initial power. The consequence of sinusoidal reactivity input to reactor without feedbacks is increase of power. This is due to the absence of prompt neutrons when reactivity is negative. While when reactivity is positive, the reactor is controlled by both prompt and delayed neutrons, and when reactivity is negative, the reactor is controlled only by delayed neutrons. Hence the envelope of net reactivity comes down initially and then saturates to lower value. Accordingly the envelope of power also comes down initially and saturates to lower value. The fuel and clad hot spot temperatures increase initially and then saturate.

TABLE 5.3: Design safety limits for category I and II events.

Temperature	Category of event	
(K)	I	II
Fuel Hot Spot	No melting	No melting
	(2998)	$(2998)^*$
Clad Hot Spot	973	973 to 1023 for 75 min and
		1023 to 1073 for 15 min
Coolant Hot Spot	No bulk coolant boiling	
	No burnout in local hot spots	

$*$ Fuel melting point

TABLE 5.4: Channel hot spot factors.

Temperature rise across	Clad mid-wall	Fuel Center
Channel	1.1000	1.1504
Film	2.3088	1.3109
Clad	1.4014	1.2656
Gap	-	1.3887
Fuel	-	1.2712

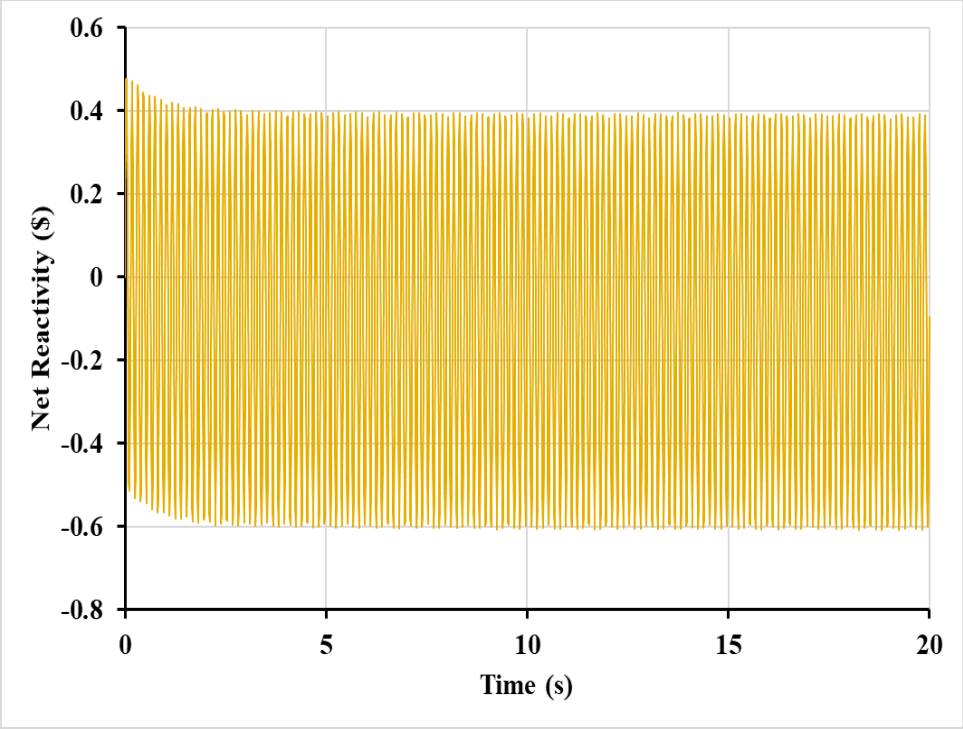

FIGURE 5.4: Net reactivity fluctuations for input sinusoidal reactivity amplitude 0.5$ frequency 7 Hz.

Behavior of net reactivity for sinusoidal reactivity input of amplitude 0.5 $ and frequency of 7 Hz is shown in Figure 5.4. It is seen that the amplitude is damped due to reactivity feedback effects. The envelope of net reactivity comes down and remains constant. This is also due to reactivity feedbacks. Figure 5.5 shows the normalized power profile. Similarly, the envelope of normalized power also comes down due to reactivity feedback effects. The Design Safety Limits (DSLs) for category I and II events have been given in Table 5.3 [69], [80]. The channel hot spot factors applicable to clad mid-wall and fuel center are given in Table 5.4 [81]. Figure 5.6 shows the peak fuel hot spot temperature and Figure 5.7 shows the peak clad hot spot temperature for sinusoidal reactivity input of amplitude 0.5 $ and frequency 7 Hz. Figure 5.8 and Figure 5.9 show the same for amplitude of 0.5 $ and frequency of 10 Hz. It is seen that both fuel and clad hot spot temperature remain below category-I DSL (2998 K for fuel, 973 K for clad).

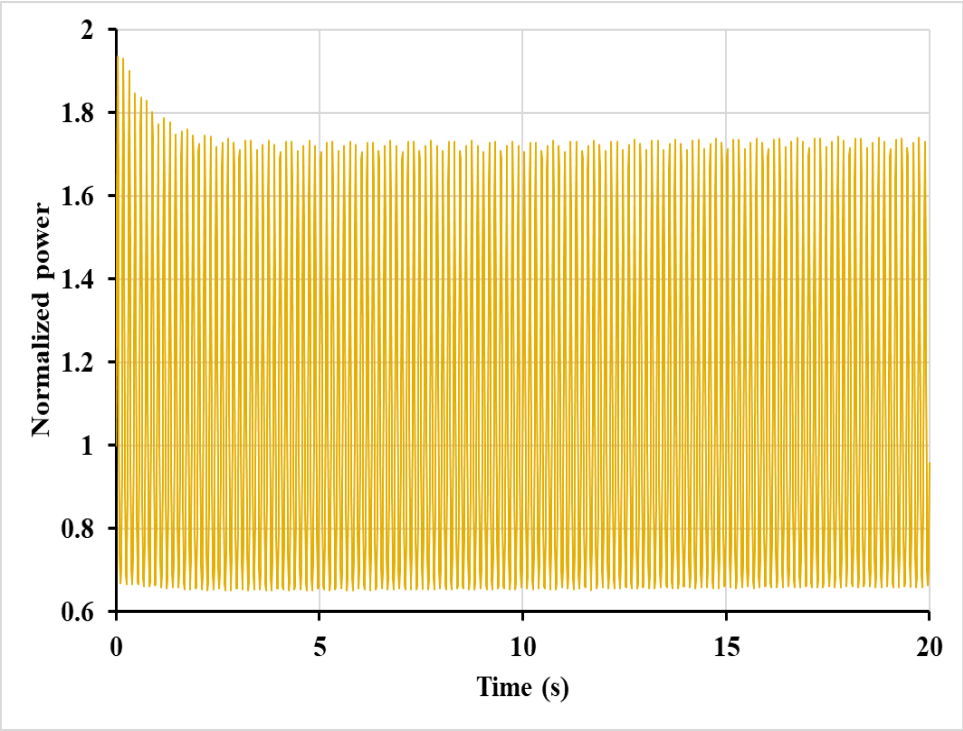

FIGURE 5.5: Normalized power fluctuations for input sinusoidal reactivity amplitude 0.5 $ frequency 7 Hz.

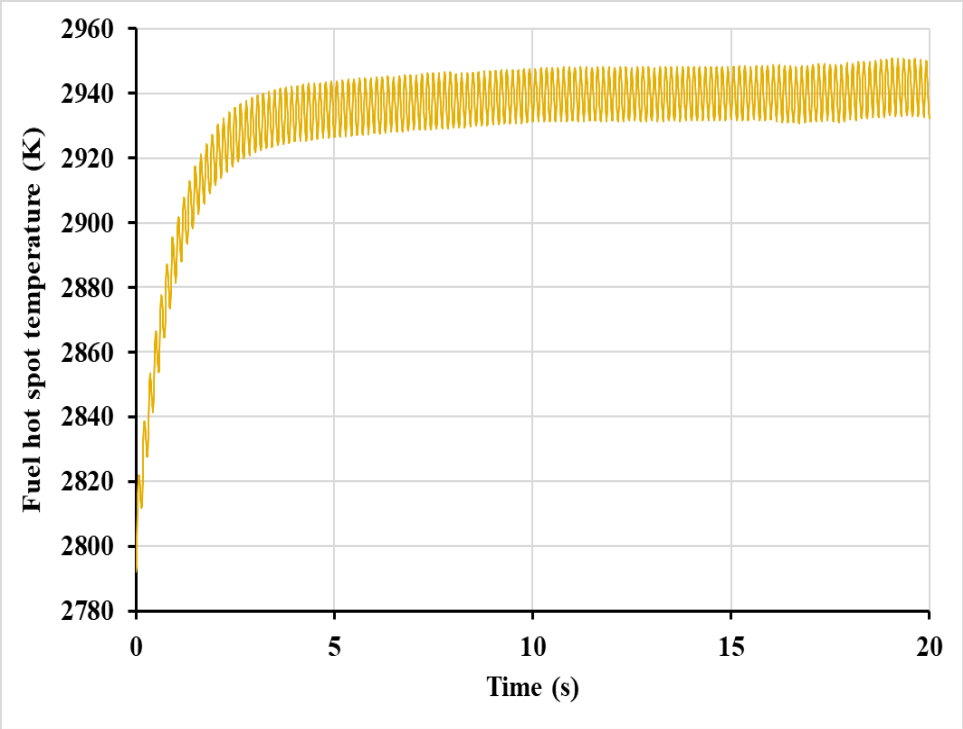

FIGURE 5.6: Sinusoidal reactivity input (0.5 $, 7 Hz) Fuel hot spot temperature.

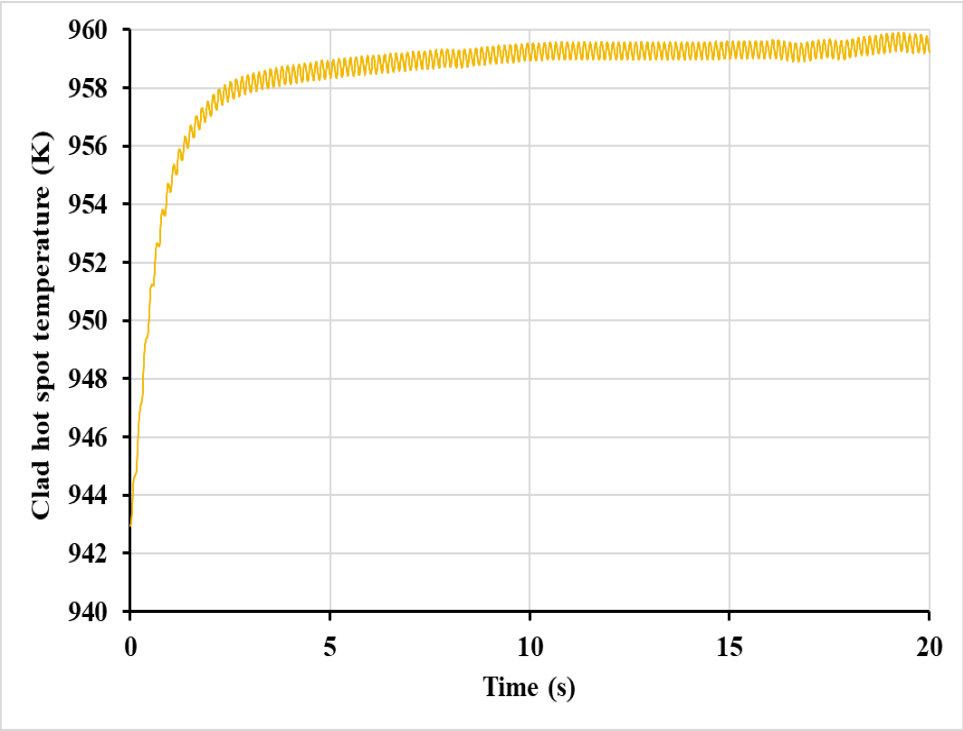

FIGURE 5.7: Sinusoidal reactivity input (0.5 $, 7 Hz) Clad hot spot temperature.

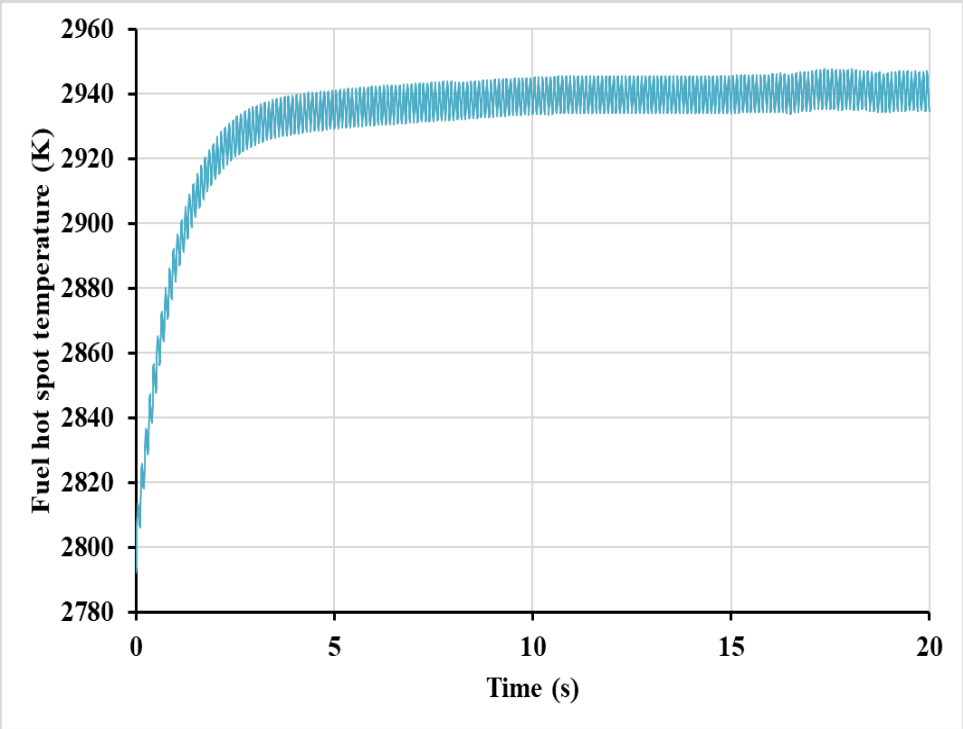

FIGURE 5.8: Sinusoidal reactivity input (0.5 $, 10 Hz) Fuel hot spot temperature.

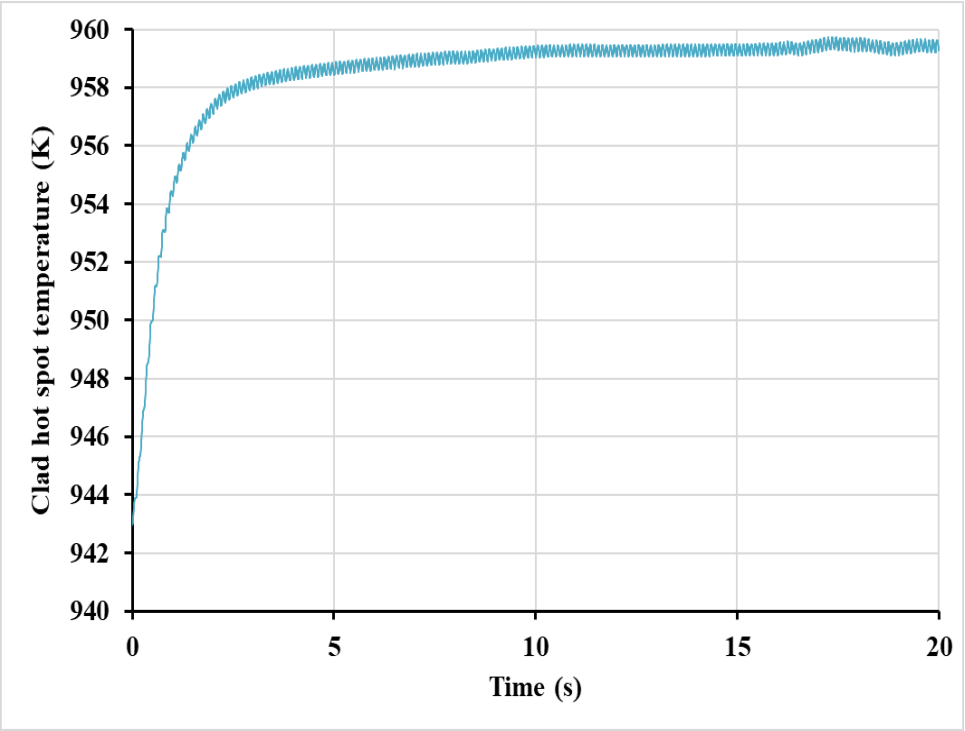

FIGURE 5.9: Sinusoidal reactivity input (0.5 $, 10 Hz) Clad hot spot temperature.

5.3.3 *Analysis with seismic excitation reactivity input*

The net reactivity fluctuations computed from the input reactivity fluctuations of Figure 5.2 for SSE is given in Figure 5.11. It is seen that the net reactivity fluctuates vary with positive and negative values. Out of 3892 pulses over the 20s period, 156 pulses are more than 0.2 $, 9 pulses are more than 0.3 $, 146 pulses are less than -0.2 $ and 9 pulses are less than -0.3 $. The peak pulse is 0.33 $. Here also the dampening effect of reactivity feedback effects is seen. The mean value of reactivity fluctuations is –0.0084 $ over the 20s period. Figure 5.10 shows the normalized power fluctuations and Figure 5.11 shows the net reactivity fluctuations. Figure 5.12 shows the behavior of peak fuel hot spot temperature and Figure 5.13, peak clad hot spot temperature. The fuel hot spot temperature attains highest value of 2835 K and clad hot spot temperature 946 K. Hence, the fuel and clad hot spot temperatures remain below category-I DSL, which corresponds to normal operation.

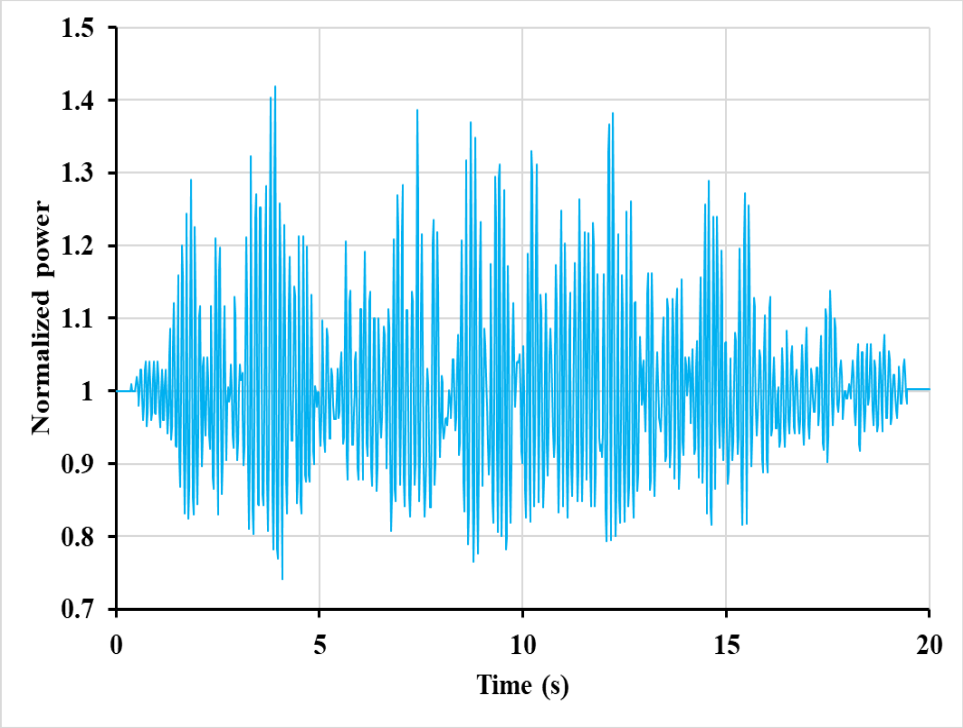

FIGURE 5.10: Fluctuations in normalized power for SSE input reactivity.

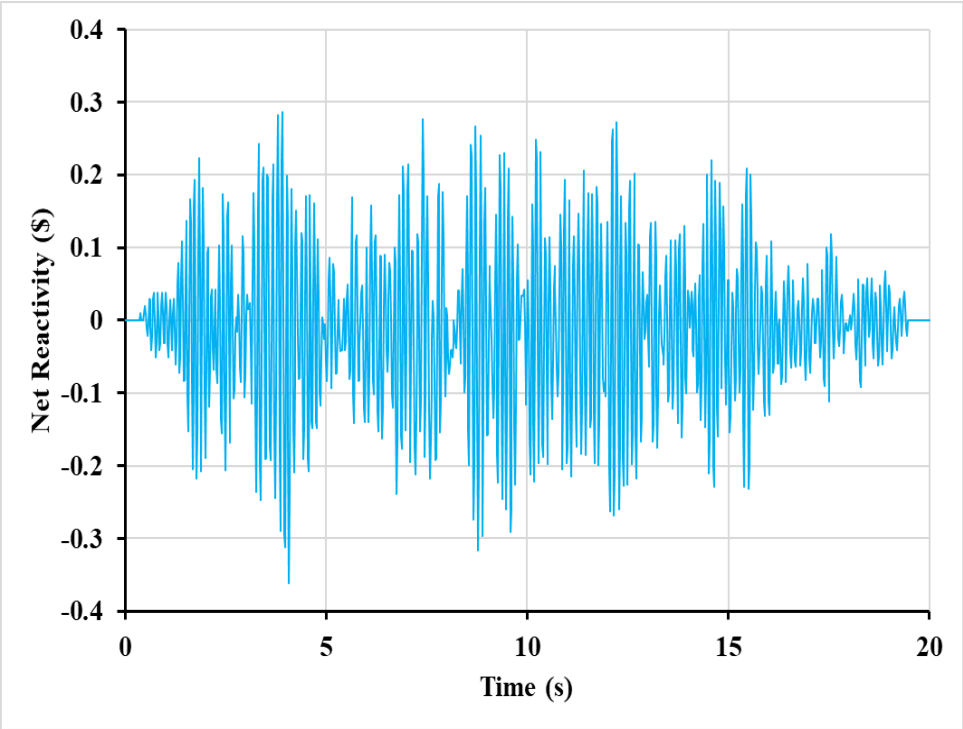

FIGURE 5.11: Net reactivity fluctuations for SSE input reactivity.

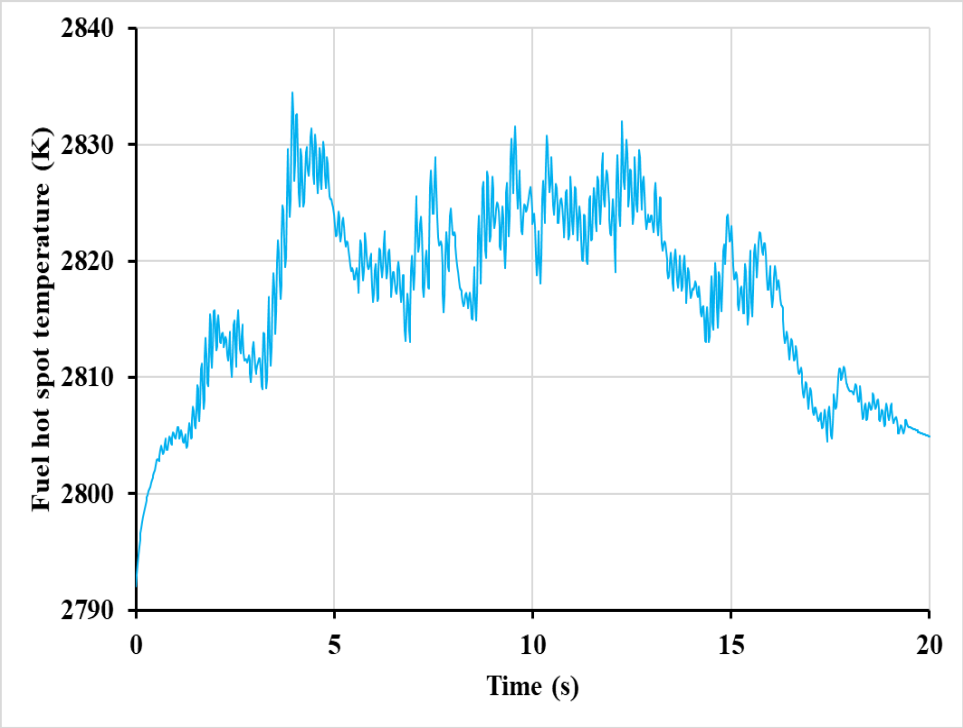

FIGURE 5.12: Fluctuations in fuel hot spot temperature for SSE.

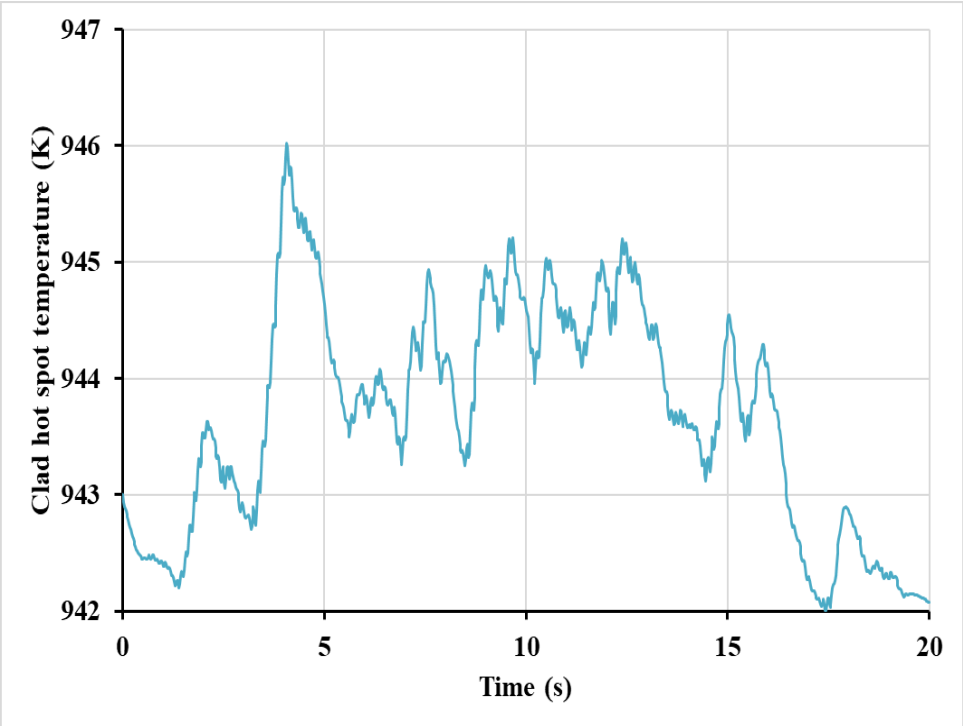

FIGURE 5.13: Fluctuations in clad hot spot temperature for SSE.

5.4 Summary

Safe Shutdown Earthquake (SSE) and Operating Basis Earthquake (OBE) are analysed by using the Design Basis Events for PFBR. Probability of occurrence of SSE is lower. It is found that considering the geographical location and analysis of geometrical changes in core, peak magnitude of reactivity fluctuations from SSE fall below 0.4$. Reactor kinetics studies have established that for these reactivity fluctuations, the fuel and clad remain below normal operation limits. The same is also further affirmed with analysis of sinusoidal reactivity with amplitude of 0.5 $, that the fuel and clad hot spot temperatures remain below normal operation limits.

Chapter 6

Summary, Conclusions and Future Directions

6.1 Summary and conclusions

The neutronics stability of a nuclear reactor has to be ensured for its safe operation under various types of reactivity perturbations. Such perturbations cause reactor power change and returns to its steady state after some time, if it is stable. Otherwise, the system will move away from the steady-state leading to an un-safe state. A stability analysis is therefore important to ascertain stable operation in a nuclear reactor under all possible reactivity perturbations. Methods of linear and non-linear stability analysis currently used in thermal and fast reactors have been reviewed in this thesis. Linear stability analysis in the frequency domain with simplified models are being widely used. The time dependence of reactor power is simulated by using point kinetics equations, and corresponding variation of temperatures for fuel, clad and coolants are studied using lumped heat transfer equations. No space dependent reactivity feedbacks are considered in all the studies reported. It is reported that a thermal reactor may become unstable due to large xenon reactivity feedbacks, whereas fast reactors are, in general, stable systems. As the core size increases, neutronic coupling in a fast reactor reduces, its stability behaviour becomes non-linear. But, limited studies have been reported in the area of fast power reactors. Hence, this thesis work is focused to characterise the stability behaviour of pool-type SFRs having different power level,

core size and fuel type. Further, safety of these reactors under various reactivity perturbations such as sinusoidal type and seismic fluctuations are also studied. Most challenging part in all of these studies are the development of methodologies and the associated computational tools. The following important works are carried out:

(a) ***Development of a transfer function based computer code DYNRCO for linear stability analysis***

A computer code DYNRCO is developed for doing linear stability analysis of fast reactor systems using transfer function method. It uses multichannel approach, in which the spatial dependence of reactivity feedbacks is considered while estimating the open-loop transfer function of the reactor system. The forward and feedback transfer functions are estimated by solving point kinetics equations along with heat transfer and reactivity equations in Laplace domain. The Nyquist criteria is used for assessment of linear stability. This code can also estimate the stability margin from the Nyquist plot.

(b) ***Assessment of linear stability in oxide and metal SFR cores using DYNRCO***

The computer code DYNRCO is used to demonstrate the stability of MOX and metal fueled FBR cores. Two core configurations of 500 MWe PFBR (oxide), i.e. fresh and equilibrium, and three metal cores (120 MWe, 500 MWe and 1000 MWe) are studied and made a relative comparison with respect to PFBR core. The study proved the stable nature of metal and oxide cores with little advantage for metal cores in terms of stability margin.

(c) ***Non-linear stability analysis using bifurcation method***

A non-linear analysis by using the bifurcation method is done for the first time to assess stability of PFBR core. The governing non-linear reactor dynamics equations with fuel, steel and coolant temperature feedbacks are used. It is concluded from this study that FBR has unique stable solution within the operating regime without any non-trivial bifurcations. Nature of its solution is compared with that of a PWR core (non-linear system).

(d) ***Studies of SFR cores response to large non-linear reactivity perturbations***

The response to large reactivity perturbations is also important to be studied in an SFR core to assess its overall safety. It is done in the time domain by using the transient analysis code PREDIS for step and sinusoidal reactivity inputs, with PFBR core as an example. It is shown that the power or system temperatures are not diverging with time. Study also shows that the negative feedbacks in PFBR is sufficient to ensure the stability of the core. Further, fuel and steel temperatures are well below their design safety limits.

(e) ***Studies of SFR cores response to seismic reactivity perturbations***

A demonstration of core safety during an earth quake induced large non-linear reactivity perturbation is very challenging in the area of fast reactors. The methodology to perform such a study using PREDIS code has been developed and it has been applied to assess the system response under Safe Shutdown Earthquake (SSE) and Operating Basis Earthquake (OBE) by taking PFBR as an example. Though the probability of occurrence of SSE is lower in PFBR, the peak magnitude of reactivity fluctuations is found to be 0.4 $, if it occurs. It is demonstrated that the design safety limits in all system components are also respected even when the reactor is not scrammed.

To conclude, the major outcome of this thesis work is the development of a transfer function-based computer code DYNRCO for linear stability analysis in fast reactor systems and its application to characterise core stability behaviour of different types of oxide and metal sodium cooled pool-type fast reactor systems. Further, methodologies have been established for non-linear stability assessment in fast reactors by using bifurcation method and time domain transient analysis. The fast reactors studied are found to be stable against small and large non-linear reactivities of step, sinusoidal and seismic excitations and their system temperatures are well within the design safety limits.

6.2 Scope for future studies

Following studies are recommended as an extension of the present study:

- The DYNRCO code requires an experimental validation. The dynamic power coefficient can be deducted from power versus time data under a rod drop experiment. Similarly, the feedback time constant can be estimated from the dynamic power coefficient by curve fitting. A rod drop or rod oscillator experiments is proposed to be carried out in the Fast Breeder Test Reactor (FBTR) for this purpose.

- Space dependent reactivity feedbacks has to be incorporated in the nonlinear stability analysis using the Liapunov method.

- Stability of the core against flow and temperature fluctuations using transfer function methods needs to be studied.

- The model used in the present study can be improved by considering both primary and secondary sodium circuits and also by including more reactivity feedback mechanisms like control rod drive line expansion, vessel expansion etc.

****

References

[1] P. G. Drazin, *Nonlinear Systems*. Cambridge University Press, 1992.

[2] G. G. Theler and F. J. Bonetto, "On the stability of the point reactor kinetics equations", *Nuclear Engineering and Design*, vol. 240, pp. 1443–1449, 2010.

[3] A. M. Lyapunov, "The general problem of the stability of motion", *International journal of control*, vol. 55, pp. 531–773, 1992.

[4] R. Seidel, *Practical bifurcation and stability analysis*. Springer, 2010, vol. 5.

[5] K. Ogata, *Modern Control Engineering*. Pearson, 2018, vol. 5.

[6] W. R. Evans, *Control system dynamics*. McGraw-HIll, 1954.

[7] H. Nyquist, "The regeneration theory", *Bell Syst. Tech. J.*, 1932.

[8] M. Ash, *Nuclear reactor kinetics*. McGraw-Hill International, 1979.

[9] P. Breeze, *Nuclear Power*. Academic Press, 2017.

[10] J. R. Lamarsh, *Introduction to Nuclear Reactor Theory*. Addison-Wesley, 1983.

[11] J. C. Lee, *Nuclear Reactor Physics and Engineering*. Wiley, 2020.

[12] IAEA, *Accident analysis for nuclear power plants with graphite moderated boiling water RBMK reactors*. Safety reports series-43, 2005.

[13] S. S. Bajaj and A. R. Gore, "The indian PHWR", *Nuclear Engineering and Design*, vol. 236, pp. 701–722, 2006.

[14] N. Kasahara, *Fast Reactor System Design*. Springer, 2017.

[15] D. A. Arostegui and M. Holt, "Advanced nuclear reactors: Technology overview and current issues", *CRS Report*, vol. R45706, 2019. DOI: www.crs.gov.

[16] D. L. Hetrick, *Dynamics of nuclear reactors*. The university of chicago press, 1971.

[17] C. Guerrieri, A. Cammi, and L. Luzzi, "An approach to the MSR dynamics and stability analysis", *Progress in Nuclear Energy*, vol. 67, pp. 56–73, 2013. DOI: 10.1016/j.pnucene.2013.03.020.

[18] S. J. Peng, M. Z. Podowski, and R. T. L. Jr., "BWR linear stability analysis", *Nuclear Engineering and Design*, vol. 93, pp. 25–37, 1986.

[19] P. Wahia and V. Kumawat, "Nonlinear stability analysis of a reduced order model of nuclear reactors: A parametric study relevant to the advance heavy water reactor", *Nuclear Engineering and Design*, vol. 241, pp. 134–143, 2011. DOI: 10.1016/j.nucengdes.2010.11.006.

[20] D. G. Cacuci, J. March-Leuba, and R. B. Parez, "Limit cycles and bifurcations in nuclear systems", *CONF-861102-11, Oak Ridge National Laboratory*, 1986.

[21] J. March-Leuba, D. G. Cacuci, and R. B. Parez, "Nonlinear dynamics and stability of boiling water reactors: Part 1- Qualitative analysis", *Nuclear science and engineering*, vol. 93, pp. 111–123, 1986.

[22] J. A. Turso, R. M. Edwards, and J. March-Leuba, "Hybrid simulation of boiling water reactor dynamics using a university research reactor", *Nuclear Technology*, vol. 110, pp. 132–144, 1995.

[23] V. A. Vyawahare and G. E. Paredes, "BWR stability analysis with sub-diffusive and feedback effects", *Annals of nuclear energy*, vol. 110, pp. 349–361, 2017.

[24] V. A. Vyawahare and G. Espinosa-Paredes, "On the stability of linear fractional-space neutron point kinetics (F-SNPK) models for nuclear reactor dynamjcs", *Annals of Nuclear Energy*, vol. 111, pp. 12–21, 2018. DOI: 10.1016/j.anucene.2017.08.060.

[25] N. Z. Cho and L. M. Grossman, "Optimal control of Xenon spatial oscillations in load follow of a nuclear reactor", *Nuclear science and engineering*, vol. 83, pp. 136–148, 1983.

[26] H. Ukai, Y. Morita, and Y. Yada, "Control of xenon spatial oscillations during load follow of nuclear reactor via robust servo systems", *Journal of Nuclear science and technology*, vol. 27, pp. 307–319, 1990.

[27] G. Li, B. Liang, X. Wang, X. Li, and K. Wang, "Stability analysis of nonlinear nuclear reactor cores adopting T-S fuzzy modeling and Lyapunov theory", *AMSM 2016*, pp. 256–259, 2016.

[28] E. Cervi, A. Cammi, and A. D. Ronco, "Stability analysis of the generation -IV nuclear reactors by means of the root locus criterion", *Progress in nuclear energy*, vol. 106, pp. 316–334, 2018.

[29] D. Yu, "Space dependent fast reactor stability", *Proc. Okla. Acad. Sci.*, vol. 50, pp. 136–139, 1970.

[30] E. V. Depiante, "Stability analysis of a liquid-metal reactor and its primary heat transport system", *Nuclear Engineering and Design*, vol. 152, pp. 361–377, 1994. DOI: SSDI0029-5493(94)00806-A.

[31] R. Ziskind and W. E. Kastenberg, "On the determination of stability domains in nonlinear point reactor dynamics", *Nuclear Science and Engineering*, vol. 44, pp. 86–94, 1971.

[32] M. Numano, H. Nishihara, and H. Abe, "Determination of stability domain of reactor with single temperature and prompt power coefficient", *Journal of nuclear science and technology*, vol. 9, pp. 157–164, 1971.

[33] J. Devooght, "Determination of stability domains in point reactor dynamics", *Nuclear Science and Engineering*, vol. 28, pp. 226–236, 1967.

[34] Y. M. Hamada, "Liapunov's stability on autonomous nuclear reactor dynamical systems", *Progress in Nuclear Energy*, vol. 73, pp. 11–20, 2014. DOI: 10.1016/j.pnucene.2013.12.012.

[35] A. Oyama, S. An, and S. Saito, "Dynamic analysis of large fast reactor", *Journal of nuclear science and technology*, vol. 4(11), pp. 545–554, 1967.

[36] B. Mitchell, "A review of reactivity feedback, stability and related operating experience in fast power reactors from EBR-I to BN 800", *Science and technology of fast reactor safety*, pp. 179–184, 1986.

[37] R. R. Smith, R. G. Matlock, F. D. McGinnis, M. Novick, and F. W. Thalgott, "An analysis of the stability of EBR-I marks I to III, and conclusions pertinent to the design of fast reactors", *Physics of fast and intermediate reactors*, vol. 3, pp. 43–91, 1962.

[38] R. R. Smith, J. F. Boland, F. D. McGinnis, M. Novick, and F. W. Thalgott, "Instability studies with EBR-I marks III", *AEC Research and Development Report*, vol. ANL-6266, 1960.

[39] T. Sofu, "A review of inherent safety characteristics of metal alloy sodium-cooled fast reactor fuel against postulated accidents", *Nuclear Engineering and Technology*, vol. 47, pp. 227–239, 2015. DOI: 10.1016/j.net.2015.03.004.

[40] H. H. Hennies, "The fast neutron breeder fission reactor: Safety issues in reactor design and operation", *Philosophical Transactions fo the Royal Society of London*, vol. 331, no. 1619, pp. 409–418, 1990.

[41] Y. I. Chang, "Technical rationale for metal fuel in fast reactors", *Nuclear engineering and technology*, vol. 39, no. 3, pp. 161–170, 2007.

[42] J Cahalan, R. Wigeland, G. Friedel, G. Kussmaul, J. Moreau, H. Perks, and P. Roy, "Performance of metal and oxide fuels during accidents in a large liquid cooled reactor", *International Conference on fast reactor safety*, vol. 4, pp. 198–211, 1990.

[43] S. C. Chetal, V. Balasubramaniyan, P. Chellapandi, P. Mohanakrishnan, P. Puthiyavinayagam, C. P. Pillai, S. Raghupathy, T. K. Shanmugham, and C. S. Pillai, "The design of the prototype fast breeder reactor", *Nuclear engineering and design*, vol. 236, pp. 852–860, 2006. DOI: 10.1016/j.nucengdes.2005.09.025.

[44] J. Graham, *Fast Reactor Safety*. Academic Press, 1971.

[45] H. H. Hummel and D. Okrent, "Reactivity coefficients in large fast power reactors", *American Nuclear Society*, 1970.

[46] W. Bolton, *Instrumentation and Control Systems*. Elsevier, 2015.

[47] K. O. Ott and R. J. Neuhold, *Introductory Nuclear Reactor Dynamics*. American Nuclear Society, 1985.

[48] R. Harish, T. Sathiyasheela, G. S. Srinivasan, and O. P. singh, "KALDIS: A computer code system for core disruptive accident analysis of fast reactors", *IGC-208*, 1999.

[49] A. E. Walter and A. B. Reynold, *Fast breeder reactors*. Pergamon Press, 1981.

[50] B. Merk, E. Fridman, and Frank-PeterWeiß, "On the use of a moderation layer to improve the safety behavior in sodium cooled fast reactors", *Annals of Nuclear Energy*, vol. 38, pp. 921–929, 2011. DOI: 10.1016/j.anucene.2011.01.024.

[51] T. Sathiyasheela, K. Natesan, G. Srinivasan, K. Devan, and P. Puthiyavinayagam, "Analysis of unprotected transients with control and safety rod drive mechanism expansion feedback in a medium sized oxide fuelled fast breeder reactor", *Nuclear Engineering and Design*, vol. 291, pp. 1–9, 2015. DOI: 10.1016/j.nucengdes.2015.04.022.

[52] D. Tenchine, "International benchmark on the natural convection test in Phenix reactor", *Nuclear Engineering and Design*, vol. 258, pp. 189–198, 2013.

[53] D. Tenchine, D. Pialla, P. Gauthe, and A. Vasile, "Natural convection test in Phenix reactor and associated CATHARE calculation", *Nuclear Engineering and Design*, vol. 253, pp. 23–31, 2012.

[54] P. Gauthe, "Data list for the calculation of Phenix End Of Life Tests", *CEA/DEN/CAD/DER/SESI/LESA/NT DO 16*,

[55] K. Mikityuk, "FAST: An advanced code system for fast reactor transient analysis", *Annals of Nuclear Energy*, vol. 32, pp. 1613–1631, 2005.

[56] A. Chenu, K. Mikityuk, and R. Chawla, "Analysis of selected Phenix EOL tests with the FAST code system – Part II: Unprotected phase of the natural convection test", *Annals of Nuclear Energy*, vol. 49, pp. 191–199, 2012.

[57] V. I. Matveev, I. V. Malysheva, and I. V. Buriyevskiy, "Physical characteristics of large fast-neutron sodium-cooled reactors with advanced nitride and metallic fuels", *Nuclear energy and technology*, vol. 1, pp. 308–312, 2015.

[58] A. Riyas and P. Mohanakrishnan, "ULOF transient behaviour of metal-fuelled fast breeder reactor cores as a function of core size and perturbation methods", *Nuclear Engineering and Design*, vol. 278, pp. 141–149, 2014. DOI: 10.1016/j.nucengdes.2014.07.018.

[59] T. Sathiyasheela, "Comparitive study of unprotected loss of flow accident analysis of 1000 MWe and 500 MWe fast breeder reactor metal (FBR-M) cores and their inherent safety", *Annals of Nuclear Energy*, vol. 38, no. 5, pp. 1065–1073, 2011. DOI: 10.1016/j.anucene.2011.01.005.

[60] R. Harish, G. S. Srinivasan, A. Riyas, and P. Mohanakrishnan, "A comparative study of unprotected loss of flow accidents in 500 MWe FBR metal cores with PFBR oxide core", *Annals of Nuclear Energy*, vol. 36, pp. 1003–1012, 2009. DOI: 10.1016/j.anucene.2009.06.004.

[61] B. Merk, K. Devan, A. Bachchan, D. Paul, P. Puthiyavinayagam, and G. Srinivasan, "Can enhanced feedback effects and improved breeding coincide in a metal fueled, sodium cooled fast reactor?", *Annals of Nuclear Energy*, vol. 105, pp. 205–218, 2017. DOI: 10.1016/j.anucene.2017.03.018.

[62] A. Riyas, K. Devan, and P. Mohanakrishnan, "Perturbation analysis of prototype fast breeder reactor equilibrium core using IGCAR and ERANOS code system", *Nuclear Engineering and Design*, vol. 255, pp. 112–122, 2013. DOI: 10.1016/j.nucengdes.2012.09.020.

[63] M. Tsuji, K. Nishio, Y. O. Masakuni Narita, and M. Mori, "Stability analysis of BWRs using bifurcation theory", *Journal of nuclear science and technology*, vol. 30, pp. 1107–1119, 1992.

[64] Rizwan-uddin, "Turning points and sub- and supercritical bifurcations in a simple BWR model", *Nuclear Engineering and Design*, vol. 236, pp. 267–283, 2005.

[65] C. Lange, D. Hennig, M. Schulze, and A. Hurtado, "Complex BWR dynamics from the bifurcation theory point of view", *Annals of Nuclear Energy*, vol. 67, pp. 91–108, 2014. DOI: 10.1016/j.anucene.2013.07.034.

[66] C. Y. Yang and N. Z. Cho, "A study of multiplicity of power distributions in a nuclear reactor subject to reactivity feedbacks", *Nuclear science and engineering*, vol. 101, pp. 242–258, 1989. DOI: 10.13182/NSE89-A23612.

[67] Q. V. Lavande, N. Maiti, and H. P. Gupta, "Investigating stability of PWR model with feedback using nonlinear approach", *Internal report, BARC*, 2002.

[68] S. Sastry, *Nonlinear systems: Analysis, stability and control*. Springer, 1999.

[69] S. C. Chetal, "Safety design of Prototype Fast Breeder Reactor", *Proc. ICAPP 2007, Nice France*, 2007.

[70] E. E. Lewis, *Nuclear power reactor safety*. John Wiley and Sons, 1977.

[71] G. Petrangeli, *Nuclear safety*. Elsevier, 2006.

[72] P. Chellapandi, "Seismic analysis of NSSS components of prototype fast breeder reactor", *Proc. 1st national conference on nuclear reactor safety*, vol. 1, 2002.

[73] P. Cecchini, "Neutronic and thermal behavior of the PEC core in an earthquake", *IAEA-IWGFR-65*, 1988.

[74] A. Preumont, "Seismic behavior of the SNR-2 core subassemblies", *Proc. BNES conference on science and technology of fast reactor safety, Guernsey*, vol. 2, pp. 553–556, 1986.

[75] S. Glasstone and A. Sesonske, *Nuclear reactor engineering*. CBS Publishers and distributors, 2003, vol. 2.

[76] P. Chellapandi, "Seismic analysis of LMFBR core part I, Development of code CORESEIS", *Proc. 10th symposium on earthquake engineering*, vol. 10, 1994.

[77] R. Ravi, "Seismic analysis of LMFBR cores part II, validation of code CORESEIS", *Proc. 10th symposium on earthquake engineering*, vol. 10, 1994.

[78] A. Gupta and P. Chellapandi, "Reactivity oscillations during seismic event", *IGCAR Report*, vol. PFBR/31100/DN/1034, 2002.

[79] E. E. Lewis, *Fundamentals of nuclear reactor physics*. Elsevier, 2008.

[80] P. P. Vinayagam and S. C. Ravichandar, "Design safety limits for fuel, clad and coolant", *IGCAR report PFBR/31100/DN/1038 Rev-C*, 2006.

[81] S. C. Ravichandar, "Hotspot factors for fuel", *IGCAR Report- PFBR/31110/DN/1064*, 2008.

Chapter 6

Summary, Conclusions and Future Directions

6.1 Summary and conclusions

The neutronics stability of a nuclear reactor has to be ensured for its safe operation under various types of reactivity perturbations. Such perturbations cause reactor power change and returns to its steady state after some time, if it is stable. Otherwise, the system will move away from the steady-state leading to an un-safe state. A stability analysis is therefore important to ascertain stable operation in a nuclear reactor under all possible reactivity perturbations. Methods of linear and non-linear stability analysis currently used in thermal and fast reactors have been reviewed in this thesis. Linear stability analysis in the frequency domain with simplified models are being widely used. The time dependence of reactor power is simulated by using point kinetics equations, and corresponding variation of temperatures for fuel, clad and coolants are studied using lumped heat transfer equations. No space dependent reactivity feedbacks are considered in all the studies reported. It is reported that a thermal reactor may become unstable due to large xenon reactivity feedbacks, whereas fast reactors are, in general, stable systems. As the core size increases, neutronic coupling in a fast reactor reduces, its stability behaviour becomes non-linear. But, limited studies have been reported in the area of fast power reactors. Hence, this thesis work is focused to characterise the stability behaviour of pool-type SFRs having different power level,

core size and fuel type. Further, safety of these reactors under various reactivity perturbations such as sinusoidal type and seismic fluctuations are also studied. Most challenging part in all of these studies are the development of methodologies and the associated computational tools. The following important works are carried out:

(a) ***Development of a transfer function based computer code DYNRCO for linear stability analysis***

A computer code DYNRCO is developed for doing linear stability analysis of fast reactor systems using transfer function method. It uses multichannel approach, in which the spatial dependence of reactivity feedbacks is considered while estimating the open-loop transfer function of the reactor system. The forward and feedback transfer functions are estimated by solving point kinetics equations along with heat transfer and reactivity equations in Laplace domain. The Nyquist criteria is used for assessment of linear stability. This code can also estimate the stability margin from the Nyquist plot.

(b) ***Assessment of linear stability in oxide and metal SFR cores using DYNRCO***

The computer code DYNRCO is used to demonstrate the stability of MOX and metal fueled FBR cores. Two core configurations of 500 MWe PFBR (oxide), i.e. fresh and equilibrium, and three metal cores (120 MWe, 500 MWe and 1000 MWe) are studied and made a relative comparison with respect to PFBR core. The study proved the stable nature of metal and oxide cores with little advantage for metal cores in terms of stability margin.

(c) ***Non-linear stability analysis using bifurcation method***

A non-linear analysis by using the bifurcation method is done for the first time to assess stability of PFBR core. The governing non-linear reactor dynamics equations with fuel, steel and coolant temperature feedbacks are used. It is concluded from this study that FBR has unique stable solution within the operating regime without any non-trivial bifurcations. Nature of its solution is compared with that of a PWR core (non-linear system).

(d) ***Studies of SFR cores response to large non-linear reactivity perturbations***

The response to large reactivity perturbations is also important to be studied in an SFR core to assess its overall safety. It is done in the time domain by using the transient analysis code PREDIS for step and sinusoidal reactivity inputs, with PFBR core as an example. It is shown that the power or system temperatures are not diverging with time. Study also shows that the negative feedbacks in PFBR is sufficient to ensure the stability of the core. Further, fuel and steel temperatures are well below their design safety limits.

(e) ***Studies of SFR cores response to seismic reactivity perturbations***

A demonstration of core safety during an earth quake induced large non-linear reactivity perturbation is very challenging in the area of fast reactors. The methodology to perform such a study using PREDIS code has been developed and it has been applied to assess the system response under Safe Shutdown Earthquake (SSE) and Operating Basis Earthquake (OBE) by taking PFBR as an example. Though the probability of occurrence of SSE is lower in PFBR, the peak magnitude of reactivity fluctuations is found to be 0.4 $, if it occurs. It is demonstrated that the design safety limits in all system components are also respected even when the reactor is not scrammed.

To conclude, the major outcome of this thesis work is the development of a transfer function-based computer code DYNRCO for linear stability analysis in fast reactor systems and its application to characterise core stability behaviour of different types of oxide and metal sodium cooled pool-type fast reactor systems. Further, methodologies have been established for non-linear stability assessment in fast reactors by using bifurcation method and time domain transient analysis. The fast reactors studied are found to be stable against small and large non-linear reactivities of step, sinusoidal and seismic excitations and their system temperatures are well within the design safety limits.

6.2 Scope for future studies

Following studies are recommended as an extension of the present study:

- The DYNRCO code requires an experimental validation. The dynamic power coefficient can be deducted from power versus time data under a rod drop experiment. Similarly, the feedback time constant can be estimated from the dynamic power coefficient by curve fitting. A rod drop or rod oscillator experiments is proposed to be carried out in the Fast Breeder Test Reactor (FBTR) for this purpose.

- Space dependent reactivity feedbacks has to be incorporated in the nonlinear stability analysis using the Liapunov method.

- Stability of the core against flow and temperature fluctuations using transfer function methods needs to be studied.

- The model used in the present study can be improved by considering both primary and secondary sodium circuits and also by including more reactivity feedback mechanisms like control rod drive line expansion, vessel expansion etc.

****

SUMMARY

A nuclear reactor core is required to have neutronics stability for ensuring safe operation under various types of reactivity perturbations. It helps system not to move away from equilibrium due to small perturbations in reactivity. Stability analysis is therefore very important for the design of nuclear reactor cores. Limited studies have been reported in the area of fast power reactor stability. The works reported in this thesis are mainly focused to characterise the stability behaviour of pool-type SFRs having different power levels, core sizes and fuel types. The required tools and the methodologies have been developed for this purpose.

The transfer function method using Nyquist criteria has been adopted for linear stability analysis and a computer code DYNRCO is developed. It has the capability to account for multichannel approach in heat transfer and reactivity feedback calculations in the frequency domain. The code is used for the stability analysis of MOX and metal fueled FBR cores and the stability margins are estimated. Even though the feedback power coefficient is larger in case of Oxide core the stability margin is lower compared to metal cores. The smaller time constant due to better heat transfer properties of the metal core gives a higher stability margin for the metal fueled FBRs.

Also, safety of PFBR under various reactivity perturbations such as sinusoidal type and seismic fluctuations are studied. The power evolution with time is simulated and it is shown that there is no unstable oscillations. It is demonstrated that design safety limits are respected during Safe Shutdown Earthquake (SSE) even when the reactor is not scrammed. Non-linear stability analysis is also performed for the first time using bifurcation method and time domain analysis. It is found that these reactors are stable even with large reactivity perturbations.

Thesis Title:

STUDIES ON STABILITY CHARACTERISTICS OF MOX AND METAL FUELED FAST REACTOR CORES

Name of candidate: ANURAJ V L

अनुराज वी एल

अनुराज वी एल

Thesis Highlight

Name of the Student: Anuraj V L

Name of the CI/OCC: IGCAR **Enrolment No.:** PHYS-02201204018

Thesis Title: Studies on stability characteristics of MOX and metal fueled fast reactor cores

Discipline: Physical Sciences **Sub-Area of Discipline:** Fast Reactor Stability

Date of viva voce: 14 December 2020

A nuclear reactor core is required to have neutronics stability for ensuring safe operation under various types of reactivity perturbations. It helps system not to move away from equilibrium due to small perturbations in reactivity. Stability analysis is therefore very important for the design of nuclear reactor cores. The works reported in this thesis are mainly focused to characterise the stability behaviour of pool-type SFRs having different power levels, core sizes and fuel types. The required tools and the methodologies have been developed for this purpose.

The transfer function method using Nyquist criteria has been adopted for linear stability analysis and a computer code DYNRCO is developed. It has the capability to account for multichannel approach in heat transfer and reactivity feedback calculations in the frequency domain. The code is used for the stability analysis of MOX and metal fueled FBR cores and the stability margins are estimated. Even though the feedback power coefficient is larger in case of Oxide core the stability margin is lower compared to metal cores. The smaller time constant due to better heat transfer properties of the metal core gives a higher stability margin for the metal fueled FBRs.

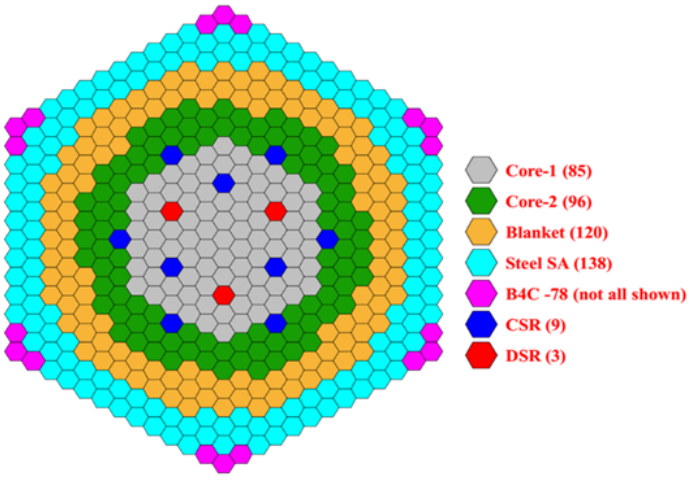

Figure 1. Core configuration of 500 MWe MOX core.

Also, safety of PFBR under various reactivity perturbations such as sinusoidal type and seismic fluctuations are studied. The power evolution with time is simulated and it is shown that there is no unstable oscillations. It is demonstrated that design safety limits are respected during Safe Shutdown Earthquake (SSE) even when the reactor is not scrammed. Non-linear stability analysis is also performed for the first-time using bifurcation method and time domain analysis. It is found that these reactors are stable even with large reactivity perturbations. processes.